Development of peptide-drug conjugates targeting mitochondria

Inaugural-Dissertation

zur

Erlangung des Doktorgrades

der Mathematisch-Naturwissenschaftlichen Fakultät

der Universität zu Köln

vorgelet von

Félix Gayraud

Köln, 2023

Die im Rahmen der vorliegenden Arbeit durchgeführten Experimente und Untersuchungen wurden im Zeitraum von April 2020 bis März 2023 am Institut für Biochemie der Universität zu Köln unter der Anleitung von Frau Prof. Dr. Ines Neundorf durchgeführt.

Abstract

Cancer is a leading cause of death worldwide and represents a challenge that scientists tend to address for decades. Due to its diffuse nature, survivability, and coexistence with healthy cells, treatments targeting this condition often lack efficacy and can lead to undesirable side effects due to the lack of targeting specificity. Through the hacking of various biological processes cancer cells can escape immune response and cellular death machinery rendering them almost immune. Such behavior results, in part, from exploiting the mitochondria organelle to its benefits. Within this work, the development of peptide-drug conjugates targeting mitochondria was explored as a way to better treat cancer through directly deliver drugs to mitochondria. The peptide strategy chosen offers a safe carrier to travel through biological medium while exhibiting interesting cell penetration and mitochondria colocalization properties. To obtain such cargo a fusion between a cell penetrating peptide (CPP) and a mitochondria targeting sequence (MTS) was achieved through peptide synthesis yielding mitochondria targeting CPP (mCPP). CPPs are a class of peptides with the ability to interact and cross cellular membranes without showing toxicity, while MTS are peptide sequences used to transport ribosomal expressed proteins to mitochondria thereof offering mitochondrial targeting. A variety of mCPPs were synthesized by modifying the sequence of the CPP part and the position of the payload. Jasmonic acid was chosen as payload, as this plant stress hormone can induce mitochondria triggered apoptosis but lacks the ability to cross cellular membranes on its own. Thereof addressing this drug directly to mitochondria might offer the ability to restore the apoptotic function of cancerous cells. In this work is presented the synthesis of those mCPPs, their structural characterization and cellular fate as well as their cytotoxicity towards healthy and cancerous cell lines. Results obtained are quite encouraging and highlight the interest of relying on such targeted strategy to address cancer.

Zusammenfassung

Krebs ist weltweit ein der Haupttodesursachen und seine Bekämpfung stellt seit Jahrzehnten eine Herausforderung für die medizinische Wissenschaft dar. Aufgrund seiner diffusen Natur, Überlebensfähigkeit und Koexistenz mit gesunden Zellen fehlt es oft an wirksamen Krebsbehandlungen. Außerdem können unerwünschte Nebenwirkungen auftreten, da zielgerichtete Therapien fehlen. Durch Ausnutzung verschiedener biologischer Prozesse können Krebszellen dem Immunsystem und den zellulären Todesmechanismen entkommen und sind nahezu immun dagegen. In dieser Arbeit wurden Peptid-Wirkstoff-Konjugate entwickelt, die Mitochondrien ansteuern und so eine direkte Wirkstoffzufuhr zu den Mitochondrien ermöglichen sollen, um Krebs besser behandeln zu können. Die gewählte Peptidstrategie bietet einen sicheren Träger und zeigt interessante Eigenschaften in Bezug auf die Zellpenetration und Mitochondrien-Kolokalisierung. Die generierten Peptide sind zusammengesetzt aus einem zellpenetrierenden Peptid (CPP) und einer Mitochondrien-Targeting-Sequenz (MTS), wodurch mitochondrienansteuernde CPPs (mCPP) entstehen. CPPs sind eine Klasse von Peptiden, die die Fähigkeit besitzen mit zellulären Membranen zu interagieren und diese zu durchqueren, ohne Toxizität zu zeigen. MTS Peptidsequenzen steuern normalerweise ribosomal exprimierte Proteine zu den Mitochondrien und können somit eine mitochondriale Targeting-Funktion bieten. In dieser Arbeit wurden unterschiedliche mCPPs durch Modifikation der Sequenz des CPP-Teils und der Position der Wirkstoffladung synthetisiert. Jasmonsäure wurde als Wirkstoff ausgewählt, da dieses pflanzliche Stresshormon eine mitochondrieninduzierte Apoptose auslösen kann, aber nicht allein die Fähigkeit besitzt, zelluläre Membranen zu überqueren. Daher könnte die direkte Anwendung dieses Wirkstoffs auf Mitochondrien die apoptotische Funktion von Krebszellen wiederherstellen. In dieser Arbeit wird die Synthese dieser mCPPs, ihre strukturelle Charakterisierung sowie ihr zelluläres Schicksal und ihre Zytotoxizität gegenüber gesunden und krebsartigen Zelllinien präsentiert. Die erzielten Ergebnisse sind vielversprechend und könnten eine Grundlage für die weitere Entwicklung einer solchen zielgerichteten Strategie zur Bekämpfung von Krebs bieten.

Contents

1. The mitochondria

1.1. Mitochondria structure

Mitochondria are essential organelles for eukaryotic cells and thus for us humans. This bean, the size of a micrometer, can be viewed as the single most important organelle for the cell owing to all the functions it fulfills and to its involvement in other metabolic processes that we will scope over in the present chapter.

This story begins with the origin of mitochondria which lies in the endosymbiotic relation developed between eukaryotic cells and non-sulphuric bacteria as theorized by Sagan.[1,2] Through enslavement of bacteria by an eukaryotic host mitochondria developed a particular morphology. This organelle is separated from the rest of the cell by a double membrane that creates an intermembrane space, which can be viewed as an adaptative medium between mitochondria and its host.
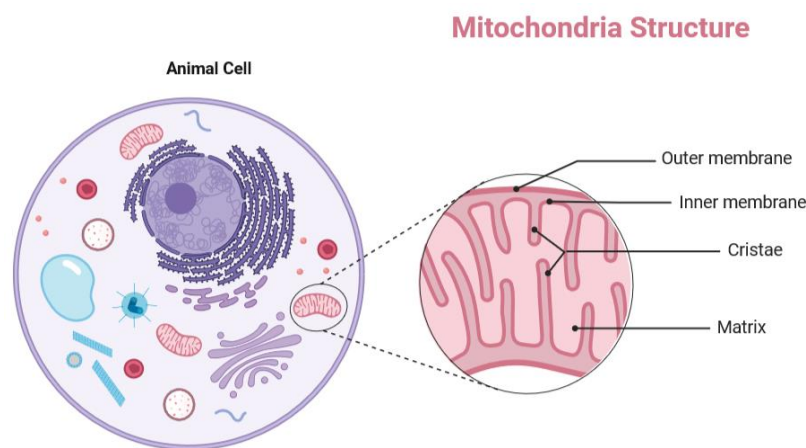
Figure 1. Schematic representation of a cell and details of a mitochondria structure. (Made on Biorender)

Mitochondria exhibit a complex structure comprising an outer membrane (OMM), an inner membrane (IMM), and an intermembrane space (IMS) serving as an exchange site. The IMM encloses the matrix of the mitochondria, where most of the organelle's activities occur. The matrix contains highly invaginated structures called cristae, which increase the surface area for exchange with the IMS. This compartmentalization, a result of the mitochondria's evolutionary history, differentiates the functions of the OMM and IMM. The OMM primarily acts as a signaling platform, while the IMM is primarily involved in cellular energy production. The IMS serves as a communication hub, ensuring the coordinated functioning of the entire mitochondrial machinery.

One of the remarkable features of mitochondria is their high adaptability. They can adjust their location within the cell to meet local energy demands and can exist as individual entities or form groups that collectively contribute to the cell's energy needs. Additionally, mitochondria can alter their shape to accommodate specific requirements, making both their outer and inner membranes dynamic and flexible. A crucial aspect of mitochondrial dynamics is the fission/fusion mechanism, which enables mitochondria to adapt to cellular demands. Fusion is mediated by mitofusin proteins that bridge neighboring mitochondria, allowing the

opening of their respective OMMs and the subsequent merging of their separate IMMs, resulting in the formation of larger mitochondrial assemblies.[3] On the other hand, fission occurs when specific parts of mitochondria need replacement, renewal, or when cellular energy demands decrease, allowing their materials to be utilized by other organelles.[3]

1.2. Mitochondria, the powerhouse of the cell

As mentioned, mitochondria are well known for their energy production fulfilling a major role for cell survival and growth. This pivotal function occurs at the inner mitochondrial membrane (IMM), which is highly invaginated to maximize the surface area for exchange. Energy is produced in the form of adenosine triphosphate (ATP), consisting of an adenine base, a ribose sugar, and three phosphate groups bonded in series.[4] ATP is obtained through ATP synthase, a complex structure located at the end of the Electron Transport Chain (ETC). The ETC, situated on the surface of the IMM, comprises five complexes that consume electrons and expel protons into the intermembrane space (IMS) (Fig 2). In return those protons can be used by the ATP synthase to finalize the transformation of Adenosine diphosphate (ADP) in ATP in a process termed Oxidative Phosphorylation (OXPHOS).[5] Therefore, OXPHOS may represent the most important process in cellular metabolism in order to sustain the cell in energy and fuel other metabolic pathways.
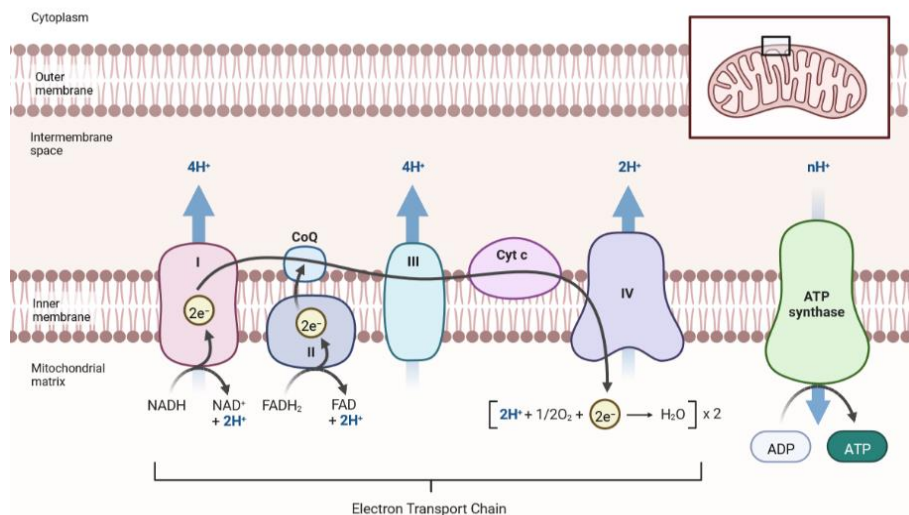
Figure 2. Schematic representation of the Electron Transport Chain. (Made on Biorender)

The energy stored in ATP is derived from the cleavage of inorganic pyrophosphate (PPi) groups. When ATP is hydrolyzed to ADP + PPi or AMP + 2 PPi, these reactions can drive energetically unfavorable transformations, enabling otherwise thermodynamically unfavorable processes to occur.[4]

To generate the electron flow required, the ETC relies on NADH and $FADH_2$, intermediates from the Tricarboxylic acid cycle (TCA) and the fatty acid oxidation, that can carry electrons. These processes occur within the cristae of mitochondria. During the TCA cycle, a pyruvate molecule is used to produce both electron carriers. Fatty acids are converted to Fatty CoA and subsequently oxidized to generate the electron carriers as well.[5]

1.3. Mitochondria a major contributor to cellular stress

Alongside the production of ATP, OXPHOS is also responsible for a major production of Reactive oxygen Species (ROS). These oxygen radical species are formed when oxygen species, utilized by the various complexes of the ETC, undergo incomplete reduction, resulting in the addition of a single electron rendering them highly reactive and potentially damaging for the cell. Within mitochondria, the two major ROS products are the superoxide anion ($O_2^-\cdot$), precursor of most ROS, and hydrogen peroxide (H_2O_2).[6,7] Production of $O_2^-\cdot$ occurs through the stepwise reduction of O_2 in the ETC, but also from diverse enzymes at the OMM and IMM of mitochondria. Subsequently, it can either dismutase spontaneously[8], or via superoxide dismutase[9]. Hydrogen peroxide is more stable and membrane permeable can diffuse through the cell to be eliminated in the cytosol or within the mitochondria through antioxidant systems.[6]

Mitochondria possess antioxidant protection systems, to counteract the harmful effects of ROS, in the form of superoxide dismutase in the matrix, converting $O_2^-\cdot$ into H_2O_2 which can be further deactivated by catalase into water and oxygen, or by glutathione peroxidase.[6,10] It can also be scavenged by peroxiredoxin enzymes in the mitochondria.[11] Finally, if not scavenged by the previous, H_2O_2 can react with oxidized cytochrome c or cytochrome oxidase.[12,13] As a result, mitochondria are equipped with effective defenses to protect themselves from the ROS they generate, enabling them to withstand significant oxidative stress.

However, unregulated ROS can cause critical problems for mitochondria. A vestige resulting from the origin of mitochondria, is their possession of mitochondrial DNA (mtDNA), which is localized on the inner leaflet of IMM in close proximity to the ROS source.[6] While mtDNA does possess several DNA repair enzymes, it is characterized by a lack of introns, histones, and DNA protecting proteins. In comparison to nuclear DNA, mtDNA has a reduced repair system, making it highly susceptible to degradation.[14,15] Consequently, mtDNA has a high mutation rate and damages altering its functioning are associated with many human diseases. This is particularly significant as mtDNA encodes essential proteins required for OXPHOS.[16] Due to its location, the respiratory chain is the primary target of ROS damage. Within the Electron Transport Chain (ETC), there are several metal-containing complexes that are sensitive to oxidative modifications. When these complexes undergo oxidative modifications, their enzymatic activity is reduced, leading to compromised ATP production and increased ROS generation. This, in turn, intensifies oxidative stress within the cell.[6]

1.4. Apoptosis and mitochondria

In contrast to energy production, synonym of life and growth, mitochondria are also executioner of apoptosis, which is a programmed cell death. When there is a need for cell renewal, a decrease in cell requirements, or the presence of intracellular damage that could be harmful to neighboring cells, mitochondria can initiate apoptosis through two pathways: the extrinsic pathway and the intrinsic pathway.

The extrinsic pathway is activated when cell surface death receptors bind to their corresponding ligands. Upon receiving this signal death receptor would induce dimerization of pro-caspase-8, resulting in its activation. Once activated, caspase-8 cleaves and activates Caspase-3 and-7 resulting in large scale cleavage of cellular components and ultimately cellular death.[17–19] Alternatively, caspase-8 cleavage can generate tBID by activating the BH3-only protein BID. tBID then initiates the intrinsic apoptotic pathway, bridging both pathways.[18]
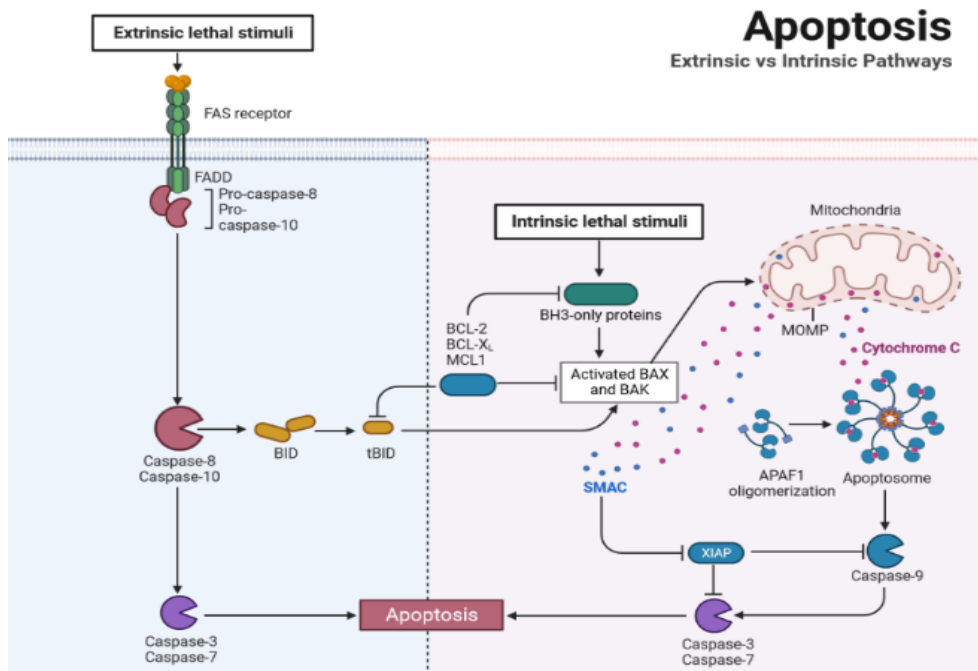
Figure 3. Schematic representation of the apoptotic triggering pathways. (Made on Biorender)

On the other hand, the intrinsic pathway is triggered in response to an intrinsic lethal signal. Intrinsic lethal signal, such as DNA damage, cellular stress or growth factor deprivation, activate BH3-only members of the B cell lymphoma 2 (Bcl-2) protein family. These BH3-only members inhibit anti-apoptotic Bcl-2 proteins while activating pro-apoptotic BCL-2 proteins, specifically BAK and BAX. Activated BAK and BAX consequently localize to the OMM, forming higher-order oligomers through their dimerization. Formation of this oligomer results in mitochondrial outer membrane permeabilization (MOMP), causing the voltage dependent anion channel (VDAC) to open and release proteins from the IMS.[18,20] Among the released proteins, cytochrome-c, a component of the ETC, binds to apoptotic peptidase activating factor 1 (APAF1), forming a heptameric structure known as the apoptosome, which activates caspase-9 causing cleavage and activation of caspases-3 and -7.[17,18] Furthermore, MOMP leads to the release of proteins such as SMAC/DIABLO and OMI, which can inhibit the caspase inhibitor XIAP, facilitating apoptosis.[18]

Apoptosis leads to distinct cellular changes, including cell surface blebbing, externalization of phosphatidylserine (PS), DNA fragmentation, and chromatin condensation. These alterations result in the formation of apoptotic bodies, which are subsequently tagged with PS to facilitate their recognition and clearance by macrophages.[21] Overall, the cell undergoes a

controlled death process leaving no trace of its existence, if not for its materials than can be re-used by other cells and inducing no inflammatory response from neighboring cells.[22]

Given the consequences of apoptosis consequences, mitochondria have to ensure cellular safety by regulating this process through a control on different apoptosis effectors in normal metabolic conditions. One key component involved is the VDAC, which mitochondria utilize as a central hub for substrate import required for OXPHOS and ATP export to the cytosol.[23] To maintain normal cellular function, the opening of VDAC is inhibited by antiapoptotic Bcl-2 proteins located on the OMM.[23]

1.5. Mitochondrial necrosis

In contrast to apoptosis, necrosis represents an alternative mechanism of cell death that occurs under stressful conditions. When cells are exposed to severe stress, they can activate necrotic pathways, involving receptor interacting protein (RIP) kinases and/or poly(ADP-ribose) polymerase-1 (PARP-1). These signals are transmitted to the mitochondria, leading to the disruption of its structure and the leakage of mitochondrial content, ultimately resulting in necrosis. [24]

Upon receiving necrotic signals, the MOMP occurs, leading to the release of ATP and ROS from the mitochondria. This release causes mitochondrial swelling, eventually leading to mitochondrial rupture and cell death under stress-induced conditions. Unlike apoptosis, necrosis triggers the release of inflammatory signals that can be detrimental to neighboring cells. Consequently, necrosis is considered a less desirable, secondary option for controlled cell death.

1.6. Mitochondria, a communication hub

In addition to its morphological heritage mitochondria also maintained substantial in-house protein production. Through ribosomes, located in matrix, mitochondria synthesize 1% of its proteins.[25] The remaining are synthesized in the cytosol and imported via a well-developed system, the translocase of the outer membrane complex (TOM) located in the OMM.[26,27]

The TOM complex serves as the initial entry port, it can sort and redirect imported proteins to a further entry gate that will dictate the final location of the protein. Sorting upon 5 different routes is decided by mitochondrial targeting sequences (MTS). Ranging from 15-50 aa, these sequences are N-terminally attached to the proteins and share the structural features of being positively charged amphipathic alpha helices, helping them to interact with the different components of TOM.[25]

Proteins destined for the OMM that possess a transmembrane beta-barrel domain are redirected through the sorting and assembly machinery (SAM) complex. These beta-barrel proteins play essential roles in transporting metabolites and other proteins across the OMM.[25,28] Alpha-helical proteins are the other OMM constituents that are redirected to this membrane via the mitochondrial import machinery (MIM). Some of these proteins may pass through the

TOM complex, while others can directly insert themselves into the OMM without relying on TOM or MIM, and the precise mechanisms of their insertion are still not fully understood.[25,26,28]

Going a layer deeper, proteins destinated to the IMS bear an IMS precursor that will help their redirection after TOM processing to the intermembrane space import and assembly (MIA). These proteins often contain cysteine residues, as MIA interacts with them through disulfide bonds, facilitating the removal of electrons via oxidation. These electrons are then transported to the respiratory chain via cytochrome c.[28,29]

Proteins destined for the IMM and matrix follow three distinct routes. Carrier proteins in the IMS are guided by small translocase of the inner membrane (TIM) proteins through the intermembrane space to the carrier translocase (TIM22 complex), which inserts these precursors into the IMM.[26,28,30] Other IMM proteins are inserted either by the oxidative assembly complex (OXA) or by TIM23. OXA can insert in the IMM matrix encoded proteins or nuclear encoded proteins depending on their origin.[28] In contrast TIM23 can mediate the insertion into the IMM or entry into the matrix depending on the MTS of the protein. In collaboration with OXA it can insert in the IMM carrier proteins that are further folded and structured by OXA.[28] Proteins bearing a matrix-targeted MTS are processed by the presequence translocase-associated motor (PAM) after entry into the matrix. PAM relies on ATP consumption to complete the translocation of these proteins into the matrix.[28] Once inside the matrix, the MTS is removed by mitochondrial processing peptidases (MPP), allowing the proteins to fold and function in their final destination.

Interestingly, MTS have been utilized for targeted delivery of therapeutics to mitochondria, presenting an attractive option due to their specific targeting capacity.[31] However, as standalone MTS often lack the ability to efficiently cross cellular membranes, customization is typically required to enhance their cellular uptake and delivery.

2. Cancer

Cancer is a disease resulting from the uncontrolled growth of normal cells lacking effective regulatory mechanisms. In 2020, it accounted for 19.3 million new cases and 10 million deaths worldwide making it a leading cause of death in current world.[32] Furthermore, those numbers are expected to raise to 28.4 million cases in 2040, hence, it is futile to mention how important the need for cancer treatment is in the hope to expand Human lifespan.

2.1. Available cancer treatments

The treatment of cancer is a complex process due to the diverse forms it can take, affecting various tissues and organs. Different therapeutic approaches are available to tackle cancer, each tailored to specific cases. These treatments include surgical removal of the tumor, radiation therapy, chemotherapy, immunotherapy, and hormone therapy. However, it is important to note that each treatment option has its advantages and drawbacks

Surgical removal of the tumor is often employed, but it is crucial to follow up with additional treatments since leaving even a single cancer cell can lead to tumor regrowth. Radiation therapy utilizes high doses of radiation to target and eliminate cancerous cells. However, it may not be suitable for advanced cancers or sensitive locations.

Chemotherapy involves the administration of anti-cancer drugs designed to kill tumor cells. This treatment can be targeted to cancer cells, enhancing drug efficiency and reducing side effects on healthy cells. Despite its effectiveness, chemotherapy can still result in side effects for patients due to the inability to exclusively target cancerous cells.

Immunotherapy focuses on enhancing the capacity of the immune system to fight against cancer. This approach aims to harness the body's immune response to specifically target cancer cells. Hormone therapy, on the other hand, aims to alter hormone levels, which are essential for certain types of cancer growth.

While these treatment methods have shown promise, they often come with side effects for patients. Insufficient targeting of cancerous cells can result in treatments affecting healthy cells, leading to undesirable side effects. It is important for healthcare professionals to carefully assess each patient's condition and select the most appropriate treatment strategy while considering potential risks and benefits.[33]

2.2. Cancer hallmarks

Cancer, as described by Hanahan and Weinberg[34,35], is characterized by a set of complementary abilities that support tumor growth and metastatic invasion, termed cancer hallmarks (Fig 4). Gaining insights into the biology of cancer is crucial for a better understanding and improved treatment of this complex disease.
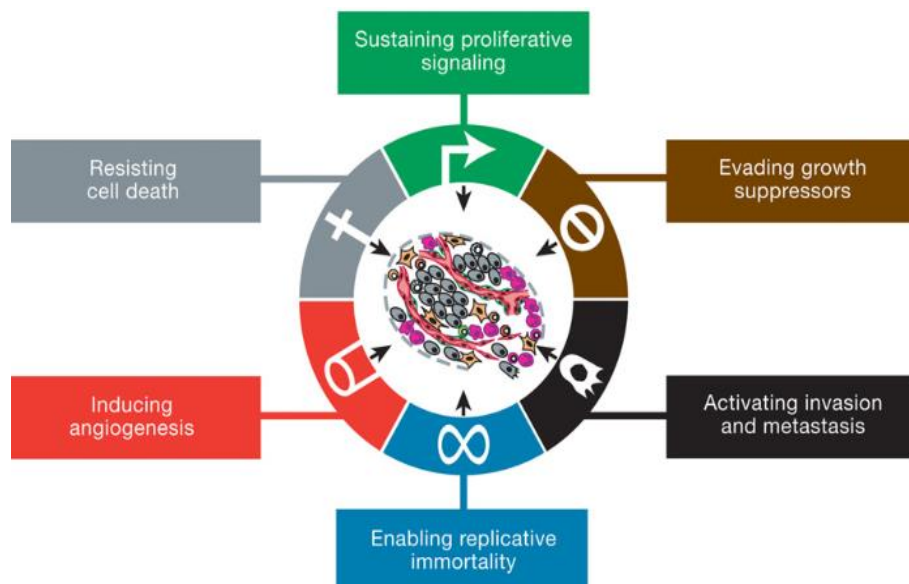
Figure 4. Schematic overview of the cancer hallmarks. Extracted from[35].

One of the hallmark features of cancer is the abnormal and uncontrolled growth of cancerous cells, in contrast to the carefully regulated growth of healthy cells. Cancer cells achieve this by deregulating growth signals, either through the overproduction of growth hormones or by hypersensitizing the associated receptors.[35–37] Furthermore, cancer cells have the ability to alter the signaling of growth suppressors, allowing them to grow into tumors without being inhibited by cell-to-cell contact.[35,38] Additionally, cancer cells acquire replicative immortality by protecting the ends of their chromosomes with telomeres, enabling them to overcome the constraints of limited growth and division cycles.[39,40]

To sustain tumor growth, cancer cells also manipulate angiogenesis, the formation of new blood vessels, and the import of nutrients and oxygen to the tumor.[41] Furthermore, cancer can progress to affect other organs through tumor metastasis, which makes it challenging to treat as it can spread to different locations. [42]

Understanding these fundamental characteristics of cancer provides valuable insights into its mechanisms and helps in the development of targeted treatment strategies. By targeting the specific vulnerabilities and dysregulated processes in cancer cells, researchers and clinicians strive to improve outcomes for patients with this complex disease.

2.3. Mitochondria and cancer

A last point to cancer hallmarks is their ability to escape cellular death, an ability acquired via the close relation of this disease with mitochondria. Regarding cancerous cells as abnormal cells, they should be eliminated as so via apoptosis, but it appears that they have the ability to escape this cell death pathway. Indeed, the proteins from the Bcl-2 family control mitochondrial apoptosis, and as observed in cancerous cell lines pro-apoptotic proteins are down regulated while anti-apoptotic proteins are overexpressed.[43,44] Furthermore, during cancer development and metastasis, cancerous cells undergo high oxidative stress and to protect themselves they rely on increased antioxidant mechanisms via an increased production of NADPH to scavenge ROS.[45,46] Through those mechanisms, cancerous cells render themselves almost immune to apoptosis death pathway and can maintain their growth and invasion.

Considering the high energy needs of cancerous cells, it was interestingly observed that they tend to maintain OXPHOS while promoting glycolysis to produce ATP termed the Warburg effect.[47] Originally thought to produce more ATP the Warburg effect has since been challenged to reveal that promoting glycolysis is used by cancerous cells to utilize the intermediates in other anabolic reactions and to sustain growth and proliferation.[47]

Finally, due its exposure and sensibility to mutations mtDNA has been found to be highly mutated favoring cancer progression and that those mutations are maintained to sustain growth and development of cancer cells.[48]

Mitochondria hacking by cancer has a multi-level influence on the fate of cancer. The reprogramming of this key organelle is of high importance for the disease. Influencing cancer

development and progression mitochondria role in cancer represent undoubtedly a target to tackle the disease.

3. Targeting mitochondria as an anticancer strategy

As discussed in the previous chapters mitochondria are organelles that play a crucial role in cellular metabolism and energy production. They also play a key role in cell death and are implicated in the development and progression of cancer. Therefore, targeting mitochondria in cancerous cells has been considered a potential strategy for cancer therapy. One of the most promising ways to address mitochondria is through targeted drug delivery. The targeting of mitochondria for drug delivery in cancerous cells has been an active area of research in recent years.[47,49,50]

This chapter will provide an overview of the various strategies that have been proposed for targeted drug delivery to mitochondria in cancerous cells. The different types of carriers, targeting moieties, and drug delivery systems that have been used to achieve this goal will be discussed. It will also present examples of recent research in each area and highlight the potential and limitations of each strategy. The goal is to provide a comprehensive understanding of the current state of the field and to identify areas that require further research to improve the efficacy of targeted drug delivery to mitochondria in cancerous cells.

3.1. Delocalized lipophilic cations

Due to the negative membrane potential across their IMM, mitochondria pose a challenge for common strategies aiming to target and access them. The negative charge across the membrane acts as a barrier that limits the entry of molecules and therapeutics into the mitochondria. This feature makes it difficult to specifically deliver drugs or other compounds to this organelle. But this characteristic also renders them sensible to targeting via cationic molecules, which can easily accumulate at its membrane for internalization. This is the strategy behind delocalized lipophilic cations (DLC), small cationic molecules that can interact with OMM through electrostatic interactions due to their cationic nature, before crossing the IMM thanks to their lipophilic character.[51] Moreover, with their small size and cationic nature they can also easily diffuse through cellular membrane allowing them to access the cytosol and thus mitochondria through membrane accumulation. Main representatives of this category are Triphenylphosphonium (TPP), Dequalinium (DQA), and Rhodamine-123.

DLC targeting ability rely on the negative membrane potential of IMM as explained previously, mitochondria possess 2 membranes exhibiting an outer membrane with large pores that let big molecules diffuse through, and the inner leaflet is positively charged due to the proton gradient from the ETC. Hence, positively charged cations would naturally accumulate inside the matrix of mitochondria. Additionally, to reach inside mitochondria compounds must first overcome the cellular membrane, which is here again positively charged with an inner cytosol more negatively charged allowing passage to those small molecules. Even if the charges are not strong DLC can slowly accumulate inside the cells and then localize to mitochondrial matrix.[51,52]

DLC present some advantages, they are easily synthesizable and conjugable, only few units are required to improve the efficacy of a cargo, they are stable in biological media, low reactivity towards other cell components, no light absorption in the visible or near infrared region and a good combination of lipophilic and hydrophilic properties. Therefore, DLC have been used as targeting moieties to enhance drug efficacy, e.g. the conjugation of chlorambucil to TPP, a DNA alkylating agent, resulted in a 12-fold reduced IC_{50} compared to the drug alone.[53] DQA as standalone does already exhibit toxicity towards cancerous cells but it can also be used to form vesicles, named DQAsomes, to encapsulate Doxorubicin resulting in increased activity for the drug.[54,55]

However, it should be noted that TPP can act as an uncoupler in mitochondria, leading to proton leakage and potential toxicity at concentrations exceeding 10 µM.[56] Furthermore, studies have shown that intravenous injection of TPP results in its rapid clearance from the bloodstream within 5 minutes, with accumulation observed in the kidneys and liver.[57] These factors highlight the common limitation of small molecules, such as TPP, which require high concentrations to be effective but may also increase the risk of off-site localization and side effects. Thus, careful consideration of dosage and optimization is necessary to balance the therapeutic benefits and potential drawbacks associated with TPP.[56,57] Despite these challenges, ongoing research aims to develop strategies and modifications to enhance the targeting efficiency, specificity, and safety of TPP-based approaches for mitochondrial delivery.

3.2. Nanocarriers

On a different scale from DLC, nanocarriers (NC) are an option that is also extensively researched on for mitochondria delivery. Nanocarriers could be defined as large scale objects that encapsulate a drug payload, positively charged NC can interact with cellular membrane and internalize via endocytosis to release their content in the cytosol for them to reach mitochondria.[58] Moreover, owing to their bigger size and charges NC can benefit from the Enhanced permeability and retention (EPR) effect to specifically accumulate at the surface of tumors.[59] Finally, NC can also protect their payload from degradation during transport in vivo.[60]

A first examples of NC, the DQAsomes, was presented in the previous part. A classic method for encapsulation relies on the use of liposomes, such objects are constituted of phospholipids assembled in sphere creating a pocket that can incorporate hydrophilic or hydrophobic drugs.[61] Such strategy was used to encapsulate two anticancer drugs to treat MCF-7 cells targeting the opening of MOMP and triggering of apoptosis.[62]

Another strategy to encapsulate drugs relies on polymeric particles. Using polymeric particles offer the advantage of a time and distribution controlled drug delivery as well as a better protection of their payload.[63] A combination of Poly(lactic-co-glycolic acid), Polyethylene glycol and TPP was used to prepare a mitochondria targeting vesicle incorporating anticancer drugs as well as drugs for treating other diseases successfully.[64]

Finally, metallic particles can be used as NC, resulting in small sized particles with unique properties associated with their metal core. Indeed, due to their photophysical properties metal complexes have been used in phototherapy as photosensitizer and this strategy has

been applied to mitochondrial targeting. In association with polymers, peptides or protein decorated metal complexes can be used to sensibilize their mitochondrial target to irradiation which in turn produce ROS and trigger cell death.[65–67] In another example Iridium complex was used as a coating to gold nanorods to constitute a mitochondria targeted NC applied to photothermal therapy with an interesting hypoxia responsive luminescence achieving a dual function.[68]

Accounting advantages of NC it is also to consider the drawbacks of those carriers which are difficult to synthesize, come at a higher cost, can be stopped by biological barriers. Moreover, NC usually being internalized by endocytosis they can suffer from endosomal entrapment not being released in the cytosol. Finally, regarding metal complexes their usage can be limited due to their poor solubility and tendency to aggregate in water.

3.3. Peptides & cell penetrating peptides

Peptides are a class of biomolecules that are composed of small chains, up to 50 amino acids (aa), assembled through amide bond between the carboxylic group of an aa and the amine of another aa. Peptides can act as hormones, neurotransmitters, antibiotics, or enzymes, among other things having implications in many physiological processes.

Cell penetrating peptides (CPP) are a category of peptides which possess unique properties. With a length ranging from 5 to 30 aa, those sequences usually bear a strong positive charge facilitating interaction with negatively charged phospholipids constituting cellular membranes, and to penetrate cells.[69] Interaction with cellular membrane would result in crossing this biological barrier in different ways depending on the sequence. Moreover, CPPs offer the advantage of penetrating cells in a noninvasive manner without affecting the integrity of the membrane being safe for the cells.[70] Historically the first CPP to be developed was TAT as it was observed that this viral protein could rapidly translocate over cellular membrane and accumulate in cells.[71]

3.3.1. Cell penetrating peptides internalization

The mode of penetration for CPPs cannot be solely predicted based on the sequence and can be categorized into two main modes: direct penetration and endocytosis.[70,72,73]

In direct penetration, several models exist for CPP internalization. In the inverted micelles model, CPP accumulation at the membrane and interaction with negatively charged phospholipids lead to the formation of a micelle that encapsulates and internalizes the CPPs. Pore formation can occur through the barrel-stave model, where CPPs adopt an amphipathic alpha-helix upon insertion in the bilayer, creating a barrel-shaped pore, or through the toroidal model, where the CPP interacts with polar groups of the phospholipids to form a pore. The

carpet model involves CPP interaction with the membrane, disrupting it and causing its reorganization, leading to CPP internalization.[70,72,73]
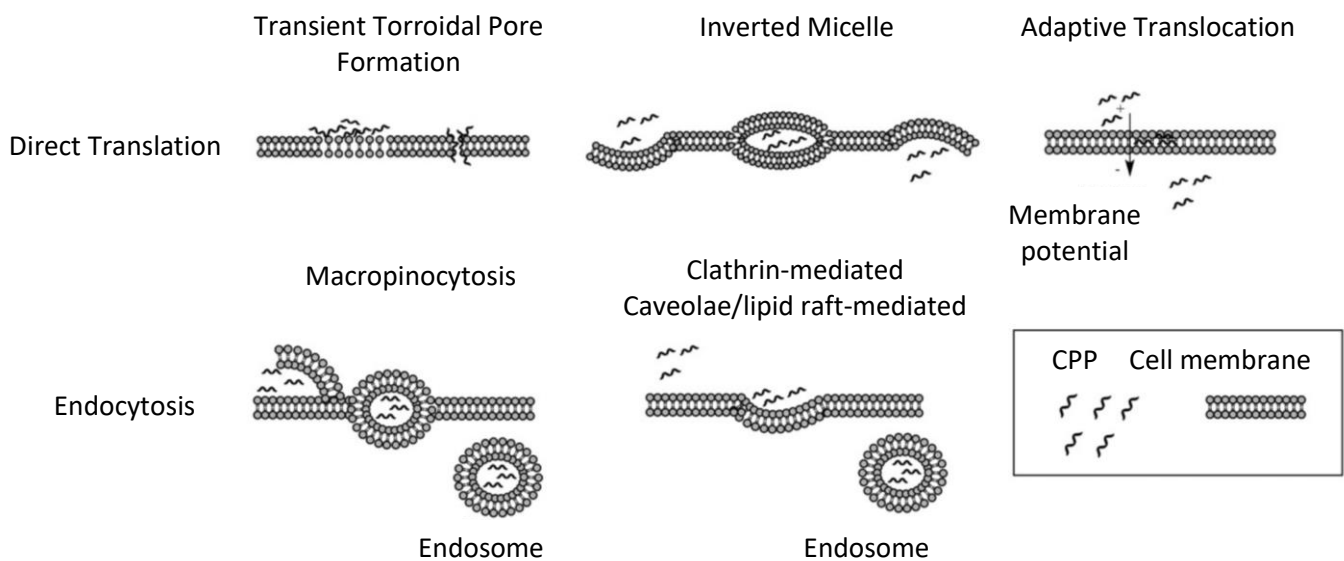
Figure 5. Schematic overview of the different cell penetration models. Modified from[81].

Endocytosis, an energy-dependent process, involves the internalization of CPPs via membrane modifications. Upon interaction with cellular membranes, CPPs are internalized through endosomal vesicles, from which they must escape once internalized. Endocytotic pathways vary based on the size of the object to be internalized. Macropinocytosis is associated with the uptake of larger particles and is often observed with arginine-rich and cationic CPP sequences, such as TAT.[74–76] Pinocytosis, on the other hand, is dedicated to the uptake of smaller objects, fluids, and solutes.[70] It can be categorized into three models: clathrin-mediated endocytosis, caveolae-mediated endocytosis, or caveolae/clathrin-independent endocytosis. Clathrin-mediated endocytosis involves the interaction between CPPs and cell surface receptors, where clathrin structures itself around the CPP, invaginating the membrane for internalization. Arginine-rich anionic CPPs are often associated with this pathway.[70,77] Caveolae-mediated endocytosis, associated with proline-rich amphipathic sequences, is characterized by the formation of flask-shaped caveosomes.[70,78] Caveolae/clathrin-independent endocytosis is less understood and observed, occurring in parallel with caveolae-mediated endocytosis but in fewer cases.[79,80]

Regardless of the specific endocytotic pathway taken for CPP cell entry, successful internalization relies on endosomes and their subsequent escape. Endosomes are the main obstacles in CPP internalization as those vesicles can trap CPP. If they don't find an escape route the transition from early to late endosomes can degrade the CPPs through acidic pH or hydrolases, additionally to inhibiting the display of their biological activity due to their entrapment.[82]

3.3.2.Cell penetrating peptides structure

Among the diversity of CPPs sequences it appears that some common features can be highlighted for favoring the cell penetrating ability of those peptides. Overall CPPs are usually positively charged, a requirement to interact with the negatively charged cellular membrane constituents.[83,84] This interaction with membranes is mainly driven by the presence of arginine and lysine residues in the sequence. Indeed, due to their guanidinium group they can offer two hydrogen donors to create bidentate hydrogen bonds with phosphate, carboxylate and sulfate groups of membranes.[84] Moreover the presence of multiple arginines can even result in the bending of the membrane due to this interaction diffused through different guanidinium groups. Regarding lysines, their interaction with membranes is solely due to the presence of a primary amine on the side chain, positively charged at physiological pH, that is an excellent H donor but can only participate in a single H bonding.[84]

Additionally, to the positive charges and interaction with membranes another important characteristic is the secondary structure adopted by the CPP. Even if most of the CPP adopt an alpha helix or a beta strand or beta turn structure upon interacting with membranes, it cannot be concluded that such structure is required for cell penetration.[84] The criteria that prevails regarding the structure appears to be its malleability, as CPP have to interact with different membrane constituents in changing parameters their adaptability and conformational malleability seems to be the defining parameters when regarding secondary structure.[85] Supporting this idea, it was also observed that CPP can be unstructured in aqueous solution but can structure themselves upon interaction with lipids, in specific buffers, as if they can adapt to their interacting partners. [86,87]

3.3.3.Cell penetrating peptides in Neundorf working group

Neundorf working group took interest in CPP development and designed an original sequence from part of a cationic antimicrobial peptide.[88] Antimicrobial peptides possess the ability to permeabilize the membranes of microorganisms and hence have been applied as CPP.[89] The C-terminal region of cathelicidin was used to design the CPP sC18. This new CPP exhibits sequence similarity with TAT and have been applied for drug delivery, performing well in cancerous cells and bacteria.[90–93]

With the aim of further improving the sequence, an Ala scan was performed on sC18, to discover that substitution of Glu[15] yielded sC18dE, a CPP with great cellular internalization and good viability resulting from the removal of the negative charge in the cationic tail of the sequence.[94] However, this increased uptake was recently observed to be mitigated as most of sC18dE peptides were entrapped in endosomes without the ability to escape.[95] In an another attempt to exploit the potential of sC18 the sequence was modified by removal of the last 4 aa of the sequence resulting in sC18*, a shorter CPP which proved to be efficient as a cargo to internalize peptide sequences.[95–97]

3.3.4. Cell penetrating peptides as mitochondria targeted drug delivery systems

Owing to their ability to safely cross cellular membranes CPPs have been widely used for the delivery of drugs in the form of peptide-drug conjugates (PDC).[81,98–100] The biological barrier of cellular membrane is usually a limiting factor in drug design, especially for small molecules which can lack the ability to cross it and therefore highly benefit of the use of carriers for their delivery. A commonly used anticancer drug, Doxorubicin, is for example highly effective but cancerous cells have developed a resistance to it and it also affect healthy cells. Conjugation to a CPP, Poly-L-Arginine, was able to increase internalization and cytotoxicity of Doxorubicin while not inducing any change in the toxicity towards healthy cells.[101]

The example of the SS (Szeto-Schiller) peptide opened the way to mitochondria penetrating peptides (mtPP). This antioxidant peptide can protect mitochondria from oxidative stress by scavenging ROS through the Tyrosine in its sequence.[102] Interestingly, the SS peptides are tetrapeptides with alternating basic and aromatic residues.[103] Similarly, other repetitive sequences emerged as mitochondria targeting with effect on mitochondria.[104,105]

Inspired by this strategy Dr. Klimpel, in Neundorf group, aimed to develop a mtPP relying on the properties of sC18.[106] Relying on the mitochondria targeting effect of MTS and acknowledging their inability to cross cellular membranes it was hypothesized that through the conjugation of a MTS to sC18 the resulting sequence would possess both properties creating an mtPP. Through the evaluation with different domains of mitochondrial proteins, aldehyde dehydrogenase 5 (ALD5) was finally chosen as the MTS. The resulting mtPP was obtained through N-terminal conjugation of ALD5 to sC18 for mimicking physiological conditions. When evaluating this peptide for cellular uptake and localization it performed well and successfully reached the matrix of mitochondria in Hela cells. Moreover, this mtPP was modified to incorporate a cytotoxic payload, chlorambucil, for anticancer action via mitochondria delivery, which resulted in an efficient drug delivery system but with a limitation due to the payload instability.

3.3.5. Cell penetrating peptides limitations

Due to their peptidic nature, CPPs are subject to proteases and plasma degradation, limiting their half life time it does affect the efficacy of their treatment.[107] Since a reduced lifetime inside the cell would result in less exposure time of the drug long lasting treatments are usually difficult to achieve through PDC and require repeated administration and fluctuating their concentration in blood.[108]

For the CPPs internalized via endocytosis, a common challenge to overcome is to escape the endosome once internalized. When trapped in the endosomes, CPPs may lack the ability to escape, resulting in reduced activity as they are not released into the cytosol.[109,110]

It is important to consider the lack of specificity of CPPs as standalone, as they cannot specifically address cancerous cells and require further customization to do so. In some cases,

certain CPPs have been observed to be limited in penetrating specific cell lines, possibly due to interactions with specific membrane components.[111,112]

Another limitation to their therapeutic application is their low oral bioavailability requiring them to be administrated via direct injection, a method which is invasive and uncomfortable for patients thus limiting their application.[107,113]

Therefore, when designing PDC, these limitations should be taken into account and addressed through modifications to the CPP sequence or decoration with cancer-targeting moieties, among other strategies.[112]

4. Aims

As presented in this introduction targeting mitochondria seems an appealing strategy in treating diseases such as cancer. However, reaching mitochondria can be a difficult challenge due to its location, metabolism and structural characteristics. In a previous project a mitochondria targeting peptide (MTP) was designed upon conjugation of a MTS to sC18, a CPP developed in the lab.[106] Design of such peptide was obtained through evaluation of different modified MTS with the final choice being ALD5, a sequence derived from aldehyde dehydrogenase 5. As stated previously, the MTS alone lacked the ability to translocate inside the cell and therefore it was coupled to sC18.

In this project, new and more efficient MTPs should be designed containing modifications in the sequence of sC18 and their biological activity should be evaluated. Moreover, the conjugation of a new payload, namely Jasmonic acid (JA), and variation in its coupling position should be investigated. Jasmonic acid is a plant stress hormone, that was described to induce apoptosis through mitochondria activation.[114–116] The drug alone cannot cross efficiently biological membranes resulting in poor activity requiring high concentrations to be efficient.[115–122] Therefore, targeting of JA to mitochondria via MTP should be used to restore apoptotic potential of cancerous mitochondria.

5. Results and discussion
5.1. Peptide synthesis

In previous work of the lab, ALD5sC18 was described as an efficient MTP targeting the matrix of mitochondria. To further explore the potential of this mitochondria targeting conjugate and to improve the cellular uptake efficiency, variants of sC18 should be introduced. (Fig 6)
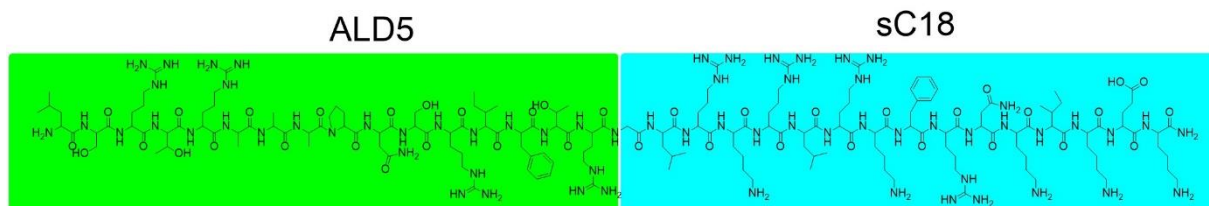
LeuSerArgThrArgAlaAlaAlaProAsnSerArgIlePheThrArgGlyLeuArgLysArgLeuArgLysPheArgAsnLysIleLysGlu Lys

Figure 6. Structure of mCPP1 peptide.

The additional sequences synthesized were built upon using sC18dE and sC18*, as they have proven to be interesting alternatives to sC18. For the aim of simplifying the reading and discussion those MTPs are named mCPPs followed by a number relative to the CPP sequence (1-sC18, 2-sC18dE, 3-sC18*) and the letter refers to the coupling position, that I will discuss later on. The following Table 1 gathers all the synthesized peptide sequences:

Table 1. List of synthesized peptides. All were obtained in purity > 95%.

Name	Sequence	Mw theo (g/mol)	Mw exp (g/mol)
ALD5	LSRTRAAAPNSRIFTR	1816,08	1816,4
CPP1	GLRKRLRKFRNKIKEK	2069,55	2070,33
CPP1aJA	GLRKRLRKFRNKIKEK(JA)	2261,85	2263,19
CPP2	GLRKRLRKFRNKIKK	1940,44	1942,13
CPP2aJA	GLRKRLRKFRNKIKK(JA)	2132,70	2133,08
mCPP1	LSRTRAAAPNSRIFTRGLRKRLRKFRNKIKEK	3868,60	3870,02
mCPP2	LSRTRAAAPNSRIFTRGLRKRLRKFRNKIKK	3739,48	3740,84
mCPP3	LSRTRAAAPNSRIFTRGLRKRLRKFRNK	3369,98	3371,40
mCPP1aCF	LSRTRAAAPNSRIFTRGLRKRLRKFRNKIKEK(CF)	4226,92	4228,74
mCPP2aCF	LSRTRAAAPNSRIFTRGLRKRLRKFRNKIKK(CF)	4097,80	4099,48
mCPP2cCF	LSRTRAAAPNSRIFTRGLRKRLRK(CF)FRNKIKK	4097,80	4098,92
mCPP3aCF	LSRTRAAAPNSRIFTRGLRKRLRKFRNK(CF)	3728,35	3729,6
mCPP1aJA	LSRTRAAAPNSRIFTRGLRKRLRKFRNKIKEK(JA)	4060,87	4062,0
mCPP1bJA	LSRTRAAAPNSRIFTRK(JA)GLRKRLRKFRNKIKEK	4189,05	4190,22
mCPP2aJA	LSRTRAAAPNSRIFTRGLRKRLRKFRNKIKK(JA)	3931,75	3933,12
mCPP2bJA	LSRTRAAAPNSRIFTRK(JA)GLRKRLRKFRNKIKK	4059,93	4061,22
mCPP2cJA	LSRTRAAAPNSRIFTRGLRKRLRK(JA)FRNKIKK	3931,75	3932,95
mCPP3aJA	LSRTRAAAPNSRIFTRGLRKRLRK(JA)FRNK	3562,30	3563,21
mCPP3cJA	LSRTRAAAPNSRIFTRGLRKRLRK(JA)FRNK	3562,30	3563,35

The MTS, CPPs and mCPPs were first synthesized as they were required as controls in biological assay as well as for structural analysis. Their synthesis was carried on solid phase via robot synthesis using the classic Fmoc/tBu strategy. In this strategy amino acids (aa) have their amine moiety protected with a fluorenylmethoxycarbonyl protecting group (Fmoc), the side chains are usually protected with tert-butyl (tBu) and their carboxylic moiety is free. This protection system is highly essential to keep control on the elongation of the peptide, as if both the amine and carboxylic functions of the amino acids were unprotected, they could react freely with each other yielding uncontrolled additions. To achieve peptide elongation, the amino acids are added in a sequential manner and coupled through the formation of an amide bond. This bond is formed by the reaction between the amine group of one amino acid and the carboxylic group of another amino acid, resulting in the loss of a water molecule. This dehydration reaction leads to the formation of a stable peptide bond, which connects the two amino acids together. To do so, the amine needs to be first deprotected from its Fmoc

group, being base labile it is removed using piperidine. Once the Fmoc group is removed the aa to be coupled is added with activation agents which will turn the carboxylic function into a reactive one that will add up on the free amine from the previous aa. Following this method peptides can be elongated directly on a resin.

In my case the resin chosen was Rinkamide, as upon cleavage it would leave out a carbox-amide on the C-terminal side. A peptide bearing a carboxamide on its C-terminal side would have its usual negative charge of the carboxylic moiety neutralized thus increasing the positive charge of the sequence, which is important for membrane interaction and hence for cell penetration.[70,123] Therefore, after peptide elongation on resin the peptide was cleaved off the resin manually using a TFA cocktail, such strong acidic mixture will also deprotect the side chain protection as tBu is acid labile. Finally, the peptides were precipitated in diethyl ether to remove most of the organic impurities coming from the synthesis. The final step of this synthesis was the purification.
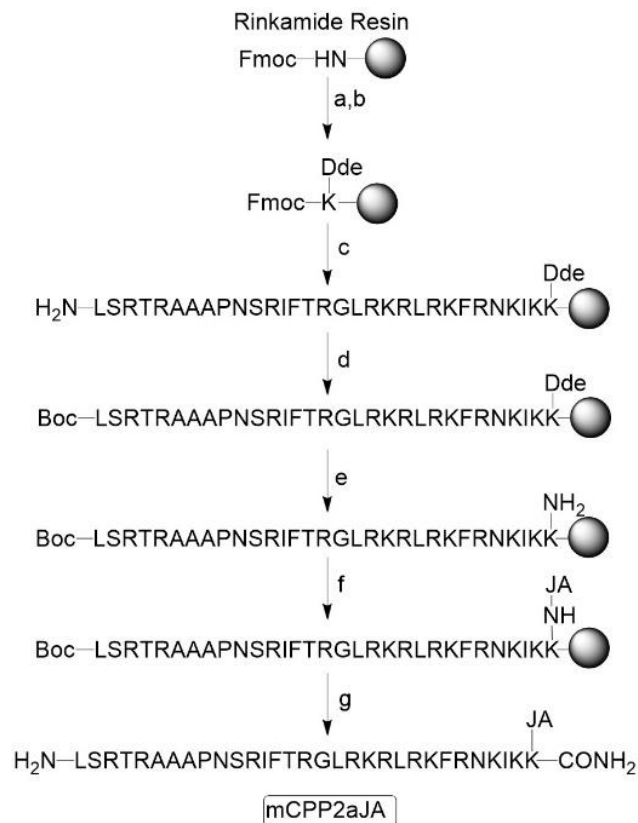
Figure 7. Overview of the synthesis of peptide conjugates. **a**: 30% piperidine in DMF, 2 x 30 min, rt; **b**: 3 eq Fmoc-Lys(Dde)-OH, 3 eq HATU, 3 eq DIPEA, 2h, rt; 3 eq Fmoc-Lys(Dde)-OH, 3 eq Oxyma, 3 eq DIC, o/n, rt; in DMF, 3 to 4 steps alternating; **c**: robot elongation; **d**: 10 eq Boc_2O, 1 eq DIPEA, in DMF, 2h, rt; **e**: 2% hydrazine in DMF, 8 x 10min; **f**: 3 eq Jasmonic acid, 3 eq HATU, 3 eq DIPEA, 2h, rt; 3 eq Jasmonic acid, 3 eq Oxyma, 3 eq DIC, o/n, rt; in DMF, 3 to 4 steps alternating; **g**: trifluoroacetic acid/triiso-propylsilane/water (95/2.5/2.5, v/v/v), 3 h, rt.

Regarding the PDC and fluorophore conjugates, the starting point was the previous design with the sequence mCPP1 having the drug payload attached via the side chain of the C-terminal Lysine. This design was kept with the Jasmonic acid drug and applied to the new mCPPs yielding the "a" generation of PDCs and fluorophore labelled mCPPs. In an attempt to better understand the processing of the internalized mCPPs I designed the "b" generation of PDC with the introduction of a lysine to bear the payload between the MTS and the CPP. Indeed, once internalized mitochondria targeted natural peptides and proteins are cleaved off their MTS via a system of proteases internal to the matrix of mitochondria. Therefore, I hypothesized that once the mCPP would reach the mitochondria the CPP could be detached from the MTS and if the drug payload is attached to the CPP its potency could be diminished. While with an attachment point on the MTS, without affecting the original sequence, the resulting MTS-JA from this hypothetical cleavage site could stay in the surrounding of mitochondria and keep its activity. Finally, a third generation of "c" conjugates was also designed in order to tackle potential protease degradation. For those conjugates the attachment point chosen was Lys[24] as this aa is still on the CPP part and present in all 3 different mCPPs.

The synthesis of conjugates presented additional challenges compared to a simple robot synthesis due to the need to attach a payload to the side chain of the peptides. This required the implementation of orthogonal protection for the attachment site. Orthogonal protection refers to the use of protecting groups that are not cleaved during the standard deprotection and coupling steps, but can be selectively removed under specific conditions without affecting the other protecting groups.

In the Fmoc/tBu strategy, as mentioned earlier, the Fmoc group is labile under basic conditions, while the tBu group is labile under acidic conditions. These two protecting groups are orthogonal to each other within this system. To introduce an additional orthogonal protection, I chose to use 2-acetyldimenone (Dde) as the amine protection. The Dde group is not labile under acidic conditions but can be removed under stronger basic conditions than those used for Fmoc deprotection. This means that the standard piperidine solution used for Fmoc deprotection will not remove the Dde group, while a hydrazine solution used for Dde deprotection will remove the Fmoc group.

By incorporating orthogonal protection, I could selectively protect and deprotect specific functional groups at different stages of the synthesis, allowing for the attachment of the payload to the desired site on the peptide side chain. This strategy ensured that the payload remained intact during the peptide synthesis process and could be selectively released at a later stage under specific conditions.

Considering the price of Dde protected Lysine and to ensure its coupling the addition of this special aa had to be performed manually so the effective coupling could be monitored via Kaiser test. The Kaiser test is a ninhydrin-based on beads test. Briefly some resin beads, with the elongated peptide, are taken and the kaiser test solution is added. After a brief heating at 95°C depending on the presence of a free amine or not the beads and solution color turn blue or remain yellow/orange. This simple color change is a trustworthy indicator of effective coupling or deprotection step.

Regardless of the payload to couple or the mCPP sequence their synthesis followed the same procedure, with the only variation being on the coupling position. For the "a" conjugates the coupling position being on the last position, which is the first to be attached on the resin, the rinkamide resin had to be loaded with a Dde protected lysine. After this first step, the peptide was elongated with the robot synthesizer. For the "b" and "c" conjugates the first part of the peptide was elongated by the robot before adding the Dde protected Lysine manually, after successful coupling assessed by a sample cleavage, the rest of the peptide was elongated with robot synthesis. After robot elongation the same procedure was followed regardless of coupling position. The robot synthesis final step being a Fmoc deprotection the obtained sequence has a free N-terminal amine which was protected with a group orthogonal to Dde; Boc which is basic stable and acid labile. After monitoring this coupling by kaiser test the Dde group was removed and finally the payload attached and assessed by a sample cleavage. It is worth to notice that the coupling of the carboxyfluorescein (CF) required more coupling steps, especially for the "a" conjugates probably due to the proximity with the polymeric resin beads which may hinder the coupling position. Finally, the peptide conjugates were obtained after full cleavage following the same method as for the unlabeled/unmodified peptides.

After precipitation in ether, the crude peptides were purified using HPLC in acetonitrile/water solvent system. During HPLC purification the appearance of a side product with a difference in mass of +72 Da and a close retention time was observed. This side product resulted probably from a partially incomplete deprotection of Pbf, the protecting group of Arginines. In an attempt to prevent the formation of this product the TFA cleavage time was elongated but it only slightly decreased its presence. The final solution I had to apply was to pursue a second purification over HPLC with an elongated increasing gradient of acetonitrile, to separate the eluting peaks when it was required.

5.2. Peptide structure characterization by Circular Dichroism Spectroscopy

As mentioned in the introduction the secondary structure that a peptide adopts will have a strong impact on its cell penetrating potency. Generally, an alpha-helical structure is beneficial for the lipid-peptide interaction. Moreover, the amphipathic helix with a charge distribution alongside the different faces of the peptide might further promote mitochondria interaction.[85,124]

Therefore, all mCPPs and PDC were characterized concerning their structure using circular dichroism (CD) spectroscopy. CD is a phenomenon resulting from the difference in absorption of polarized light between chiral molecules. Indeed, due to their structural configuration chiral molecules do not absorb left and right polarized light to the same extent resulting in different spectra. In the case of peptides and proteins this technique is used to get information on their secondary structure as it has been observed that the different peptides structures exhibit a characteristic spectrum. In the case of alpha helices, a negative band at 208 nm and a positive band at 222 nm are expected, while for a beta sheet structure a positive band will be present at 196 nm and a negative one at 216 nm.

Considering the water-soluble character of the peptides aqueous buffer was chosen as primary solvent for this measurement. In an attempt to promote structuration of the peptides a co-solvent was also used, namely trifluoroethanol (TFE). TFE is used in order to promote structuration of peptides and proteins, in an aqueous solvent. It acts by disrupting H bonding between water molecules and the polar groups present on the aa side chains. Disrupting those interactions leads to increased intra-molecular interactions thus yielding more ordered and structured peptides.[125,126] Therefore, the use of TFE must come with special attention to interpreting results as its concentration can yield biased data. To overrule this point, I decided to evaluate the peptides with an increasing concentration of TFE, up to 50% as the results cannot be interpreted above this point.
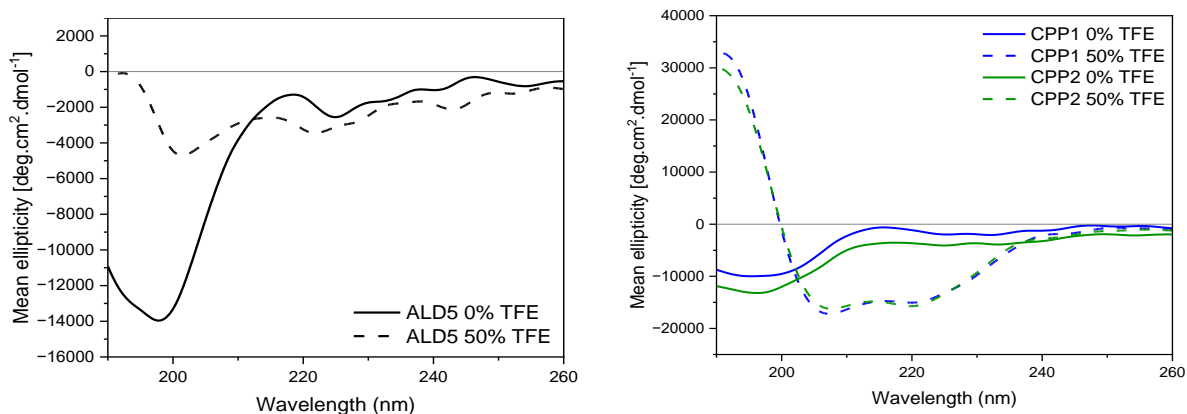
Figure 8. CD spectra of ALD5 (right), CPP1 and CPP2 (left). Spectra were recorded at 20 µM peptide concentration in 10 mM phosphate buffer, pH 7.0, with or without addition of TFE. R-value 50% TFE CPP1: 0.85, CPP2: 0.92.

When investigating ALD5 alone, even with the addition of TFE, no structuration can be observed (Fig 8), the spectrum presents a wide absorption band before 220 nm which is characteristic of a random coil. In such case the peptide is folded onto itself without adopting a specific structure. A similar behavior can be observed for CPP1 and CPP2 when in water alone. But upon addition of TFE their spectra change to present two strong absorption peaks at 208 and 222 nm which is the characteristic signature of an alpha-helix secondary structure (Fig 8). To evaluate the alpha helix character of a peptide, sequence the R-value is a helpful
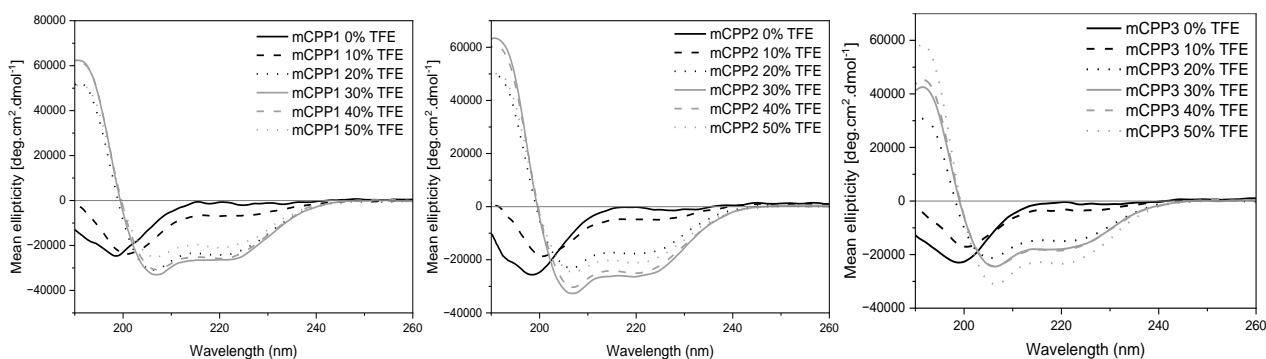
Figure 9. CD spectra of mCPP1 (left), mCPP2 (middle), mCPP3 (right). Spectra were recorded at 20 µM peptide concentration in 10 mM phosphate buffer, pH 7.0, with or without addition of TFE. R-value 50% TFE mCPP1: 0.84, mCPP2: 0.93, mCPP3: 0.75.

index that is obtained as follow: R-value = $[\theta]_{222\,nm}/[\theta]_{208\,nm}$, and for the CPPs with addition of TFE their value is in agreement with recent datas.[95,127]

Upon coupling of ALD5 to the different CPPs resulting in the mCPPs sequence the profile of those peptides was changed (Fig 9). Indeed, with increasing TFE, a clear alpha helix character appeared, highlighting the benefit of this coupling for ALD5 which can structure itself under the influence of the CPPs. As mentioned, TFE has to be used cautiously and therefore I pursued an experiment where I recorded the spectra of the peptides under the influence of increasing TEF concentrations up to 50% in water. Thereafter when calculating the R-value for each concentration it appears that with a minimum concentration of 30% the alpha helix structure is adopted by all three mCPPs. Moreover, some differences were noticed between mCPP1-2 and mCPP3. For the first 2 sequences an R-value of 0,80 was reached with only 20 % of TFE whereas for mCPP3 this concentration had to be increased. Even comparing the R-value at 50% TFE revealed a stronger structuration for mCPP1-2 compared to mCPP3. This result might go back to the fact that mCPP3 is a shorter version of mCPP1 with the deletion of 4 aa which may have been involved in the structuration via stabilizing the structure through H bonding for example. Nevertheless, an alpha helix structure was obtained for all mCPPs in presence of small amount of TFE.
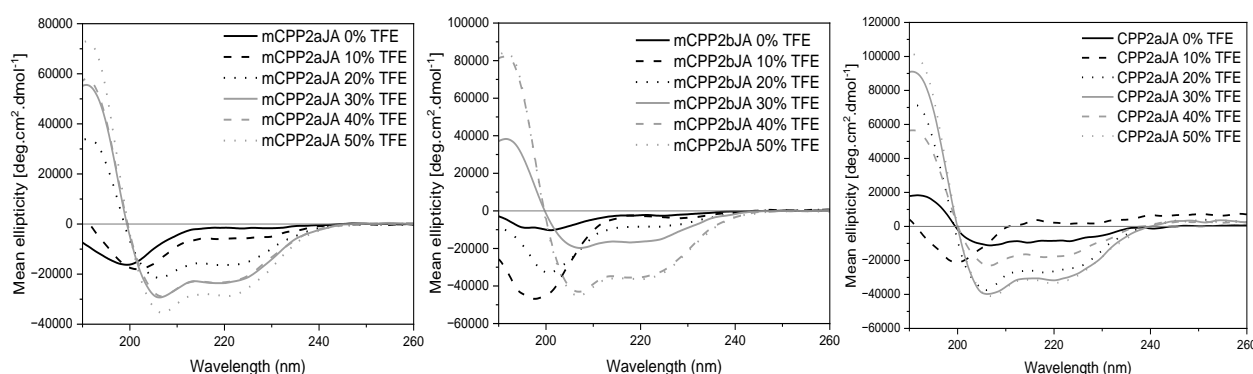
Figure 10. CD spectra of mCPP1 (left), mCPP2 (middle), mCPP3 (right). Spectra were recorded at 20 µM peptide concentration in 10 mM phosphate buffer, pH 7.0, with or without addition of TFE. R-value $_{50\%\,TFE}$ mCPP2aJA: 0.80, mCPP2bJA: 0.84, CPP2aJA: 0.80.

Considering the influence of deleting aa in the sequence on the structuration for the overall peptide it also had to be considered that the coupling of the drug at different positions could also affect the structure. Therefore, the same experiment was pursued with the drug conjugates of version 2. It appeared that the conjugation of JA on the C-terminal lysine did not affect the structuration of mCPP2aJA which exhibited a similar spectrum as mCPP2 (Fig 10). Interestingly the addition of an aa bearing JA, in the case of mCPP2bJA, seemed to have little influence on its structure as the alpha helix was reached but requiring a slight increase in TFE compared to mCPP2. Finally, conjugation of JA to the CPP alone did not perturbate the structure of the peptide. Overall, it can be concluded that neither the deletion nor addition of aa or payload disrupts the structuration into alpha helix of the different mCPPs which is an important trait for the cell penetrative potency of the peptides. (See supplementary for other conjugates spectrum)

As stated in the introduction and above structuration of CPP and also MTS plays an important role for membrane interaction and internalization. Regarding MTS the formation of an amphipathic alpha helix can be necessary for interacting with mitochondrial import system.[124] As for the alpha helix it was observed that the CPP adopts this structure but this also applies to the different mCPPs and drug conjugates. Therefore, the amphipathic character of the mCPPs had to be evaluated. To pursue such evaluation, I had to rely on calculators that can give the organization of the different aa along alpha helical peptides.
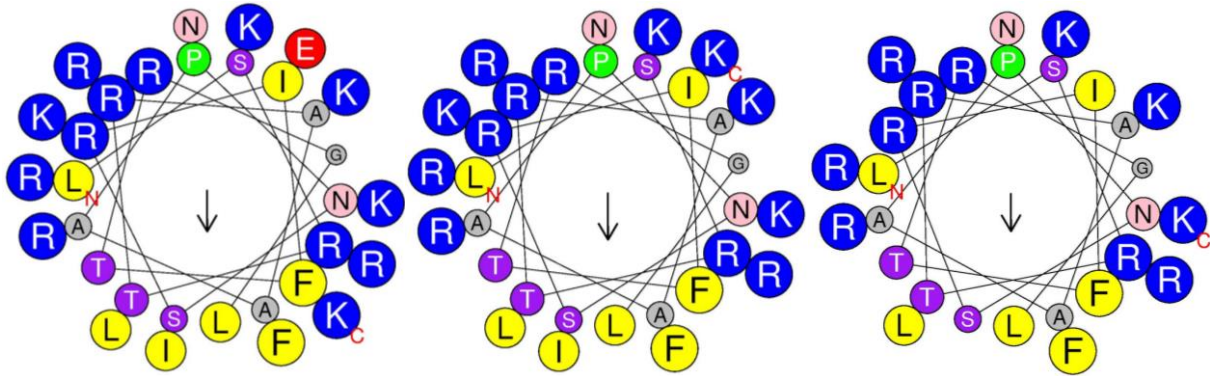
Figure 11. Helix projection with size proportional to residues. mCPP1 (left), mCPP2 (middle), mCPP3 (right). Colors refers to residues properties: blue for hydrophilic/positively charged aa, yellow for hydrophobic/non-polar aa, grey, pink and purple for uncharged aa, green for special aa, red for hydrophilic/negatively charged aa. Additionally terminal aa are marked with a red letter; N for N-termini and C for C-termini.

Using this tool, the profile of the 3 different mCPPs appears to have a good distribution of hydrophobic residues and charged residues characteristic of amphipathic sequences (Fig 11). It can be observed that the deletion of Glu[31] seems to have a positive effect as it removes a negative charge in a positively charged face, especially when comparing mCPP1 and mCPP2 the distribution of mCPP2 offers a better distinction between hydrophobic and hydrophilic faces. Nevertheless, it can be observed that due to its shorter sequence the mCPP3 sequence has a weaker amphipathic character due to less aa distribution. This has also to be associated with its decreased alpha helix character and therefore this sequence has to be considered in a slightly different way than mCPP1 and mCPP2. Regarding the different drug conjugates, version a/c or b with the additional Lys, it appears that the amphipathicity is not affected by the payload introduction. (See supplementary for projections)

5.3. Biological evaluation of novel mCPPs

In this project, I conducted evaluations of the biological profile of the novel mCPPs and PDCs in various cell lines that are relevant for their potential application as cancer therapeutics.

The Hela cell line was used as a cancerous cell line for these evaluations. It should be noted that the Hela cell line was obtained without consent from tissues of Henrietta Lacks, a patient who suffered from cervical cancer. Despite the controversial origin of this cell line, it has been widely utilized in research since its establishment.[128]

Molt-4 is a cell line derived from a patient with acute lymphoblastic leukemia, which is a specific type of blood cancer. It is important to mention that Molt-4 cells are non-adherent, requiring slight modifications to the protocols in order to accommodate this characteristic. It should be noted that the results obtained in this cell line are still preliminary and incomplete. Therefore, any conclusions drawn from these results should be subject to further investigation and deeper study with this cell line.

HEK-293 cells, derived from human embryonic kidney cells, were utilized as a model for healthy cells. It is essential to consider that HEK-293 cells are an immortalized cell line, indicating that they have undergone a mutation that has rendered them virtually immortal, allowing for indefinite cultivation. These cells serve as a valuable model system for studying the behavior and characteristics of healthy cells.

By conducting evaluations in these different cell lines, I aimed to gain insights into the potential effectiveness and specificity of the mCPPs and PDCs as cancer therapeutics, as well as their impact on healthy cells. These findings contribute to the ongoing research and development efforts in the field of cancer treatment.

5.4. Internalization in different cell lines

Influence of FBS on internalization

In the previous part it was observed that the mCPPs possess the structural characteristics favoring their cell penetration. In this part I will take a deeper look into the internalization and cellular fate of the mCPPs. For the purpose of this study fluorophore labeled versions of the mCPPs were required and their synthesis was described in the first part. The method chosen for a first evaluation of the peptides was flow cytometry. After an incubation period in presence of fluorophore labeled peptides, internalized fluorophores are excited via a laser in a single cell analysis. Through this process the flow cytometer can measure the scattered light and fluorescence signal emitted.[129]

For cell culture, the medium need to be supplemented with different additives to sustain the growth and development of the cells. A classic supplement is fetal bovine serum (FBS), which is the main source of food and energy for the cells when growing. In this protocol, peptide incubation was pursued in an FBS deprived medium which I was curious about, therefore I pursued a comparative experiment with Hela cells.

In this experiment, two different incubation methods were employed to investigate the effect of FBS (fetal bovine serum) supplementation on the internalization of mCPPs. In one case, the mCPPs were incubated in a medium supplemented with FBS, while in the other case, FBS was removed from the medium. The results obtained from comparing these two incubation methods (Fig 12) revealed a significant difference, indicating a clear interaction between FBS and the mCPPs.

It can be observed that the internalization of mCPPs is significantly decreased in the presence of FBS. Based on these findings, a hypothesis can be proposed that the highly positive charges of the mCPPs may interact with certain proteins present in FBS. This interaction is strong and stable, making it difficult for the mCPPs to penetrate the cells effectively. It is likely that this interaction between the mCPPs and FBS proteins forms a complex that hinders
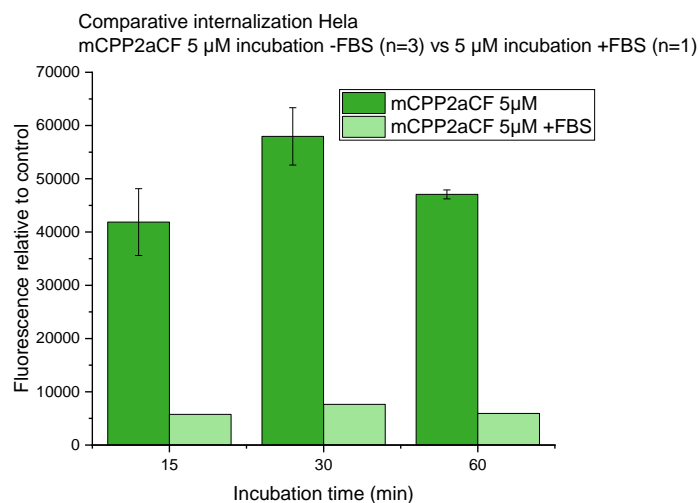
Figure 12. Comparative flow cytometry analysis of cellular uptake of mCPP2aCF in Hela cells. Peptide was incubated at 5 µM concentration for 15, 30 and 60 min in medium supplemented or not with FBS.

the availability of mCPPs for cellular internalization. These observations highlight the importance of considering the presence of FBS and its potential influence on the behavior and efficacy of mCPPs. Therefore, following biological evaluation were carried in a FBS deprived medium during peptide incubation.

Comparative uptake of mCPPs

Comparing cellular internalization of mCPPs, a striking observation from Fig 13 is the ranking of uptake between sequences: mCPP2 gives the highest signal, hence the highest cell penetration, followed by the original sequence mCPP1 and lastly mCPP3 that has a highly decreased internalization. This result can be associated with the structure of those sequences as

the R-value of mCPP3 is slightly decreased compared to mCPP1 and mCPP2. Moreover, this first observation confirms the hypothesis that by removing a Glutamic acid, bearer of a negative charge at physiological pH, it would increase the overall positive charge of the C-terminal peptide tail hence increasing its interaction with cellular membrane resulting in better cellular uptake when comparing mCPP1 and mCPP2. This pattern is also maintained independently of the concentration even if the difference is more striking at 5 µM. Those results are in agreement with the data recently collected about the different CPP.[95]

Considering the concentration used it is observed that with increasing concentration the internalization is also increased which highlights the concentration dependent uptake of the mCPPs. The uptake of mCPP2 is even more affected by the concentration used thus revealing its potential and confirming its advantage over mCPP1.

Finally, influence of incubation time on cellular uptake was evaluated with short time frame. Interestingly, uptake is already satisfactory after a short incubation of 15 minutes revealing the potential of those mCPPs. Moreover, uptake pattern is consistent with the different incubation time. Another point to consider for mCPP1 and mCPP2 is that it seems that their uptake reaches a maximum at 30 minutes with 5 µM whereas the uptake increases in a time dependent manner for mCPP3. It can be observed different internalization behavior with mCPP1 and mCPP2 exhibiting a fast uptake while mCPP3 requires more time to accumulate which could influence the efficiency of relative PDCs.
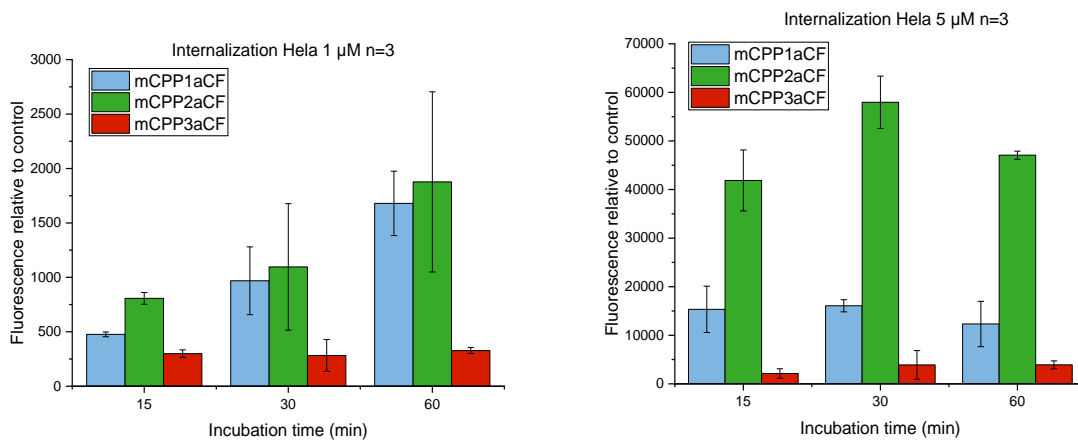
Figure 13. Comparative flow cytometry analysis of cellular uptake of CF labeled mCPPs in Hela cells. Peptide were incubated at 1 or 5 µM concentration for 15, 30 and 60 min.

Interestingly similar results, to the one obtained with Hela, were observed in Molt-4: the pattern in uptake profiles is unchanged, the uptake is concentration dependent, at 1 µM the different peptides are increasingly taken up over time while for 5 µM a maximal uptake seems to be reached after 30 minutes, which is translated in a time dependent uptake. Therefore, as for Hela cells, the uptake of the mCPPs is time and concentration dependent but when comparing uptake in both cell lines a striking observation can be made regarding the intensity of

the signals received. Indeed, in Molt-4 the relative signal obtained is 10 times higher than in Hela cells. This first result is thus quite encouraging as the cell penetrative capacity of the mCPPs is increased in this cell line this could result in increased potency for the PDCs.
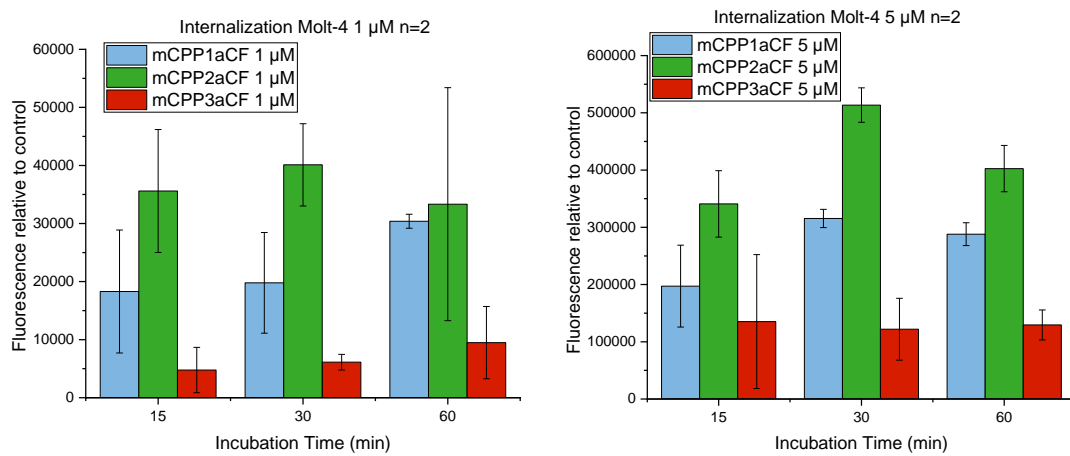
Figure 14. Comparative flow cytometry analysis of cellular uptake of mCPPs in Molt-4 cells. Peptides were incubated at 5 µM concentration for 15, 30 and 60 min.

Finally, uptake was evaluated in HEK-293 cells with increasing concentrations and incubation times. Uptake follows the same trend as in the other cell lines, with a time and concentration dependent uptake and mCPP2aCF still performing the best. Nevertheless, as with Molt-4 cells, the relative fluorescence signal received as to be taken into consideration as it is 20 times lower than in Hela cells and 200 times lower than in Molt-4. This strong difference in internalization is a good sign for selectivity as it appears that the mCPPs cannot cross the membrane of HEK cells. An explanation for this result may lie in the fact that the membrane of cancerous cells is more negatively charged than the ones of healthy cells which can result in a stronger interaction with mCPPs.[36,130]
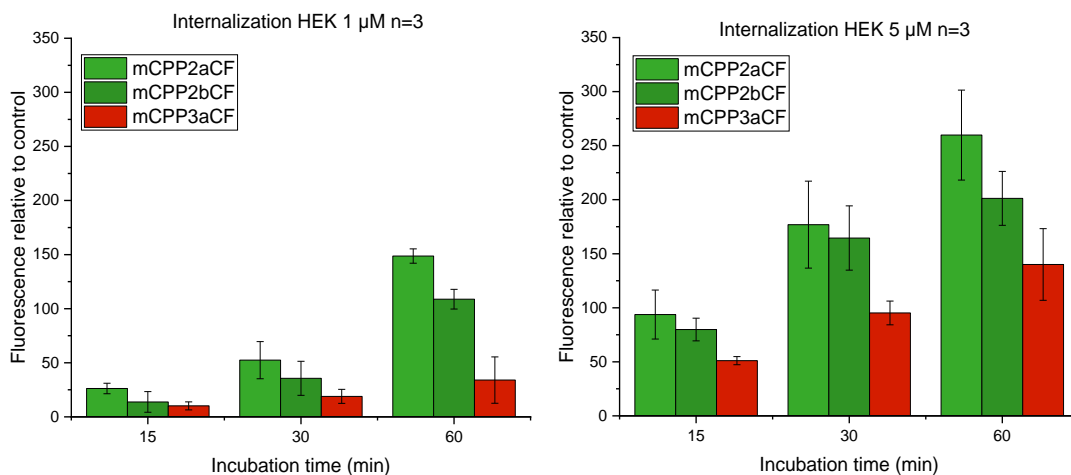
Figure 15. Comparative flow cytometry analysis of cellular uptake of mCPPs in HEK cells. Peptides were incubated at 1 or 5 µM concentration for 15, 30 and 60 min.

5.5. Fluorescence microscopy in Hela and HEK cells

With the different information on internalization at hand; behavior, concentration and incubation time, it was possible to pursue this study with fluorescence microscopy to obtain more information on the intracellular fate of the mCPPs. Principle of fluorescence microscopy lies on the excitation, at a specific wavelength, of fluorophore that will, when reversing to ground state, emit specific wavelengths. Such technique allows the observation of individual organelles, upon use of specific dyes, and the potential colocalization resulting from internalization of fluorophore labeled objects. According to flow cytometry experiments the protocol for fluorescence microscopy was designed as follows: after a growing period of 24 hours Hela cells were first incubated with CMXRos, a red mitochondria stain that specifically binds to cardiolipin, a phospholipid presents in the inner mitochondrial membrane. Due to its cationic nature this dye can specifically accumulate in the mitochondria in a membrane potential dependent manner, for 30 minutes. After this, medium was replaced by a peptide solution at 5 µM and the cells incubated for 30 minutes. Finally, Hoechst, a blue nuclear stain, was added and the incubation pursued for an additional 10 minutes. Cells were then washed, to reduce background signal from the different fluorophores, and ready to be observed under the microscope in a relatively short time frame to avoid quenching of the fluorescence due to light exposure. Due to this triple stain different fluorophores had to be used in order to avoid any overlapping signals. The mitochondria stain has a λ_{abs} 579 nm/ λ_{em} 599nm and thus emits a red light, Hoechst has a λ_{abs} 350 nm/ λ_{em} 461nm and thus emits a blue light, finally Carboxyfluorescein, the fluorophore attached to the mCPPs, has a λ_{abs} 494 nm/ λ_{em} 518nm and emits a green light that does not overlap with the other two fluorophores. To investigate the internalization pattern of the mCPPs over time, different time points were evaluated using flow cytometry. These experiments were conducted in collaboration with the "Istituto Superiore di Sanità" in Italy. The institute performed the experiments with an additional fixation step and graciously provided the resulting images that are presented hereafter. It is worth noting that cell fixation can have an impact on peptide internalization, which initially made me somewhat hesitant.
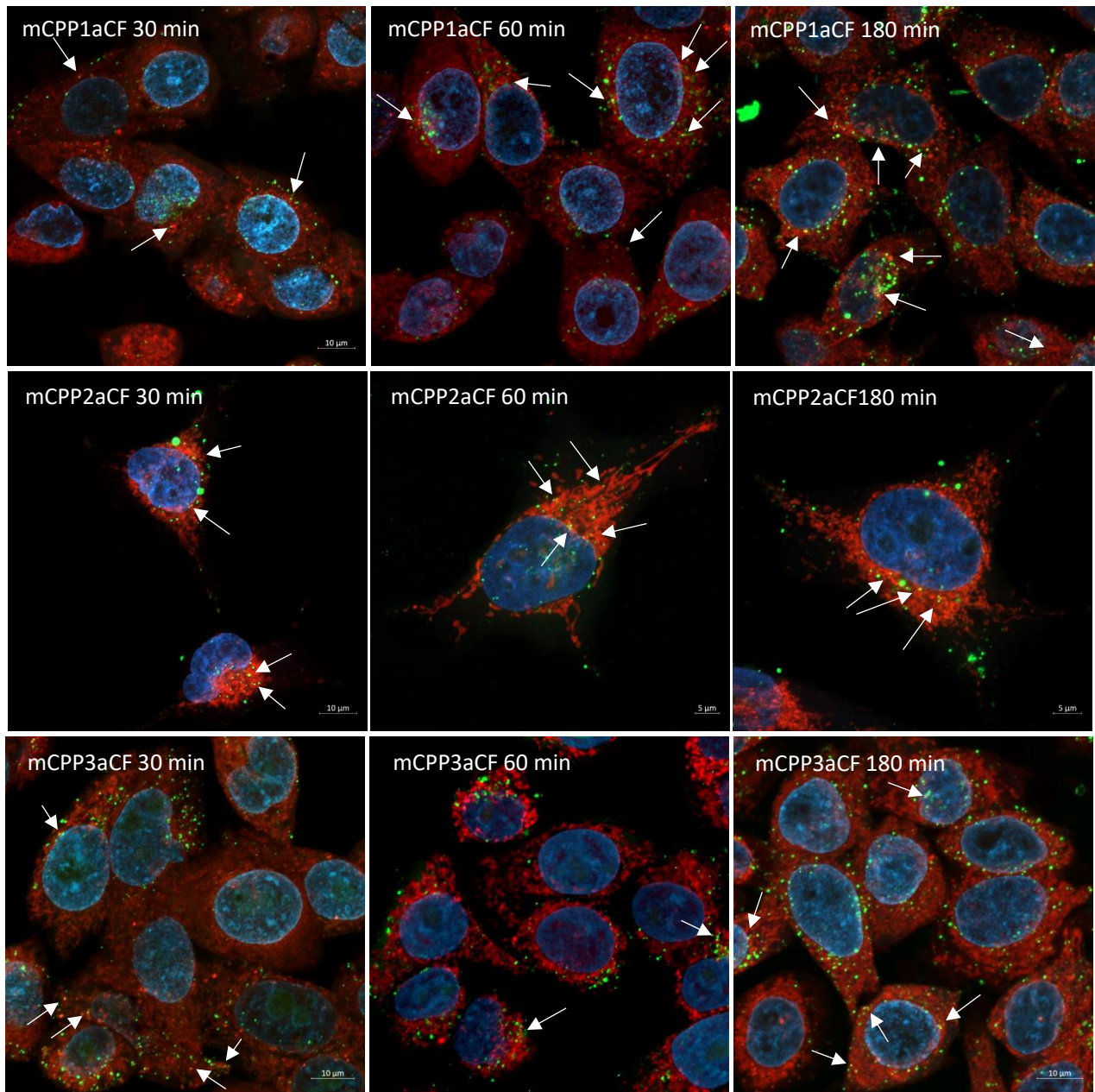
Figure 16. Confocal images of fluorophore labeled peptides in Hela cells fixed. Samples were incubated with CMXRos mitotracker (red) for 30 min then with mCPP-CF (green) for 30, 60 or 180 min at 5µM and finally with Hoechst (blue) nucleus dye for 10 min before fixation with 3% Paraformaldehyde in complete medium for 30 min at 4°C. Co-localization spots are indicated with arrows.

After a brief incubation period of 15 minutes, the peptide signal is predominantly detected outside of the cell, with only a few colocalized spots observed in the cytoplasm and mitochondria. After 30 minutes of incubation, the peptide signal remains outside of the cell or inside the cytoplasm, but a few more colocalization points can be observed. Extending the incubation time to 60 minutes further enhances the colocalization effect, with more observable spots. Finally, after a longer incubation time of 180 minutes, the colocalization spots become more prominent. The remaining signals seem to overlap with the mitochondria, although they do not appear as yellow, possibly due to being on a different plane (Fig 17). Correlating

with the flow cytometry data, it is evident that mCPP1aCF exhibits a similar behavior to mCPP2aCF, demonstrating rapid internalization and colocalization. However, for mCPP3aCF, the peptide signal appears relatively low and is primarily localized outside of the cell at 30 and 60 minutes. Nevertheless, after an extended incubation time of 180 minutes, mCPP3aCF shows increased internalization and an enhanced colocalization effect becomes noticeable.

Considering the three-dimensional nature of cells, it is important to acknowledge that organelles and internalized peptides may not align perfectly on the same plane when visualized using microscopy. Consequently, the peptide signal that initially appears to be off-target may actually be colocalizing with mitochondria. To investigate this further, Figure 18 presents a comparison of merged images from a single section. Upon closer examination, it becomes evident that the colocalization between the peptide signal and mitochondria appears more pronounced in the single section view.
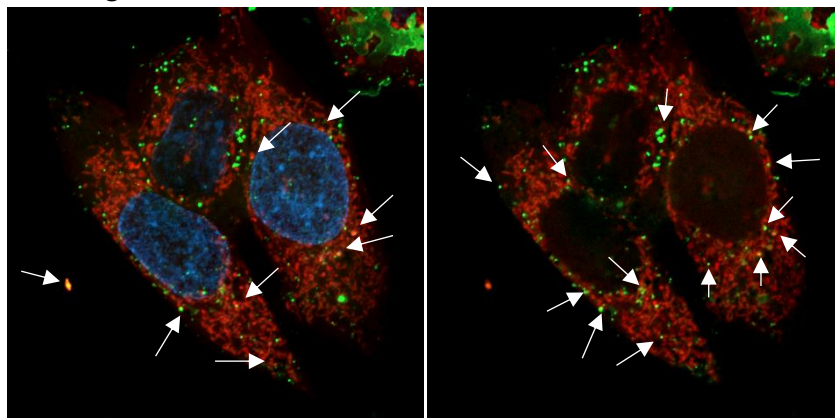
Figure 17. Confocal images of mCPP2aCF 5 µM, 30min fixed. Full image (left), single section (right).

In order to gain insights into the distinct behavior observed in flow cytometry, fluorescence microscopy was employed to examine HEK cells. The experimental conditions were kept consistent with a 30-minute incubation time and concentrations of 5 and 10 µM for comparison purposes. Figure 20 illustrates the results obtained at the higher concentration of 10 µM, as the images obtained at 5 µM (Fig S23) presented challenges due to reduced internalization at this concentration.

Consistent with the findings from flow cytometry, it is evident that internalization in this particular cell line is diminished and necessitates a higher concentration of the peptides. The microscopy images reveal that only a few peptides are internalized, with the majority appearing to aggregate in distinct shiny spots within or outside of the cells. However, for the peptides that do enter the cells, they seem to retain their ability to target mitochondria, as evidenced by the presence of colocalization spots. Notably, no significant differences are observed among the various sequences tested, with mCPP2aCF exhibiting the most favorable performance.
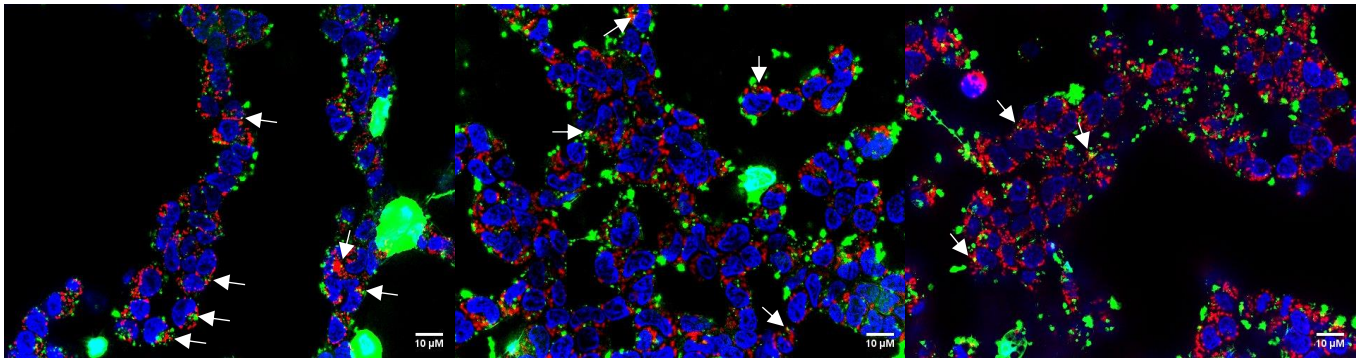
Figure 18. Microscopy images in HEK-293 cells. All images obtained with a peptide concentration of 10 µM and an incubation time of 30 min. mCPP2aCF (left) mCPP2bCF (middle) mCPP3aCF (right).

These microscopy results provide further support to the findings obtained through flow cytometry, highlighting a reduced internalization in HEK cells and the tendency of the peptides to aggregate rather than distribute uniformly within the cell. The observations of mitochondrial colocalization suggest that the peptides retain their targeting capability, albeit at a limited extent.

5.6. Cytotoxicity of mCPPs in different cell lines

Assessment of mCPPs influence on viability in different cell lines is a key point as the cargo should not induce any toxicity for the PDC efficiency to be solely attributed to its cargo. Due to my secondment in a different laboratory two readout methods were used for cytotoxic evaluation.

When in Köln the method used was relying on resazurin, a weakly fluorescent dye which is non-toxic and cell permeable with a deep blue color. Upon aerobic respiration resazurin is reduced in resofurin irreversibly, this compound is highly fluorescent and can be detected due to its absorbance at 530-570 nm and emission at 580-590 nm which gives a pink color to the solution. Therefore, when in a presence of viable cells resazurin is reduced due to the respiration through mitochondria and in absence of viable cells it will remain blue. This colorimetric difference can then be monitored to deduct the cells viability upon exposure to treatment.

During my secondment period in Rome, I was using a different readout based on Cell-Titer glo. Similarly, to resazurin this dye requires to be reduced, indirectly, by mitochondria as it reacts with ATP. But in order to react with ATP the cells must be lysed, as the dye is not cell permeable, and therefore a final vortexing step is required to disrupt membranes and release the present ATP. The molecule behind Cell-titer glo is luciferin which upon reduction turns into oxyluciferin, a molecule that emits light and can be titrated by following the luminescence. ATP being directly proportional to the number of viable cells and the advantage of cell-titer glo being an "add-mix-measure" solution highly reduce potential errors resulting from exchanging media and pipetting.

Biological evaluation in Hela cells

In the initial assessment of the peptide carrier alone, no toxicity was observed within the tested concentration range after a 24-hour incubation period (Fig 21). However, when evaluating the mCPPs, toxic effects became apparent, starting at 25 µM and increasing with higher concentrations. Notably, the highest toxicity was observed with mCPP1, while mCPP2 and mCPP3 exhibited a slightly delayed toxic response at higher concentrations, suggesting a beneficial effect of changing the peptide sequence. It is worth noting that the observed toxicity at 100 µM should be considered in the context of the high concentration used.
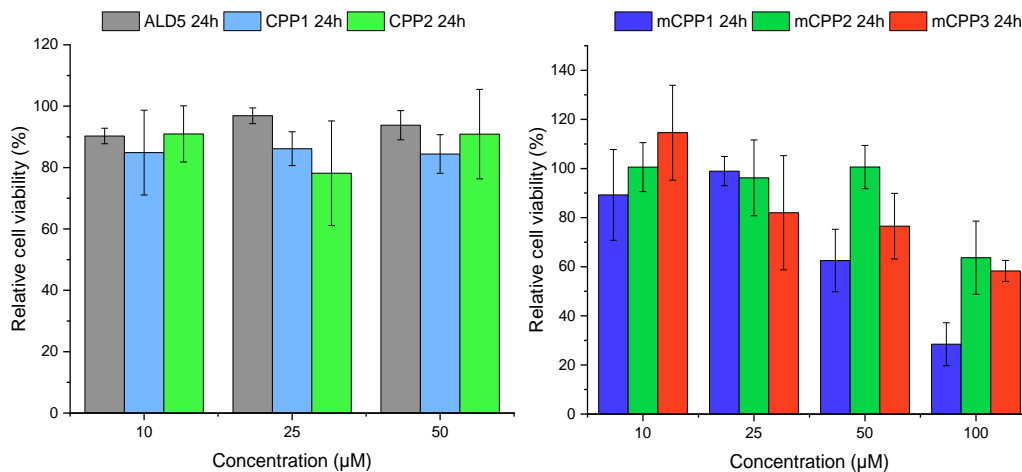
Figure 19. Cytotoxic profile of peptides in Hela cells. Peptides were incubated for 24 hours before assessment of cell viability with a resazurin based test.

The toxicity observed with the mCPPs can be attributed to their high concentration-dependent membrane interaction. At elevated concentrations, CPPs can trigger a switch from endocytosis to direct penetration, which may lead to membrane destabilization and pore formation.[74] These effects contribute to the observed toxicity at high concentrations.

The results indicate that the mCPPs possess a concentration-dependent toxic effect, with mCPP1 exhibiting the highest toxicity and mCPP2 and mCPP3 showing attenuated toxic response at higher concentrations.

To gain a deeper understanding of the toxicity, the incubation time of the peptides was extended to 48 hours in the study conducted in Rome. Prolonging the incubation time resulted in a decreased toxic effect not only for the carrier alone (CPP1 and ALD5) but also for the mCPPs. This decrease in toxicity is a positive indication for the potential long-lasting effect of the PDCs. It can also be observed that mCPP1 seems more toxic than mCPP3 highlighting the better tolerability of this new sequence in Hela cells.

Overall evaluation in Hela cells revealed a great tolerability for the mCPPs. Some noticeable toxicity can be observed when reaching concentration of 100 µM for mCPP2 and mCPP3 after 24 hours while the tolerability is reduced to a maximum of 50 µM for mCPP1 in the same conditions.
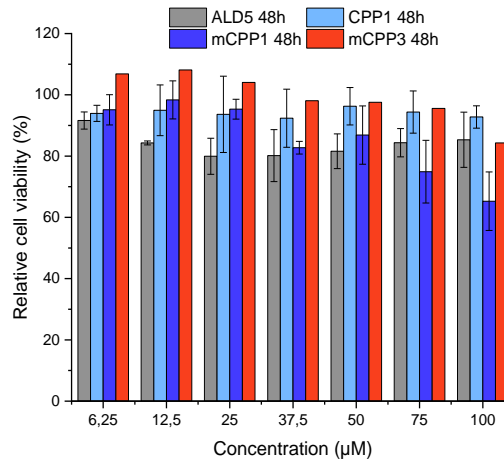
Figure 20. Cytotoxic profile of peptides in Hela cells. Peptides were incubated for 48 hours before assessment of cell viability with a cell-titer glo based test.

Based on these findings, it can be concluded that the new mCPP sequences benefit from the modifications in comparison to the original mCPP1. As previously discussed, the observed toxic effects of the mCPPs can be attributed to their strong membrane interaction, which can lead to membrane disruption at high concentrations and induce toxicity.

Biological evaluation in Molt-4 cells

When searching into literature for Jasmonic acid it appears that very few studies took interest into investigating its toxic effect on cancerous cells but the few papers investigating this subject highlight the sensibility of a specific cell line to this plant stress hormone.[117,118,122] This cell line is Molt-4, a cell line obtained from a patient suffering from acute lymphoblastic leukemia. Leukemia is a specific blood cancer and therefore is still a tumorigenic cell line. Interestingly this cell line is not adherent and therefore protocols had to be slightly modified to adapt to this change. It also has to be mentioned that the results presented here are preliminary and incomplete yet, therefore any conclusion taken is subjected to be challenged by a deeper study with this cell line.
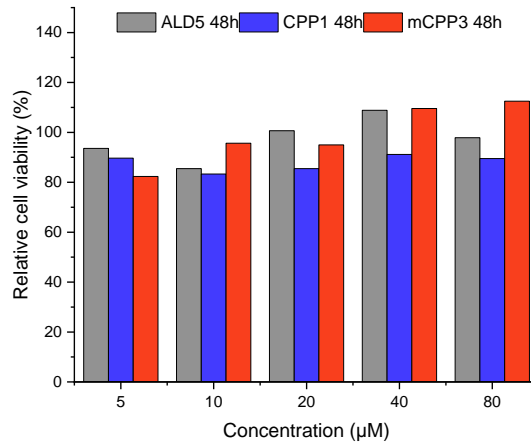
Figure 21. Cytotoxic profile of peptides in Molt-4 cells. Peptides were incubated for 48 hours before assessment of cell viability with a cell-titer glo based test.

Cytotoxic evaluation in this cell line was only pursued over 48 hours without triplicates, but the results obtained from it are quite encouraging. For the peptide part as well as for mCPP3 an increase in the tolerability was observed as no toxic effect was observed up to a concentration of 80 µM. Considering the strong uptake observed in flow cytometry evaluation it can be concluded that mCPPs are virtually well better tolerated than in Hela cells where toxic effect was noticeable at high concentration.

Biological evaluation in HEK-293 cells

Finally, evaluation with HEK cells was pursued with a cytotoxic evaluation at 24- and 48-hours incubation time points. Evaluation with mCPPs revealed low to nontoxic effect at both incubation times. Indeed, a slight decrease in viability appeared at 75 µM, for 24 hours
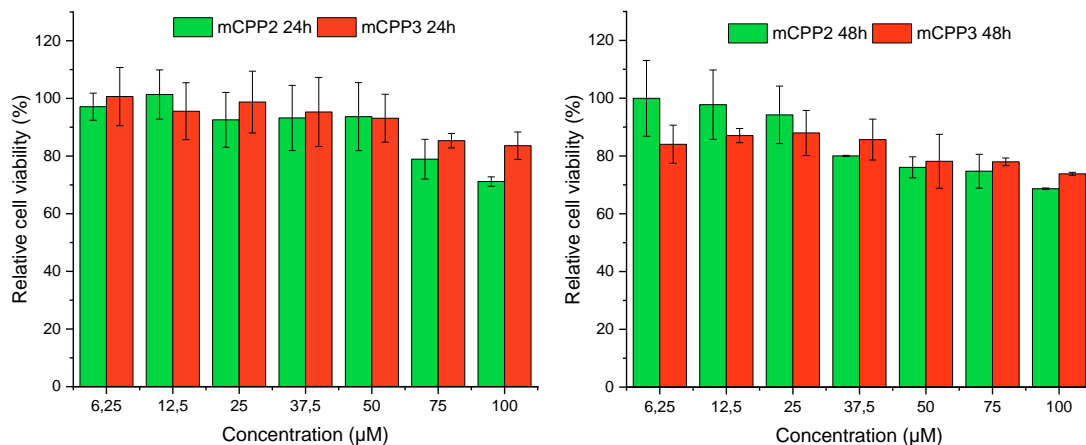
Figure 22. Cytotoxic profile of peptides in HEK-293 cells. Peptides were incubated for 24 or 48 hours before assessment of cell viability with a resazurin based test.

incubation, and at 37,5 µM for 48 hours incubation. A slight difference in viability can be observed between incubation time but overall mCPPs are really well tolerated, even at high concentration. This result goes in accordance to the uptake efficiency, as in this cell line internalization was highly decreased, suggesting that if no toxicity is observed this can be connected to a lesser membrane interaction. Overall, it can be concluded that mCPPs are safe for healthy cells which can be explained by a decreased membrane interaction as the highly cationic sequences will preferably interact with the negative surface of cancerous membranes while healthy cells are less likely to internalize them. Therefore, mCPPs exhibit a partial cancer targeting without relying on specific targeting moieties.

5.7. Effect on red blood cells

Continuing the biological evaluation of the mCPPs and PDC a parameter to consider for potential in vivo application and testing is the transport of the PDC to its target. To do so PDC are dependent on blood transportation and therefore they must be evaluated as nontoxic for blood cells to ensure a safe travel. Performing a hemolysis assay thus revealed an important testing for the PDC. Similarly, to a cytotoxic evaluation red blood cells would be incubated with the peptides before measuring the amount of hemoglobin released, due to lysis of the cells, from a plasma sample by an absorbance measurement.
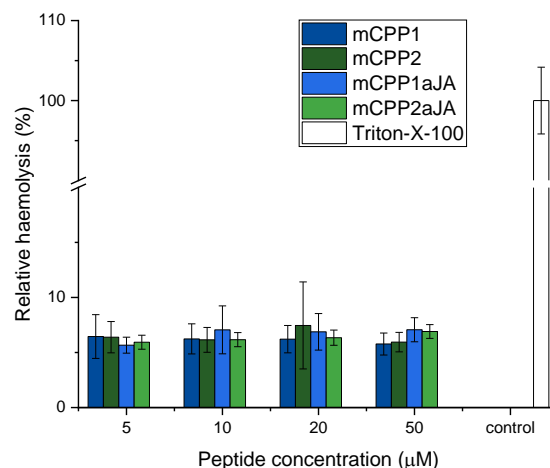
Figure 23. Hemolytic profile of peptides and PDC after 24h incubation.

Interestingly when incubating either mCPPs or PDC at different concentration no significant lysis was observed. Triton-X-100, a cell detergent, was used as positive control to obtain a sample with 100% cell lysis. In comparison all the peptides tested did not induce more than 10% and this independently of the concentration tested. Therefore, it can be concluded that the use of those mCPP and their conjugates is safe for blood samples confirming a safe profile towards healthy cells.

5.8. Cytotoxicity of PDC in different cell lines

<u>Biological evaluation of CPP-drug conjugates</u>

To evaluate the specificity and targeting efficiency of the PDCs, a control was performed using a PDC lacking the mitochondria targeting sequence. This control was important to assess whether the toxicity observed in the PDCs was specifically due to mitochondrial targeting. In this control, the CPP alone cannot localize to the mitochondria, so it was expected to have no toxic effect on the cells.

In Hela cells, the treatment with CPP1aJA for 24 hours resulted in noticeable toxicity starting at 50 µM, Fig 25, which can be attributed to the membrane interaction of the CPP at high concentrations, as previously described.[88,90] However, when the incubation time was extended to 48 hours, no toxicity was observed even at concentrations up to 100 µM. This suggests that the toxicity observed at 24 hours is likely due to a fast-killing effect, which aligns with the membrane disruption mechanism.
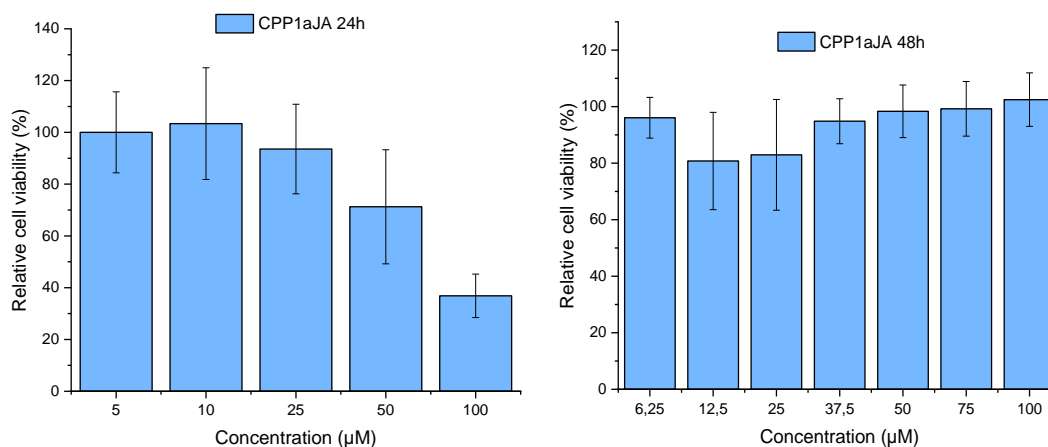
Figure 24. Cytotoxic profile of CPP1aJA in Hela cells after 24h incubation (assessment of cell viability with resazurin) and 48h incubation (assessment of cell viability with Cell Titer Glo).

Similar results were obtained in Molt-4 cells (Fig 26) when evaluating the same sequence. The CPP-drug conjugate was not toxic for this cell line, despite the increased uptake observed in FACS study.
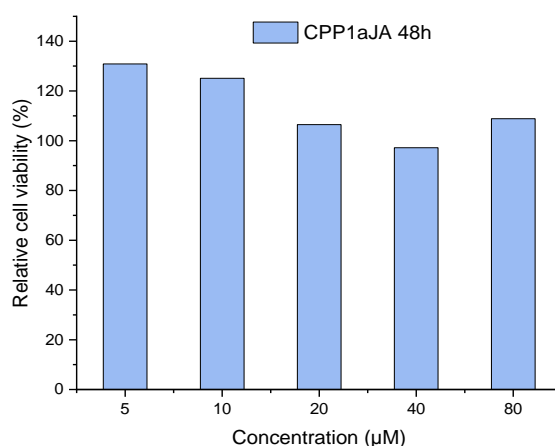
Figure 25. Cytotoxic profile of CPP1aJA in Molt-4 cells after 48h incubation assessment of cell viability with Cell Titer Glo.

In HEK cells treated with the CPP2 drug conjugate, a concentration-dependent toxicity was observed, similar to the behavior of the mCPPs in this cell line. However, the incubation time did not have a significant influence on cytotoxicity, indicating limited activity of the drug payload (JA) in these cells.
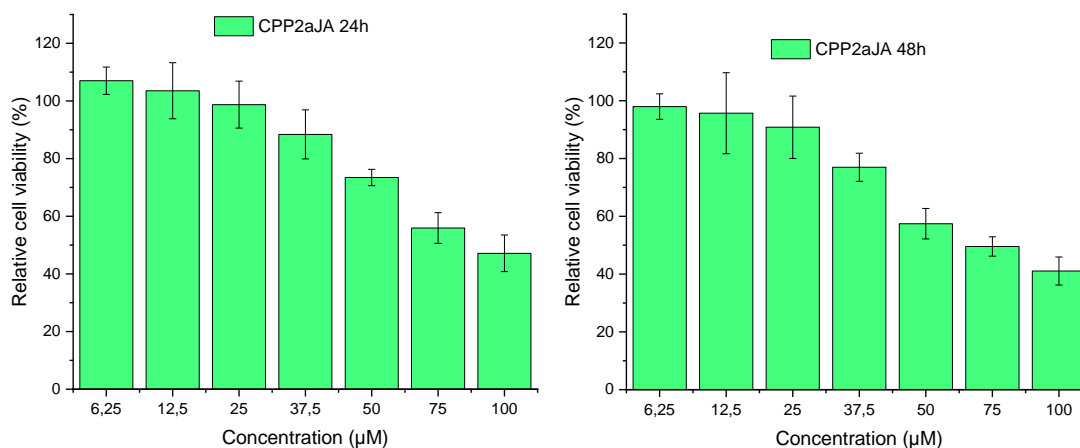
Figure 26. Cytotoxic profile of CPP2aJA in Hela cells after 24 and 48h incubation assessment of cell viability with resazurin.

The evaluation of PDCs lacking the mitochondria targeting sequence in different cell lines reveals diverse behaviors and toxic effects. In cancerous cell lines, Hela and HEK-293, no toxicity is observed for 48 hours incubation suggesting a great tolerabilty of the sequence. However, a shorter incubation time of 24 hours resulted in some toxicity for Hela cells. On the other hand, CPP-drug conjugate has a different behavior in healthy cells. A time and concentration dependent toxicity is observed. The toxic effect observed has to be put into perspective, when calculating the EC_{50} high concentrations obtained suggest a good tolerabilty for the PDCs lacking the mitochondria targeting sequence (Table 2).

Table 2. EC$_{50}$ concentration for CPP-drug conjugates in different cell lines.

Sequence/cell line	CPP1aJA/Hela	CPP1aJA/Molt-4	CPP2aJA/HEK-293
EC50 24h (µM)	75,56±1,25	-	89,53±1,27
EC50 48h (µM)	>100	>80	67,06±1,86

Biological evaluation of PDCs in Hela cells

Similarly, to mCPPs evaluation, PDCs were first evaluated after cell treatment for 24 hours. Based on Figure 27 and Table 3, the curve profiles of the various PDCs appear to be quite similar, indicating that the sequence used has minimal influence on their efficiency. Nevertheless, distinctions can be made when comparing sequences and coupling position. For mCPP1 there is a strong evidence that the "b" conjugate decreases PDC efficiency in comparison to "a" conjugate. This decreased efficiency is also observable, to lesser extent, with mCPP2 which leads to the conclusion that the coupling position has influence on the activity and an optimal payload coupling position must be located on the CPP part of the mCPP. The "b" coupling position having JA between the MTS and the CPP might hinder its activity by masking the moiety. Moreover, according to the difference in activity in can be concluded that mitochondrial proteases does not cleave mCPPs after their MTS but at an unknown position.

Table 3. EC$_{50}$ concentration for drug conjugates in Hela cells 24h.

Sequence	CPP1aJA	mCPP1aJA	mCPP1bJA	mCPP2aJA	mCPP2bJA	mCPP2cJA	mCPP3aJA	mCPP3cJA
EC$_{50}$ 24h (µM)	75,56±1,25	13,81±2,71	33,64±1,25	21,62±1,17	23,75±1,64	26,35±1,47	22,29±1,61	39,52±1,29
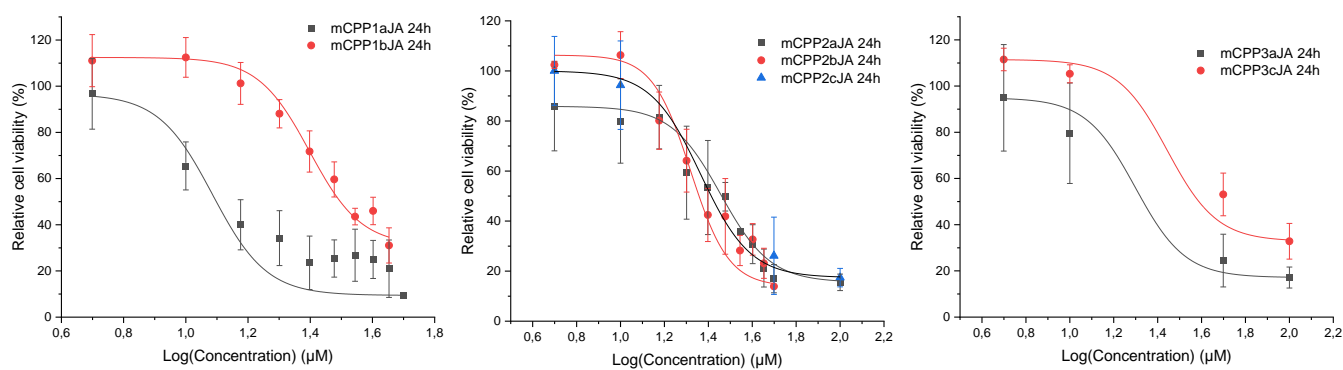
Figure 27. EC$_{50}$ curves for the drug conjugates in Hela cells at 24h.

According to the coupling position it can be deducted that the CPP part of the PDC is not degraded upon internalization in the cells as the toxicity for "a" and "c" have similar EC_{50}, even if "a" conjugates are slightly more potent. This could be due to the drug being hindered when in the "c" position whereas for "a" conjugates the drug being on the C-terminal can be more easily accessible and thus effective. It is worth to notice the strong difference in activity between CPP drug conjugate and PDC which highlight the influence of the mitochondria targeting gained through MTS coupling. Overall, coupling position can be ranked as follow with "a" drug conjugates being the most efficient conjugates, followed by "c" conjugates and lastly "b" conjugates. Moreover, mCPP2 seems to yield the best conjugates as the PDCs exhibit similar activity independently of the coupling position of the payload and that their activity seems increased when compared to mCPP1 and mCPP3.

Unfortunately, increasing the incubation time decreased the PDC potency with almost doubling the EC_{50} concentration for the "b" conjugates (Table 4, Fig 28). Furthermore, the difference in potency between "a" and "b" conjugates is increased with this extended incubation time. It is worth to notice that the efficiency of the "a" conjugates is slightly affected, especially for mCPP2aJA which almost retain its activity. Considering the reduced EC_{50} from this experiment it can be concluded that all the PDCs does not have a long-lasting effect.

Table 4. EC50 curves for the drug conjugates in Hela cells 48h.

Sequence	CPP1aJA	mCPP1bJA	mCPP2aJA	mCPP2bJA	mCPP3aJA
EC_{50} 48h (µM)	>100	40,34±1,56	25,27±1,07	44,84±1,94	32,03±0,42
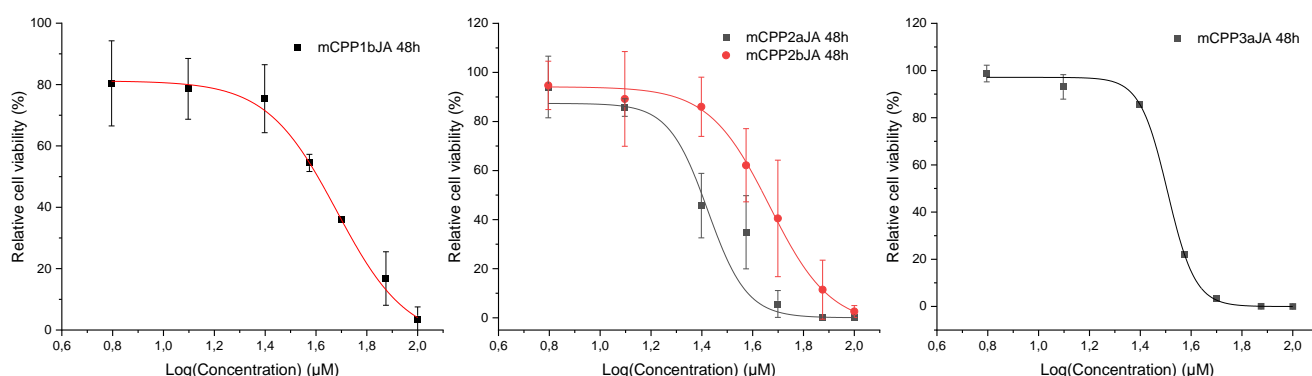
Figure 28. EC50 curves for the drug conjugates in Hela cells.

Biological evaluation in Hela cells revealed a time and concentration dependent toxicity for the PDCs. Observing such difference when increasing incubation time could be related to a toxic effect not lasting. It can be hypothesized that the PDCs have a rapid toxic effect which is not sufficient to completely remove cancer population, resulting in repopulation over 48 hours which decrease the EC_{50}. Activity of mCPP2aJA is less affected and appears as the best PDC.

Biological evaluation of PDCs in Molt-4 cells

Extending the investigation to the available PDCs in Molt-4 cells, it can be appreciated that the mCPP2 drug conjugates toxicity is greatly increased in this cell line (Table 5, Fig 29). Interestingly, a strong difference between mCPP1bJa and mCPP2bJA can be observed, highlighting the improvement resulting from the change in sequence. Finally, the close similarity in potency for the "a" and "b" conjugates for mCPP2 suggests that the coupling position is not affecting the potency of the resulting PDCs in this cell line.

Table 5. EC_{50} concentration of PDC in Molt-4 48h.

Sequence	CPP1aJA	mCPP1bJA	mCPP2aJA	mCPP2bJA
EC_{50} 48h (µM)	>80	58	11	10
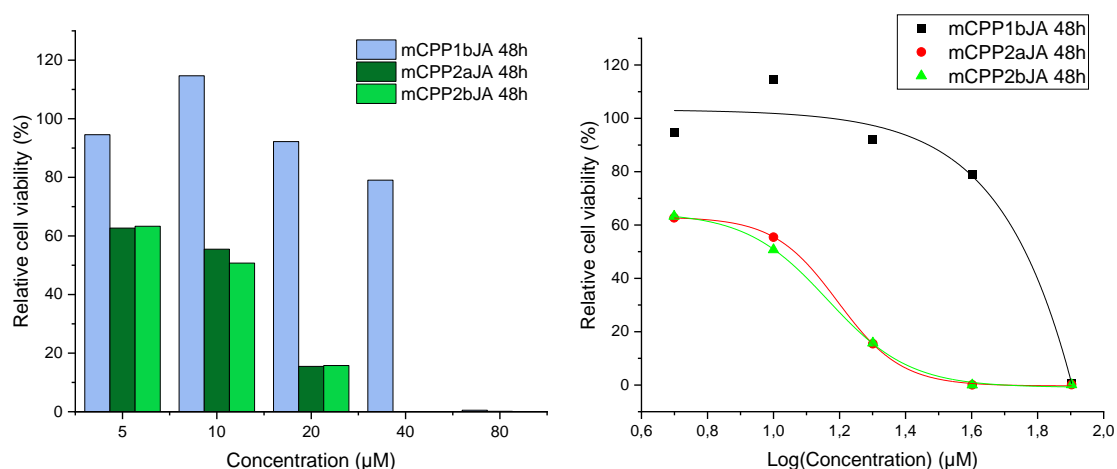
Figure 29. Cytotoxic profile of peptides in Molt-4 cells and EC_{50} curves. Peptides were incubated for 48 hours before assessment of cell viability with a Cell Titer Glo based test.

The small and incomplete biological evaluation in Molt-4 cells provides encouraging results regarding the potency of the PDCs. The observations indicate a better tolerability of the peptide cargo in Molt-4 cells compared to other cell lines. Additionally, there is a notable increase in potency for the PDCs, indicating an improved therapeutic effect in Molt-4 cells.

The difference in activity between mCPP2 and mCPP1 drug conjugates further supports the notion that the sequence change in the peptide has resulted in an improvement in activity. This improvement is consistent with the enhanced uptake observed in the cells. Furthermore, the activity of mCPP2 drug conjugates appears to be independent of the coupling position for the payload, indicating that the activity is primarily associated with the mCPP sequence and its improved uptake.

These findings emphasize the importance of evaluating PDCs in different cancerous cell lines to assess their activity. Different cancer cell lines can exhibit varying responses to PDCs, highlighting the need for comprehensive studies to identify the most effective PDCs for specific cancer types. Further investigations in Molt-4 cells and other relevant cancer cell lines are necessary to confirm and expand upon these initial observations.

Biological evaluation of PDCs in HEK-293 cells

Biological evaluation was pursued in HEK-293 cells with the PDCs. Potency of the PDCs increase in a linear relation with the concentration (Fig 30), a behavior can be associated to a toxic effect from mCPP internalization. As seen in microscopy, the peptides seem to aggregate which could disturb cellular membrane leading to cytotoxicity. Considering the EC_{50} in Table 6, these values are highly increased for the PDCs compared the other cell line, highlighting a decreased potency. Looking at mCPP2 drug conjugates, a similar behavior to the one observed in Molt-4 is observed, with similar activity independent of the payload coupling position. On the other hand, in this cell line, mCPP3aJA is more efficient than mCPP2aJA. To elaborate on this difference, mCPP3aJA activity is also maintained upon longer incubation which correlate with the reduced uptake of this sequence. One can hypothesize that mCPP3 reduced uptake is more distributed overtime thus explaining a better activity after 48 hours incubation when compared to mCPP2.

Table 6. EC_{50} concentration for PDC in HEK cells at 24 and 48h

Sequence	CPP2aJA	mCPP2aJA	mCPP2bJA	mCPP3aJA
EC_{50} 24h (µM)	89,53±1,27	71,76±1,38	70,58±1,13	54,41±1,31
EC_{50} 48h (µM)	67,06±1,66	85,34±1,19	86,23±1,22	57,64±0,97
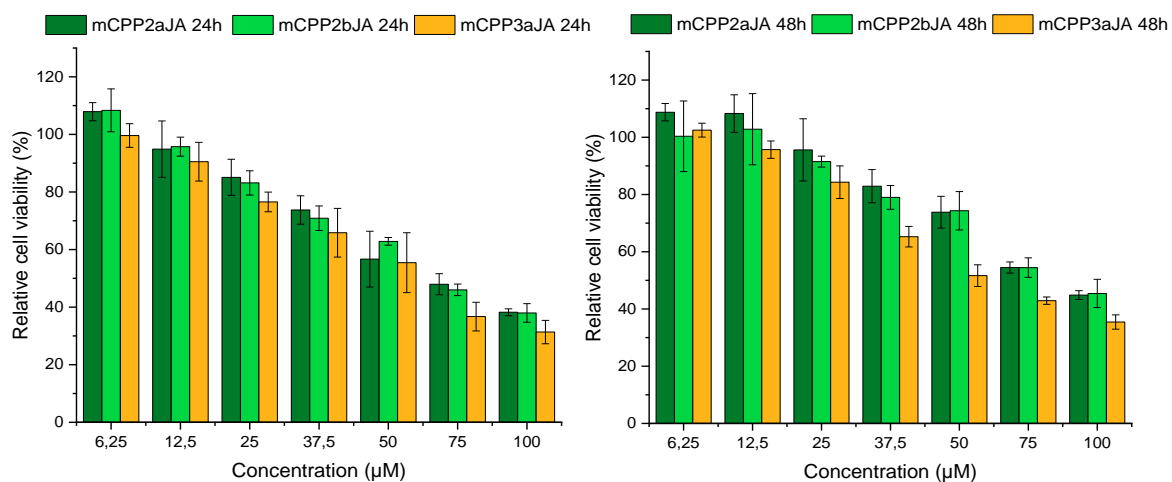
Figure 30. Cytotoxic profile of PDC in HEK cells. Peptides were incubated for 24 or 48 hours before assessment of cell viability with a resazurin based test.

The biological evaluation of PDCs in HEK-293 cells, a healthy cell model, yielded interesting results. As shown in Fig 30, there is a linear decrease in cell viability associated with the PDCs, which could be attributed to the peptide aggregation observed in microscopy. This aggregation may alter the toxic effect of the PDCs in this cell line. The overall decreased potency of the PDCs in HEK-293 cells suggests that they are less effective compared to their activity in cancer cell lines. This finding indicates a better tolerability of the PDCs in healthy cells, which could be attributed to the structural differences in membranes. Cancer cell membranes are known to be more negatively charged, which can facilitate better interaction and internalization of the PDCs. [36,130] However, in healthy cells with more positively charged membranes, this cancer-targeting ability may be diminished.

5.9. Apoptosis evaluation

Considering the potency of the PDC, especially mCPP2aJA, further testing of the killing effect had to be pursued. According to literature the killing effect of JA is an apoptotic cell death triggered via mitochondrial activation. Therefore, an apoptotic assay was pursued to verify this statement and to observe if mCPP2aJA follows the same path. This assay relies on the attachment of annexin V to phosphatidylserine (PS), a marker of apoptosis, which is present in the inner leaflet of cellular membranes in healthy cells but is re-localized to the outer leaflet upon apoptosis. Therefore, annexin V can attach to PS in cells that have undergone apoptosis but cannot attach to healthy cells, and a fluorophore is attached to annexin V so it can be viewed with flow cytometry at a specific wavelength. A second path for cell death is necrosis, when the cell dies with its membrane being disrupted. To follow this event, it relies on Propidium iodide (PI) a fluorescent marker that will bind to the DNA of cells but cannot cross cellular membranes. This inability to cross cellular membranes enables to distinguish necrotic cells, which would be completely disrupted and have their DNA freely accessible, from apoptotic and healthy cells with a membrane still intact hence blocking PI from accessing the DNA. Considering the autofluorescence from the cells it is important to add a control sample for setting the quadrant that will allow separation of healthy from apoptotic, necrotic or dead cells. Finally, to get a better overview on the triggering of apoptosis it was decided to pursue this experiment in a time course manner with 3 time points 6, 24 and 48 hours in Hela cells.
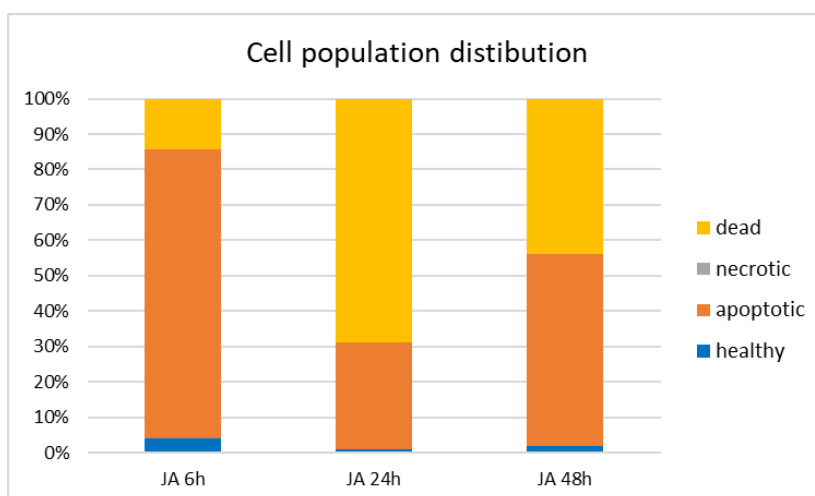
Figure 31. Cell population distribution resulting from Hela treatment with Jasmonic Acid at 20 mM for different incubation time.

Setting up a control sample allows to view the population of cells which are healthy, after examination under the microscope the cells were looking healthy and undisturbed and therefore this population, measured via flow cytometry, can be attributed to healthy cells that have undergone no treatment. When incubating the drug alone, an apoptosis triggering effect that seems to last up to 48 hours but doesn't induce an immediate apoptosis and also doesn't affect the whole population of cells was observed.
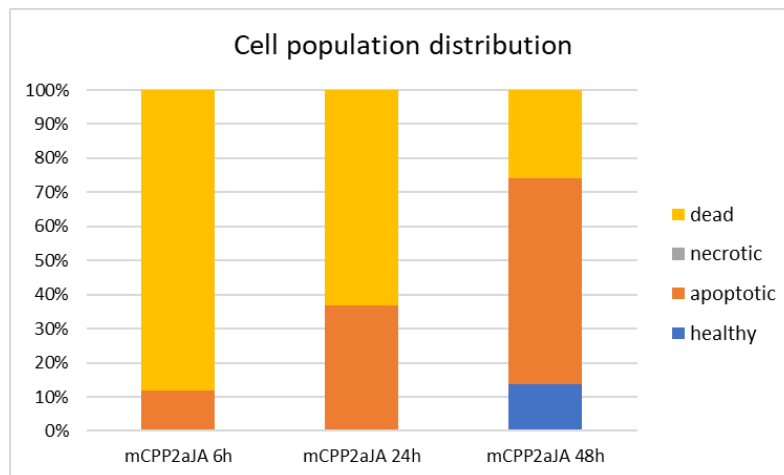
Figure 32. Cell population distribution resulting from Hela treatment with mCPP2aJA at 20 µM for different incubation time

Investigation with mCPP2aJA revealed that it does indeed trigger apoptosis and not necrosis (Fig 32). Contrary to the effect observed with the drug alone, the PDC exhibit a rapid response. Apoptosis is initiated as early as 6 hours, resulting in a significant reduction in the number of viable cells. After 24 and then 48 hours this effect is slowed down and some healthy cells repopulate, backing up the hypothesis that this conjugate exhibit a fast-killing effect that is unfortunately not strong enough to kill the whole population resulting in some leftover cells that can re proliferate once the peptide is degraded. The overall conclusion from this biological evaluation is that mCPP2aJA does indeed have a toxic effect on cancerous cells but only a limited one that does not result in full clearance of the cell population which can thereafter survive.

6. Conclusion

Addressing cancer is indeed a complex challenge due to the characteristics of this disease.[131] Cancer cells have acquired various mechanisms to promote their survival and invasion, leading to resistance against many therapeutic approaches. These characteristics are often referred to as the hallmarks of cancer.[35] One crucial aspect of cancer progression is the hijacking of mitochondria by cancer cells. Mitochondria play a crucial role in sustaining the proliferative growth of tumors. Cancer cells often undergo metabolic reprogramming, shifting their energy production from OXPHOS to glycolysis, a phenomenon known as the Warburg effect.[35,36] This altered metabolism allows cancer cells to rely more on glycolysis for ATP production, even in the presence of oxygen. This metabolic adaptation provides them with the necessary energy and building blocks for rapid proliferation.

Mitochondria also play a vital role in regulating apoptosis, a programmed cell death pathway that eliminates abnormal cells.[43] Cancer cells exhibit dysregulation of apoptosis, often evading this cellular death pathway. One key aspect is the overexpression of anti-apoptotic proteins from the Bcl-2 family in cancer cell mitochondria. These proteins prevent the release of pro-apoptotic factors and inhibit the initiation of apoptosis. Additionally, cancer cells often downregulate the expression of pro-apoptotic proteins, further tilting the balance towards cell survival.[43]

Thereof this close relation between mitochondria and cancer has attracted attention from scientist as a potential way to treat cancer in the last decades.[49,50] However, targeting of mitochondria for drug delivery requires specific characteristics as this organelle is located in the cytosol and possesses a double membrane rendering it particularly difficult to target. Nevertheless, a variety of targeting drug delivery systems have been developed relying on targeting moieties such as DLC or MTS.[132] MTS are the transporter of nuclear proteins essential to mitochondria and can be exploited as a natural targeting system to target this organelle with the drawback of not being able to cross cellular membranes.[30,133] To overcome this limitation in the frame of this project I associated MTS to CPP to obtain mCPPs for mitochondria drug delivery. The design of the original mCPP was presented in a previous work, with the fusion of ALD5, a modified MTS, and sC18 a CPP derived from an antimicrobial peptide with the ability to safely cross cellular membranes.[106] Inspired by this promising work the design of this mCPP was optimized by modifying the CPP part, as well as, the drug payload. In place of Chlorambucil, which suffered from degradation, Jasmonic acid was chosen for its ability to induce mitochondrial apoptosis. This plant stress hormone possesses the ability to restore apoptosis in cancerous cell lines with the limitation of not being able to cross cellular membrane and having a poor activity.[117,134] Therefore, coupling it to a mitochondria targeted carrier has the potential of countering those limitations and revealing the full potential of JA. Finally, in order to better understand the activity of PDC, payload coupling position was varied yielding "a", "b" and "c" conjugates.

The structure of peptides plays a crucial role in their cell penetrative capacity. In the project, the first evaluation focused on the structure characterization of the mCPPs. The individual parts of the mCPPs were evaluated separately in a buffer, and both exhibited a random coil structure. However, upon the addition of TFE (trifluoroethanol), a structuring additive, an interesting observation was made.

The TFE had no effect on the structuration of the mitochondrial targeting sequence (MTS), indicating that it does not possess any inherent structure. On the other hand, the addition of TFE induced a strong alpha-helix structuration in the cell-penetrating peptide (CPP) part, with R-values (representing the percentage of alpha-helix content) exceeding 80% at 50% TFE concentration. This effect was consistent across different versions of the mCPPs, indicating that the CPP part is primarily responsible for inducing the structuration of the MTS. This finding suggests that the CPP part plays a crucial role in the overall structure and function of the mCPPs.

Further evaluation was conducted by increasing the TFE concentration for the different mCPP versions. It was observed that an alpha-helix structure was achieved for the mCPPs starting at 20% TFE concentration. Interestingly, mCPP2 exhibited a stronger alpha-helix structuration with an R-value of 93% at 50% TFE, while it was 84% for mCPP1 and 75% for mCPP3. This suggests that the removal of the negative charge associated with Glu31 in mCPP2 resulted in a stronger structuration compared to the original mCPP1. On the other hand, the removal of the last four amino acids in mCPP3 led to a loss in structuration, which can be attributed to the overall shorter sequence and reduced intramolecular interaction.

The evaluation was completed by examining the structure of the peptide-drug conjugate (PDC). It was observed that the addition of a payload, regardless of its position, did not affect the structuring effect induced by the mCPPs. This suggests that the cargo did not interfere with the structural characteristics of the mCPPs.

Another parameter to consider for cellular internalization is the amphipathicity of the sequence as this specific charge distribution can influence membrane interaction with constituting phospholipids.[85] Moreover, amphipathicity is a structural feature of MTS required for their interaction with mitochondrial membranes and internalization.[124] Considering this dual importance of amphipathicity, mCPPs sequence were evaluated via a wheel projection tool to observe the charge distribution adopted by the peptides. Upon the different sequences a charge distribution exhibiting a hydrophilic face and a hydrophobic face to the helix was observed attesting the amphipathicity of the mCPPs. An important observation is the reduced hydrophilic face size of mCPP3, which can be attributed to the deletion of amino acids. Finally, those observations also apply to the different PDC, confirming that the payload conjugation doesn't affect structure.

The cellular uptake evaluation of fluorophore-labeled mCPPs provided valuable insights into the influence of structural modifications on cell penetrative capacity. In Hela cells, a

cancerous cell line, it was observed that the uptake of mCPP2 was significantly increased compared to the original mCPP1, regardless of the concentration or incubation time. This suggests that the structural modifications in mCPP2 enhance its ability to enter the cells effectively.

On the other hand, the uptake of mCPP3, which had amino acid deletions compared to mCPP1, was reduced in comparison to mCPP1. This highlights the detrimental influence of the deleted amino acids on the cell penetrative capacity of the peptide. The presence or absence of specific amino acids can have a significant impact on the peptide's interaction with the cellular membrane and its ability to internalize.

Furthermore, it was observed that the presence of FBS during incubation caused a strong decrease in the cell penetrative efficiency of the mCPPs. This can be attributed to the interaction between the mCPPs and the protein mix present in FBS, leading to a strong association that the mCPPs cannot dissociate from. As a result, the mCPPs are unable to effectively internalize in the cells.

3 different incubation times and 2 concentrations were evaluated, and it was observed that the uptake increased with those two factors revealing a time-concentration dependent uptake. Next was evaluated the uptake in Molt-4 cells, a blood cancer cell line in suspension. In this cell line the same time-concentration dependent uptake was observed with the same ranking between sequences. However, the uptake in Molt-4 was highly increased in comparison to the one observed in Hela cells suggesting a stronger membrane-peptide interaction. Finally, uptake was evaluated in HEK-293 cells, a human kidney embryonic cell line, as a model of healthy cells and interestingly the uptake of the mCPPs was highly decreased in comparison to the previous two cell lines. From this result it can be hypothesized that the mCPPs exhibit cancer targeting features that can be associated to the difference in membranes.[36]

Tracking peptides in the cells with fluorescence microscopy deepened the understanding of each mCPP behavior. The time-concentration uptake was confirmed in images where a stronger signal can be observed with higher concentration while for short incubation only partial signal was received from internalized mCPPs. Following the uptake profiles, it appeared that mCPP2 exhibit the fastest uptake, as at equal incubation time, it has the most signal internalized in comparison to mCPP1 and mCPP3. In Hela cells, only partial mitochondria co-localization is observed but it seems to be following the same behavior as for the uptake, with longer incubation time the co-localization increased. Rest of the peptides seems to be either stuck at the membrane or entrapped in vesicles which can be attributed to endosomal entrapment. Among the different mCPPs different behavior can be observed with mCPP1 and mCPP2 exhibiting a fast uptake, for mCPP2 co-localization spot can be observed after 15 minutes only, that increase over time. Regarding mCPP3, the uptake process is slower and

requires more time compared to mCPP1 and mCPP2. However, after 180 minutes, significant co-localization spots can be observed. Despite the lower accumulation profile of mCPP3, the overall results are comparable to those obtained with mCPP1 and mCPP2. Evaluation in HEK-293 cells revealed a different behavior. Uptake in this cell line is still time and concentration dependent, however most of the peptide signal seems to be either at the cellular membrane or colocalized with mitochondria. Therefore, the targeting ability of the mCPPs seems to be retained in this healthy cell line but the difference in membrane with Hela cells seems to be resulting in a low uptake, which might require even longer incubation period.

Finally, the cytotoxicity of the peptides and PDCs was evaluated in the different cell lines. For all cell lines the peptide parts and the mCPPs are proven to be non-toxic at 24 and 48 hours of incubation, HEK-293 seems to tolerate mCPPs more than the other cell lines as a good viability is maintained up to 100 µM with mCPP3 being the less damaging for the cells. In Hela cells the limit concentration is at 50 µM for mCPP2, the most well tolerated sequence, followed by mCPP3 while mCPP1 is only tolerated up to 25 µM. In Molt-4 cells, the few peptides tested were really well tolerated exhibiting no toxicity up to 100 µM.

Regarding PDCs, in Hela cells the different PDCS are quite efficient in killing cells with EC_{50} in the low µM range. Evaluation of drug conjugate missing the MTS revealed a low activity, that can be associated to the tolerability of the CPPs and not the drug, thus highlighting the importance of mitochondrial targeting for JA effectiveness. Among all the PDCs, mCPP2aJA is the most efficient both at 24 and 48 hours, this result follows all the previous regarding mCPP2 sequence having the highest and fastest uptake. Comparing the PDCs on their sequence, their activity follows their uptake profile with mCPP2 drug conjugates having increased activity followed by mCPP1 and mCPP3 exhibiting decreased activity. However, similarly to uptake profile, for mCPP3 drug conjugates it is observed that their activity increase over longer incubation in Hela cells. Discussing the payload coupling position, there is no clear evidence that the drug position influences the efficacy of the PDC as all activities are in the same concentration range. However, comparing mCPP2 drug conjugates coupling the drug on the C-terminal side appears to be the most effective for the PDC activity, while the "b" position results in a decreased toxicity with even more effect over longer incubation, in contrast the "c" conjugate has a small decreased toxicity but more comparable to the "a" conjugate. Therefore, it can be concluded that for optimal toxicity the drug should be carried by the CPP part as it is probably interacting with mitochondrial membrane while the MTS takes the role of internalizing the mCPP.

Surprisingly, in Molt-4 cells mCPP2 drug conjugates were highly effective over 48 hours incubation in comparison the mCPP1bJA which exhibited a poor toxicity. Regardless of the coupling position "a" or "b" mCPP2 drug conjugates have an EC_{50} around 10 µM, suggesting that the coupling position have low effect in this cell line but the mCPP sequence plays the most. Considering the great tolerability of the mCPP alone it can be concluded that this cell line is highly sensible to JA due to the difference in viability between the mCPP and PDC, this results

goes in the direction of literature which was highlighting the sensibility of this cell line to JA.[115,117]

Finally, in HEK-293 cells the toxicity profile of different PDC followed a concentration dependent toxicity that cannot be fully attributed to the presence of JA. Indeed, in this cell line the EC_{50} are in the high µM range for both incubation time, suggesting that the activity could be associated to a toxic effect of high concentration of mCPPs. It is known that at high concentrations, the internalization pathway of CPPs can shift from endocytosis to direct penetration..[135] This change in mechanism, along with the potential membrane disturbance caused by high concentrations of CPPs, can contribute to the observed toxicity. Additionally, microscopy analysis revealed peptide aggregation, which could be correlated with this hypothesis. A noticeable result from cytotoxic evaluation in this cell line is the increased activity of mCPP3aJA in comparison to mCPP2 drug conjugates.

Completing this evaluation in healthy models, the hemolysis assay revealed a great tolerability for mCPPs and PDC even at high concentration. This parameter has a great significance for in vivo application has the PDC has to be well tolerated by the biological medium ensuring its safe passage.

In order to further characterize the cytotoxic activity of mCPP2aJA an apoptosis inducing assay was pursued in Hela cells over different incubation times. JA was first evaluated for its apoptosis inductive capacity which required only 6 hours to induce a strong apoptotic effect that evolve in dead cells over longer incubation. In contrast mCPP2aJA induced a fast-killing effect with a majority of dead cells at short incubation time, which evolves in a distribution between dead and apoptotic cells after 48 hours of incubation with a low concentration of 20 µM.

In conclusion, the design of new PDC based on an original mCPP revealed the influence of peptide sequence for uptake and activity. Removal of a simple Glu[31], for mCPP2, resulted in noticeable increase in uptake, highlight the influence of a negative charge in an overall highly cationic tail. Evaluation in different cell lines revealed an improved uptake, of those amphipathic helices in cancer cells in comparison to healthy model, suggesting a preferential interaction with tumors over healthy cells resulting in a potential cancer targeting ability of the mCPPs. Microscopy fluorescence confirmed the mitochondrial targeting of mCPPs; however, this targeting ability is limited as in Hela cells most of the signal received seems to be trapped in endosomes while in HEK-293 the peptide seems stuck on the membrane with good mitochondria colocalization for the internalized peptides. Interestingly, cytotoxicity in Hela cells revealed mCPP2aJA as the best candidate upon different incubation time. In comparison other mCPPs and payload coupling position have little influence on the activity. Further evaluation in Hela cells revealed an apoptosis triggering effect of both JA and mCPP2aJA with an observable fast killing effect of the PDC that can be associated to its fast uptake and internalization. Evaluation in another cancerous cell line, Molt-4, revealed a highly increased activity of PDC with a great tolerability of nude mCPPs, as this cell line is more sensible to JA.

In contrast to microscopy images, for HEK-293 where few colocalization spots were observed, PDCs activity in this cell line is highly decreased. This observation can be associated to the ability of JA to act only on cancerous cells while not disturbing healthy cells.[115] Completing the biological profile the relation of mCPPs and PDC with red blood cells is safe as they don't induce any hemolysis, an important factor for drug applicability.

Indeed, the findings from the evaluation of different PDCs highlight the impact of sequence changes on their efficiency and mode of action. The mCPP2aJA PDC demonstrates fast up-take, leading to rapid apoptosis and effective killing of cancerous cells. However, there is a potential for relapse as not all cancerous cells may be completely eliminated during the initial treatment. On the other hand, the PDC resulting from mCPP3 shows slower accumulation in cells but provides a longer-lasting effect with an increasing killing effect over time.

Designing and optimizing mitochondria-targeting delivery systems is an important strategy for improving cancer treatment. Peptides, as a delivery approach, offer promising options. However, one challenge is protease degradation, which can limit the effectiveness of peptide-based carriers. Nevertheless, this degradation can also be utilized advantageously to create traceless drug carriers, where the carrier peptide is efficiently degraded, leaving behind the active drug within the target cells. Other improvement could lie in the use of a more efficient payload. A limiting factor regarding usage of JA is the high concentration required for this ac-tivity which implies a consequent concentration for the PDCs.

There are still ample opportunities for further research and optimization to significantly en-hance the performance of this mitochondria targeted strategy. The performances of these second-generation mCPPs are highly encouraging, particularly due to their ability to induce toxicity at significantly lower concentrations than JA alone. The evaluation of viability in dif-ferent cell lines highlights the importance of assessing the behavior of mCPPs in various cel-lular contexts.

7. Materials and methods

7.1. Materials

All Nα-Fmoc protected amino acids were purchased from IRIS Biotech (Marktredwitz, Germany). Used chemicals and consumables, unless otherwise noted, were obtained from Fluka (Taufkirchen, Germany), Merck (Darmstadt, Germany), Sarstedt (Nümbrecht, Germany), Sigma-Aldrich (Taufkirchen, Germany) and VWR (Darmstadt, Germany).

7.2. Peptide synthesis

All peptides were synthesized following standard Fmoc/tBu-strategy using an automated multiple solid-phase peptide synthesizer Syro I (multiSynTech). Peptides were prepared as C-terminal amides using Rink amide resin.

7.3. Peptide drug conjugates and fluorophore-labeled synthesis

To let the amine on the N-terminal side free, conjugation of CF or JA had to be performed on the C-terminal side via side-chain modification of the Lysine at this position. Rink amide resin was loaded with Fmoc-Lys(Dde)-OH, as Dde is orthogonal to tBu/BOC and quasi-orthogonal to Fmoc. Therefore, Fmoc-protected resin (1 eq 15 μmol, 32 mg) was swelled in DCM (500 μL), in a syringe, for 30 min. After rinsing the resin with DMF (2x1mL) Fmoc protecting group was removed by exposing the resin to piperidine in DMF solution (30% v/v, 500 μL) for 30 min, and effective cleavage was monitored by Kaiser test. The coupling of Lys-Dde was performed with manual coupling conditions. Manual couplings were usually performed in 2 steps, the first being a reaction with 3 eq of Oxyma, DIC and to be coupled chemical for an overnight reaction at rt, then a second coupling was run with 3 eq of HATU, 3 eq of DIPEA and 3 eq of the chemical to be coupled for 2 to 3 hours at rt. Elongation was then pursued using robot synthesis. After full synthesis, the free N-termini of the peptides were protected using 10 eq of di-tert-butyl-dicarbonate and 1 eq of DIPEA in DCM (500μL) (2 h, rt). Afterward, Dde was cleaved using a 2% hydrazine in DMF solution (10*10 min* 500 μL). Finally, side chain modification was carried out with 2 to 3 manual coupling steps using the corresponding chemical to couple.

For conjugates with a coupling position inside the peptide sequence the first part of the sequence was synthesized via robot synthesis. Thereafter, Lys-Dde was introduced via 2-3 manual couplings and monitored via Kaiser test and finally following the previous protocol for elongation.

7.4. Peptide purification

Peptides were cleaved from the resins using trifluoroacetic acid TFA/TIS /water (95:2.5:2.5, v/v/v/, 1 mL) within 3 h at rt, whereby also all acid-label protecting groups were removed. In the following the peptides were precipitated in ice-cold diethyl ether (10 mL), washed, dissolved in a mixture of H_2O: tert-butanol (3:1, v/v, 1 mL), and lyophilized.

Analytical data were obtained from RP-HPLC (Chromolith®Performance RP-18e, 100-4.6mm, Merck) using a gradient from 10 to 60% of acetonitrile (ACN) in H2O with 0.1% formic acid for sample separation, followed by electrospray ionization mass spectrometry (ESI/MS, Thermo Scientific LTQ-XL) measurements.

Purification of peptides was achieved by preparative RP-HPLC (Hitachi Elite LaChrom) on a Nucleodur C18ec;100-5; Macherey-Nagel using linear gradients of 10–60% B in A (A = 0.1%TFA in water; B = 0.1% TFA in ACN) over 45 min and a flow rate of 6 mL.min−1. After the combination of the peptide-containing fractions, samples were again freeze-dried and stock solutions were prepared.

7.5. Circular dichroism (CD) spectroscopy

CD spectra were recorded using a JASCO J-715 spectropolarimeter (JASCO, Pfungstadt, Germany) in an N2 atmosphere. The CD spectra were measured from 180 nm to 270 nm in 0.5 nm intervals at 20 °C using a 1 mm quartz cuvette and the instrument parameters were set as follows: sensitivity, 100 mdeg; scan mode, continuous; scan speed, 50 nm/min; response time, 2 s and bandwidth, 1.0 nm; 20 µM peptide solutions in 10 mM potassium phosphate buffer (pH 7.0) were inspected containing either 0 or 50% (v/v) trifluoroethanol (TFE). The resulting signal was converted from ellipticity (mdeg) to molar ellipticity $[\Theta]$ in deg.*cm2*dmol-1. R-values are a good indicator to confirm the α-helical character of peptides. They were calculated by taking the ratio between the molar ellipticity at 222 nm and 207 nm (R-value = $[\Theta]$222/ $[\Theta]$207).[127]

7.6. Cell culture

HeLa (human epithelial cervical cancer) and HEK-293 (immortalized human embryonic kidney) cells were cultured as sub confluent monolayers in 10 cm petri dishes at 37 °C, in a humidified atmosphere containing 5% CO2.

Molt-4 (human T lymphoblast) cells were cultured in suspension in 50 mL flask within the same atmosphere.

All cell lines were maintained in RPMI 1640 medium with 10% FBS and 4 mM glutamine.

When reaching confluency ~ 80–90%, adherent cells were splitted by using trypsin-EDTA w/ phenol red (euroclone) for cell detachment. Molt-4 cells were passaged when reaching 2x106 cells/mL and diluted to 2-4x105 cells/mL. The seeding of the cells for each experiment was adjusted to the cell line and disclosed in the associated part. However, cells were always grown to a confluency of up to 80%. All experiments were performed a minimum of twice in triplicates.

7.7. Cell viability

To determine the cell viability and cytotoxic effect of our peptides, cells were seeded (HeLa: $1\text{-}2\times10^3$; HEK-293: $2.5\text{x}10^4$ Molt-4: $2\text{x}10^4$) in 96-well plates and grown over 24h. On the next day, cells were incubated with different peptide concentrations in the appropriate FBS-free medium.

After 24 the cell viability was determined using a resazurin-based cytotoxicity assay (Sigma Aldrich), which is based on the reduction of resazurin to resofurin by metabolically active cells. Cells were washed twice with PBS, while the positive controls were treated for 10 min with 70% EtOH. Cells were incubated with a 1:10 dilution of the reagent (v/v, in FBS-free medium) for 1–2 h at 37 °C The resofurin product was monitored at 595 nm (λex= 550 nm) on a Tecan infinite M200 plate reader.

After 48h the cell viability was determined using CellTiter-Glo® (Promega) Luminescent Cell Viability Assay which is a homogeneous method for the determination of viable cells via quantitation of the ATP present, an indicator of metabolically active cells. After adding 50 µL/well of CellTiter-Glo plates were incubated for 10 min in the dark on a plate shaker at rt before reading luminescence using a microplate reader (Victor Nivo Multimode plate reader) with an emission filter blocking over 700 nm wavelengths.

7.8. Cellular uptake

To investigate the cellular uptake of the designed peptides, flow cytometry experiments were performed. Cells were seeded (Hela: 1×10^5; HEK-293: 2×10^5; Molt-4: 1×10^5) in 12-well plates and grown to subconfluency ($\sim$ 70 - 80%) o/n. On the next day, fluorophore-labeled peptides were incubated for 30 min in the appropriate FBS-free medium. After the incubation, Hela cells were washed with PBS, detached, and resuspended complete medium before centrifugation at 1200 rpm for 5 min. For Molt-4 cells, the same protocol was followed with centrifugation steps before removing medium.

The cell pellet was resuspended in 200 µL PBS and 100 µL transferred to a 96 U-well transparent plate. Cellular uptake was determined with the guava easyCyte™System (Merck) using the GRN-B (525/30) and the RED-B (695/50) channel, counting 20,000 cells per well.

7.9. Peptide internalization and subcellular colocalization

To get more insights into the internalization of the peptides, confocal laser scanning microscopy was pursued. Therefore, cells were seeded (HeLa: $3 - 4 \times 10^4$) in a µ-slide eight-well plate (Ibidi) and grown to subconfluency ($\sim$ 70 - 80%). On the next day, cells were stained with Mitotracker™ (100 nM of Red CMXRos, Thermo Fischer Scientific) for 30 min. Then medium was replaced with fluorophore-labeled peptides in the appropriate FBS-free medium and incubated for 15, 30, 60 or 180 min before adding Hoechst 33342 nuclear dye, for an additional 10 min nuclear staining. Finally, the cells were washed twice with PBS and fresh

medium added. For fixation cells were incubated in medium supplemented with 4% para-formaldehyde for 30 min at 4°C. Microscopic analysis was performed on a Nikon Eclipse Ti confocal laser scanning microscope equipped with a 60× oil-immersion objective (N.A. 1.4, Plan APO VC; Nikon). Pictures were taken with EZ-C1 3.91 software and processed with Image J.

7.10. Apoptosis evaluation via annexin V/Propidium iodide staining

Cells were seeded (Hela: 1×10^5) in 12 wells plates and grown over 24h. On the next day, cells were incubated with different peptide concentrations in the appropriate FBS-free medium. After different incubation time points, cells were washed in PBS, detached via trypsinization, and resuspended in FBS-completed media. After centrifugation at 1200 rpm for 5 min, the cell pellet was resuspended in Annexin-V Buffer (50 mM HEPES, 700 mM NaCl, 12.5 mM CaCl2, pH 7.4 diluted from 5X to 1X) and diluted to reach 1×10^6 cells/mL, 100 µL of this cell solution were transferred to an Eppendorf tube. Alexa Fluor® 488 annexin V (Solution in 25 mM HEPES, 140 mM NaCl, 1 mM EDTA, pH 7.4, 0.1% bovine serum albumin (BSA), 5 µL) and Propidium iodide (1 mg/mL, final concentration 50 ng/mL, solution in deionized water diluted to 50 µg/mL with Annexin V buffer, 1 µL) were added and samples incubated in the dark for 15 min at rt. Samples were then diluted by gently adding 400 µL of annexin V buffer and 100 µL of this final solution was transferred to a transparent U bottom 96 wells-plate and ana-lyzed using a BD Accuri™ C6 Plus Flow Cytometer with a laser (λex= 488 nm) and FITC (λem= 533/30 nm) PerpCP (λem= 670 nm) filters counting a minimum of 10.000 events. Data were analyzed using FCS express software.

7.11. Hemolysis assay

In order to investigate the hemolytic activity of peptides, human red blood cells (RBCs) were washed five times with PBS at 4 °C and centrifugated at 3.000 g for 5 min and diluted to 5 % (v/v in PBS). 100 µL of this solution were transferred into a fresh 96-well plate. 50 µL peptide solution (0.5 µM – 25 µM) were added and gently resuspended. Red blood cells were incu-bated for 24 h at 37 °C and 5 % CO2. 50 µL of 10 % Triton-X-100 were added 10 min prior to the ending of incubation time and served as positive control. After incubation, cells were cen-trifuged (rt, 2.500 g, 3 min). The supernatant was carefully transferred into a fresh 96-well plate and the absorption at 560 nm was measured on a Tecan infinite M200 plate reader. The measured absorption was correlated to the hemoglobin concentration.

8. References

(1)   Cavalier-Smith, T. Origin of Mitochondria by Intracellular Enslavement of a Photosynthetic Purple Bacterium. *Proc. R. Soc. B Biol. Sci.* **2006**, *273* (1596), 1943. https://doi.org/10.1098/RSPB.2006.3531.

(2)   Sagan, L. On the Origin of Mitosing Cells. *J. Theor. Biol.* **1967**, *14* (3), 225-IN6. https://doi.org/10.1016/0022-5193(67)90079-3.

(3)   Giacomello, M.; Pyakurel, A.; Glytsou, C.; Scorrano, L. The Cell Biology of Mitochondrial Membrane Dynamics. *Nat. Rev. Mol. Cell Biol. 2020 214* **2020**, *21* (4), 204–224. https://doi.org/10.1038/s41580-020-0210-7.

(4)   Walsh, C. T.; Tu, B. P.; Tang, Y. Eight Kinetically Stable but Thermodynamically Activated Molecules That Power Cell Metabolism. *Chem. Rev.* **2018**, *118* (4), 1460. https://doi.org/10.1021/ACS.CHEMREV.7B00510.

(5)   Spinelli, J. B.; Haigis, M. C. The Multifaceted Contributions of Mitochondria to Cellular Metabolism. *Nat. Cell Biol. 2018 207* **2018**, *20* (7), 745–754. https://doi.org/10.1038/s41556-018-0124-1.

(6)   Marchi, S.; Giorgi, C.; Suski, J. M.; Agnoletto, C.; Bononi, A.; Bonora, M.; De Marchi, E.; Missiroli, S.; Patergnani, S.; Poletti, F.; Rimessi, A.; Duszynski, J.; Wieckowski, M. R.; Pinton, P. Mitochondria-Ros Crosstalk in the Control of Cell Death and Aging. *Journal of Signal Transduction*. June 26, 2011. https://www.hindawi.com/journals/jst/2012/329635/.

(7)   Murphy, M. P. How Mitochondria Produce Reactive Oxygen Species. *Biochem. J.* **2009**, *417* (1), 1–13. https://doi.org/10.1042/BJ20081386.

(8)   Loschen, G.; Azzi, A.; Richter, C.; Flohé, L. Superoxide Radicals as Precursors of Mitochondrial Hydrogen Peroxide. *FEBS Lett.* **1974**, *42* (1), 68–72. https://doi.org/10.1016/0014-5793(74)80281-4.

(9)   Giannopolitis, C. N.; Ries, S. K. Superoxide Dismutases: I. Occurrence in Higher Plants. *Plant Physiol.* **1977**, *59* (2), 309–314. https://doi.org/10.1104/pp.59.2.309.

(10)   Radi, R.; Turrens, J. F.; Chang, L. Y.; Bush, K. M.; Crapo, J. D.; Freeman, B. A. Detection of Catalase in Rat Heart Mitochondria. *J. Biol. Chem.* **1991**, *266* (32), 22028–22034. https://doi.org/10.1016/s0021-9258(18)54740-2.

(11)   Taylor, S. W.; Fahy, E.; Zhang, B.; Glenn, G. M.; Warnock, D. E.; Wiley, S.; Murphy, A. N.; Gaucher, S. P.; Capaldi, R. A.; Gibson, B. W.; Ghosh, S. S. Characterization of the Human Heart Mitochondrial Proteome. *Nat. Biotechnol.* **2003**, *21* (3), 281–286. https://doi.org/10.1038/nbt793.

(12)   Joubert, F.; Fales, H. M.; Wen, H.; Combs, C. A.; Balaban, R. S. NADH Enzyme-Dependent Fluorescence Recovery after Photobleaching (ED-FRAP): Applications to Enzyme and Mitochondrial Reaction Kinetics, In Vitro. *Biophys. J.* **2004**, *86* (1 I), 629–645. https://doi.org/10.1016/S0006-3495(04)74141-7.

(13)   Orii, Y. The Cytochrome c Peroxidase Activity of Cytochrome Oxidase. *J. Biol. Chem.* **1982**, *257* (16), 9246–9248. https://doi.org/10.1016/s0021-9258(18)34056-0.

(14)   Clayton, D. A. TRANSCRIPTION OF THE MAMMALIAN MITOCHONDRIAL GENOME. *Annu. Rev. Biochem.* **1984**, *53* (1), 573–594. https://doi.org/10.1146/annurev.bi.53.070184.003041.

(15)   Croteau, D. L.; Bohr, V. A. Repair of Oxidative Damage to Nuclear and Mitochondrial DNA in Mammalian Cells. *Journal of Biological Chemistry*. Elsevier October 10, 1997, pp 25409–25412. https://doi.org/10.1074/jbc.272.41.25409.

(16)   Wallace, D. C. Mitochondrial DNA Mutations in Disease and Aging. *Environ. Mol. Mutagen.* **2010**, *51* (5), n/a-n/a. https://doi.org/10.1002/em.20586.

(17)   Seol, S.-Y. J. & D.-W.; *. The Role of Mitochondria in Apoptosis. *BMB Rep.* **2008**, *41* (1), 011–022.

(18)   Bock, F. J.; Tait, S. W. G. Mitochondria as Multifaceted Regulators of Cell Death. *Nature Reviews Molecular Cell Biology*. Nature Research February 1, 2020, pp 85–100. https://doi.org/10.1038/s41580-019-0173-8.

(19)   Boatright, K. M.; Renatus, M.; Scott, F. L.; Sperandio, S.; Shin, H.; Pedersen, I. M.; Ricci, J. E.; Edris, W. A.; Sutherlin, D. P.; Green, D. R.; Salvesen, G. S. A Unified Model for Apical Caspase Activation. *Mol. Cell* **2003**, *11* (2), 529–541. https://doi.org/10.1016/S1097-2765(03)00051-0.

(20)   Tsujimoto, Y.; Shimizu, S. The Voltage-Dependent Anion Channel: An Essential Player in Apoptosis. *Biochimie* **2002**, *84* (2–3), 187–193. https://doi.org/10.1016/S0300-9084(02)01370-6.

(21)   Sinha, K.; Das, J.; Pal, P. B.; Sil, P. C. Oxidative Stress: The Mitochondria-Dependent and Mitochondria-Independent Pathways of Apoptosis. *Archives of Toxicology*. Springer July 30, 2013, pp 1157–1180. https://doi.org/10.1007/s00204-013-1034-4.

(22)   Circu, M. L.; Aw, T. Y. Glutathione and Modulation of Cell Apoptosis. *Biochimica et Biophysica Acta - Molecular Cell Research*. Elsevier October 1, 2012, pp 1767–1777. https://doi.org/10.1016/j.bbamcr.2012.06.019.

(23)   Mayer, B.; Oberbauer, R. Mitochondrial Regulation of Apoptosis. *Physiology* **2003**, *18* (3), 89–94. https://doi.org/10.1152/nips.01433.2002.

(24)   Baines, C. P. Role of the Mitochondrion in Programmed Necrosis. *Front. Physiol.* **2010**, *1 NOV*. https://doi.org/10.3389/fphys.2010.00156.

(25)   Chacinska, A.; Koehler, C. M.; Milenkovic, D.; Lithgow, T.; Pfanner, N. Importing Mitochondrial Proteins: Machineries and Mechanisms. *Cell* **2009**, *138* (4), 628. https://doi.org/10.1016/J.CELL.2009.08.005.

(26)   Campo, M. L.; Peixoto, P. M.; Martínez-Caballero, S. Revisiting Trends on Mitochondrial Mega-Channels for the Import of Proteins and Nucleic Acids. *J. Bioenerg. Biomembr. 2016 491* **2016**, *49* (1), 75–99. https://doi.org/10.1007/S10863-016-9662-Z.

(27)   Gakh, O.; Cavadini, P.; Isaya, G. Mitochondrial Processing Peptidases. *Biochim. Biophys. Acta - Mol. Cell Res.* **2002**, *1592* (1), 63–77. https://doi.org/10.1016/S0167-4889(02)00265-3.

(28)   Wenz, L. S.; Opaliński, Ł.; Wiedemann, N.; Becker, T. Cooperation of Protein Machineries in Mitochondrial Protein Sorting. *Biochimica et Biophysica Acta - Molecular Cell Research*. Elsevier May 1, 2015, pp 1119–1129. https://doi.org/10.1016/j.bbamcr.2015.01.012.

(29)   Becker, T.; Böttinger, L.; Pfanner, N. Mitochondrial Protein Import: From Transport Pathways to an Integrated Network. *Trends Biochem. Sci.* **2012**, *37* (3), 85–91. https://doi.org/10.1016/j.tibs.2011.11.004.

(30)   Schatz, G. The Protein Import System of Mitochondria. *J. Biol. Chem.* **1996**, *271* (50), 31763–31766. https://doi.org/10.1074/JBC.271.50.31763.

(31)   Jean, S. R.; Ahmed, M.; Lei, E. K.; Wisnovsky, S. P.; Kelley, S. O. Peptide-Mediated Delivery of Chemical Probes and Therapeutics to Mitochondria. *Acc. Chem. Res.* **2016**, *49* (9), 1893–1902. https://doi.org/10.1021/acs.accounts.6b00277.

(32)   Sung, H.; Ferlay, J.; Siegel, R. L.; Laversanne, M.; Soerjomataram, I.; Jemal, A.; Bray, F. Global Cancer Statistics 2020: GLOBOCAN Estimates of Incidence and Mortality Worldwide for 36 Cancers in 185 Countries. *CA. Cancer J. Clin.* **2021**, *71* (3), 209–249. https://doi.org/10.3322/CAAC.21660.

(33)   Debela, D. T.; Muzazu, S. G. Y.; Heraro, K. D.; Ndalama, M. T.; Mesele, B. W.; Haile, D. C.; Kitui, S. K.; Manyazewal, T. New Approaches and Procedures for Cancer Treatment: Current Perspectives. *SAGE Open Medicine*. SAGE Publications Ltd 2021. https://doi.org/10.1177/20503121211034366.

(34)   Hanahan, D.; Weinberg, R. A. The Hallmarks of Cancer. *Cell* **2000**, *100* (1), 57–70. https://doi.org/10.1016/S0092-8674(00)81683-9.

(35)   Hanahan, D.; Weinberg, R. A. Hallmarks of Cancer: The Next Generation. *Cell* **2011**, *144* (5), 646–674. https://doi.org/10.1016/J.CELL.2011.02.013.

(36)   Pavlova, N. N.; Thompson, C. B. THE EMERGING HALLMARKS OF CANCER METABOLISM. *Cell Metab.* **2016**, *23* (1), 27. https://doi.org/10.1016/J.CMET.2015.12.006.

(37)   Cheng, N.; Chytil, A.; Shyr, Y.; Joly, A.; Moses, H. L. Transforming Growth Factor-β Signaling-Deficient Fibroblasts Enhance Hepatocyte Growth Factor Signaling in Mammary Carcinoma Cells to Promote Scattering and Invasion. *Mol. Cancer Res.* **2008**, *6* (10), 1521–1533. https://doi.org/10.1158/1541-7786.MCR-07-2203.

(38)   Shaw, R. J. Tumor Suppression by LKB1: SIK-Ness Prevents Metastasis. *Science Signaling*. American Association for the Advancement of Science September 1, 2009. https://doi.org/10.1126/scisignal.286pe55.

(39)   Shay, J. W.; Wright, W. E. Hayflick, His Limit, and Cellular Ageing. *Nature Reviews Molecular Cell Biology*. European Association for Cardio-Thoracic Surgery 2000, pp 72–76. https://doi.org/10.1038/35036093.

(40)   Blasco, M. A. Telomeres and Human Disease: Ageing, Cancer and Beyond. *Nature Reviews Genetics*. Nature Publishing Group August 2005, pp 611–622. https://doi.org/10.1038/nrg1656.

(41)   Hanahan, D.; Folkman, J. Patterns and Emerging Mechanisms of the Angiogenic Switch during Tumorigenesis. *Cell*. Cell Press August 9, 1996, pp 353–364. https://doi.org/10.1016/S0092-8674(00)80108-7.

(42)   Talmadge, J. E.; Fidler, I. J. AACR Centennial Series: The Biology of Cancer Metastasis: Historical Perspective. *Cancer Research*. American Association for Cancer Research July 15, 2010, pp 5649–5669. https://doi.org/10.1158/0008-5472.CAN-10-1040.

(43)   Chaudhry, G.-E.-S.; Akim, A. M.; Sung, Y. Y.; Sifzizul, T.; Muhammad, T. Cancer and Apoptosis. **2022**, 191–210. https://doi.org/10.1007/978-1-0716-2553-8_16.

(44)   Vyas, S.; Zaganjor, E.; Haigis, M. C. Mitochondria and Cancer. *Cell*. Cell Press July 28, 2016, pp 555–566. https://doi.org/10.1016/j.cell.2016.07.002.

(45)   Piskounova, E.; Agathocleous, M.; Murphy, M. M.; Hu, Z.; Huddlestun, S. E.; Zhao, Z.; Leitch, A. M.; Johnson, T. M.; DeBerardinis, R. J.; Morrison, S. J. Oxidative Stress Inhibits Distant Metastasis by Human Melanoma Cells. *Nature* **2015**, *527* (7577), 186–191. https://doi.org/10.1038/nature15726.

(46)   Denicola, G. M.; Karreth, F. A.; Humpton, T. J.; Gopinathan, A.; Wei, C.; Frese, K.; Mangal, D.; Yu, K. H.; Yeo, C. J.; Calhoun, E. S.; Scrimieri, F.; Winter, J. M.; Hruban, R. H.; Iacobuzio-Donahue, C.; Kern, S. E.; Blair, I. A.; Tuveson, D. A. Oncogene-Induced Nrf2 Transcription Promotes ROS Detoxification and Tumorigenesis. *Nature* **2011**, *475* (7354), 106–110. https://doi.org/10.1038/nature10189.

(47) Yang, Y.; Karakhanova, S.; Hartwig, W.; D'Haese, J. G.; Philippov, P. P.; Werner, J.; Bazhin, A. V. Mitochondria and Mitochondrial ROS in Cancer: Novel Targets for Anticancer Therapy. *J. Cell. Physiol.* **2016**, *231* (12), 2570–2581. https://doi.org/10.1002/jcp.25349.

(48) Wagner, A.; Kosnacova, H.; Chovanec, M.; Jurkovicova, D. Mitochondrial Genetic and Epigenetic Regulations in Cancer: Therapeutic Potential. *Int. J. Mol. Sci.* **2022**, *23* (14), 7897. https://doi.org/10.3390/IJMS23147897.

(49) Sainero-Alcolado, L.; Liaño-Pons, J.; Ruiz-Pérez, M. V.; Arsenian-Henriksson, M. Targeting Mitochondrial Metabolism for Precision Medicine in Cancer. *Cell Death Differ. 2022* **2022**, 1–14. https://doi.org/10.1038/s41418-022-01022-y.

(50) Cho, H.; Cho, Y. Y.; Shim, M. S.; Lee, J. Y.; Lee, H. S.; Kang, H. C. Mitochondria-Targeted Drug Delivery in Cancers. *Biochim. Biophys. Acta - Mol. Basis Dis.* **2020**, *1866* (8), 165808. https://doi.org/10.1016/J.BBADIS.2020.165808.

(51) Zielonka, J.; Joseph, J.; Sikora, A.; Hardy, M.; Ouari, O.; Vasquez-Vivar, J.; Cheng, G.; Lopez, M.; Kalyanaraman, B. Mitochondria-Targeted Triphenylphosphonium-Based Compounds: Syntheses, Mechanisms of Action, and Therapeutic and Diagnostic Applications. *Chem. Rev.* **2017**, *117* (15), 10043–10120. https://doi.org/10.1021/ACS.CHEMREV.7B00042/ASSET/IMAGES/MEDIUM/CR-2017-00042Z_0036.GIF.

(52) Modica-Napolitano, J. S.; Aprille, J. R. Delocalized Lipophilic Cations Selectively Target the Mitochondria of Carcinoma Cells. *Adv. Drug Deliv. Rev.* **2001**, *49* (1–2), 63–70. https://doi.org/10.1016/S0169-409X(01)00125-9.

(53) Millard, M.; Gallagher, J. D.; Olenyuk, B. Z.; Neamati, N. A Selective Mitochondrial-Targeted Chlorambucil with Remarkable Cytotoxicity in Breast and Pancreatic Cancers. *J. Med. Chem.* **2013**, *56* (22), 9170–9179. https://doi.org/10.1021/jm4012438.

(54) Song, Y. F.; Liu, D. Z.; Cheng, Y.; Liu, M.; Ye, W. L.; Zhang, B. Le; Liu, X. Y.; Zhou, S. Y. Dual Subcellular Compartment Delivery of Doxorubicin to Overcome Drug Resistant and Enhance Antitumor Activity. *Sci. Rep.* **2015**, *5* (1), 1–19. https://doi.org/10.1038/srep16125.

(55) Christman, J. E.; Miller, D. S.; Coward, P.; Smith, L. H.; Teng, N. N. H. Study of the Selective Cytotoxic Properties of Cationic, Lipophilic Mitochondrial-Specific Compounds in Gynecologic Malignancies. *Gynecol. Oncol.* **1990**, *39* (1), 72–79. https://doi.org/10.1016/0090-8258(90)90402-7.

(56) Trnka, J.; Elkalaf, M.; Anděl, M. Lipophilic Triphenylphosphonium Cations Inhibit Mitochondrial Electron Transport Chain and Induce Mitochondrial Proton Leak. *PLoS One* **2015**, *10* (4), e0121837. https://doi.org/10.1371/journal.pone.0121837.

(57) Porteous, C. M.; Logan, A.; Evans, C.; Ledgerwood, E. C.; Menon, D. K.; Aigbirhio, F.;

Smith, R. A. J.; Murphy, M. P. Rapid Uptake of Lipophilic Triphenylphosphonium Cations by Mitochondria in Vivo Following Intravenous Injection: Implications for Mitochondria-Specific Therapies and Probes. *Biochim. Biophys. Acta - Gen. Subj.* **2010**, *1800* (9), 1009–1017. https://doi.org/10.1016/j.bbagen.2010.06.001.

(58)   Buchke, S.; Sharma, M.; Bora, A.; Relekar, M.; Bhanu, P.; Kumar, J. Mitochondria-Targeted, Nanoparticle-Based Drug-Delivery Systems: Therapeutics for Mitochondrial Disorders. *Life*. MDPI May 1, 2022, p 657. https://doi.org/10.3390/life12050657.

(59)   Wu, J. The Enhanced Permeability and Retention (Epr) Effect: The Significance of the Concept and Methods to Enhance Its Application. *Journal of Personalized Medicine*. MDPI August 1, 2021. https://doi.org/10.3390/jpm11080771.

(60)   Wongrakpanich, A.; Joiner, M. A.; Anderson, M. E.; Salem, A. K. Mitochondria-Targeting Particles. **2014**, *9*, 2531–2543.

(61)   Akbarzadeh, A.; Rezaei-Sadabady, R.; Davaran, S.; Joo, S. W.; Zarghami, N.; Hanifehpour, Y.; Samiei, M.; Kouhi, M.; Nejati-Koshki, K. Liposome: Classification, Preparation, and Applications. *Nanoscale Res. Lett.* **2013**, *8* (1), 1–9. https://doi.org/10.1186/1556-276X-8-102.

(62)   Zhang, L.; Yao, H. J.; Yu, Y.; Zhang, Y.; Li, R. J.; Ju, R. J.; Wang, X. X.; Sun, M. G.; Shi, J. F.; Lu, W. L. Mitochondrial Targeting Liposomes Incorporating Daunorubicin and Quinacrine for Treatment of Relapsed Breast Cancer Arising from Cancer Stem Cells. *Biomaterials* **2012**, *33* (2), 565–582. https://doi.org/10.1016/j.biomaterials.2011.09.055.

(63)   Vilar, G.; Tulla-Puche, J.; Albericio, F. Polymers and Drug Delivery Systems. *Curr. Drug Deliv.* **2012**, *9* (4), 367–394. https://doi.org/10.2174/156720112801323053.

(64)   Marrache, S.; Dhar, S. Engineering of Blended Nanoparticle Platform for Delivery of Mitochondria-Acting Therapeutics. *Proc. Natl. Acad. Sci. U. S. A.* **2012**, *109* (40), 16288–16293. https://doi.org/10.1073/pnas.1210096109.

(65)   Lv, W.; Zhang, Z.; Zhang, K. Y.; Yang, H.; Liu, S.; Xu, A.; Guo, S.; Zhao, Q.; Huang, W. A Mitochondria-Targeted Photosensitizer Showing Improved Photodynamic Therapy Effects Under Hypoxia. *Angew. Chemie Int. Ed.* **2016**, *55* (34), 9947–9951. https://doi.org/10.1002/anie.201604130.

(66)   Chen, D.; Zhang, J.; Tang, Y.; Huang, X.; Shao, J.; Si, W.; Ji, J.; Zhang, Q.; Huang, W.; Dong, X. A Tumor-Mitochondria Dual Targeted Aza-BODIPY-Based Nanotheranostic Agent for Multimodal Imaging-Guided Phototherapy. *J. Mater. Chem. B* **2018**, *6* (27), 4522–4530. https://doi.org/10.1039/c8tb01347k.

(67)   Li, G.; Wang, Q.; Liu, J.; Wu, M.; Ji, H.; Qin, Y.; Zhou, X.; Wu, L. Innovative Strategies for Enhanced Tumor Photodynamic Therapy. *J. Mater. Chem. B* **2021**, *9* (36), 7347–7370. https://doi.org/10.1039/d1tb01466h.

(68) Ke, L.; Zhang, C.; Liao, X.; Qiu, K.; Rees, T. W.; Chen, Y.; Zhao, Z.; Ji, L.; Chao, H. Mitochondria-Targeted Ir@AuNRs as Bifunctional Therapeutic Agents for Hypoxia Imaging and Photothermal Therapy. *Chem. Commun.* **2019**, *55* (69), 10273–10276. https://doi.org/10.1039/c9cc05610f.

(69) Zhang, D.; Wang, J.; Xu, D. Cell-Penetrating Peptides as Noninvasive Transmembrane Vectors for the Development of Novel Multifunctional Drug-Delivery Systems. *J. Control. Release* **2016**, *229*, 130–139. https://doi.org/10.1016/J.JCONREL.2016.03.020.

(70) Ruseska, I.; Zimmer, A. Internalization Mechanisms of Cell-Penetrating Peptides. *Beilstein J. Nanotechnol. 1110* **2020**, *11* (1), 101–123. https://doi.org/10.3762/BJNANO.11.10.

(71) Järver, P.; Langel, Ü. Cell-Penetrating Peptides—A Brief Introduction. *Biochim. Biophys. Acta - Biomembr.* **2006**, *1758* (3), 260–263. https://doi.org/10.1016/J.BBAMEM.2006.02.012.

(72) Gagat, M.; Zielińska, W.; Grzanka, A. Cell-Penetrating Peptides and Their Utility in Genome Function Modifications (Review). *International Journal of Molecular Medicine*. Spandidos Publications December 1, 2017, pp 1615–1623. https://doi.org/10.3892/ijmm.2017.3172.

(73) Trabulo, S.; Cardoso, A. L.; Mano, M.; de Lima, M. C. P. Cell-Penetrating Peptides-Mechanisms of Cellular Uptake and Generation of Delivery Systems. *Pharmaceuticals*. MDPI AG March 30, 2010, pp 961–993. https://doi.org/10.3390/ph3040961.

(74) Duchardt, F.; Fotin-Mleczek, M.; Schwarz, H.; Fischer, R.; Brock, R. A Comprehensive Model for the Cellular Uptake of Cationic Cell-Penetrating Peptides. *Traffic* **2007**, *8* (7), 848–866. https://doi.org/10.1111/j.1600-0854.2007.00572.x.

(75) Nakase, I.; Hirose, H.; Tanaka, G.; Tadokoro, A.; Kobayashi, S.; Takeuchi, T.; Futaki, S. Cell-Surface Accumulation of Flock House Virus-Derived Peptide Leads to Efficient Internalization via Macropinocytosis. *Mol. Ther.* **2009**, *17* (11), 1868–1876. https://doi.org/10.1038/mt.2009.192.

(76) Wadia, J. S.; Stan, R. V.; Dowdy, S. F. Transducible TAT-HA Fusogenic Peptide Enhances Escape of TAT-Fusion Proteins after Lipid Raft Macropinocytosis. *Nat. Med.* **2004**, *10* (3), 310–315. https://doi.org/10.1038/nm996.

(77) Xiang, S.; Tong, H.; Shi, Q.; Fernandes, J. C.; Jin, T.; Dai, K.; Zhang, X. Uptake Mechanisms of Non-Viral Gene Delivery. *Journal of Controlled Release*. Elsevier March 28, 2012, pp 371–378. https://doi.org/10.1016/j.jconrel.2011.09.093.

(78) Pujals, S.; Giralt, E. Proline-Rich, Amphipathic Cell-Penetrating Peptides. *Advanced Drug Delivery Reviews*. Elsevier March 1, 2008, pp 473–484. https://doi.org/10.1016/j.addr.2007.09.012.

(79)   Taylor, B. N.; Mehta, R. R.; Yamada, T.; Lekmine, F.; Christov, K.; Chakrabarty, A. M.; Green, A.; Bratescu, L.; Shilkaitis, A.; Beattie, C. W.; Das Gupta, T. K. Noncationic Peptides Obtained from Azurin Preferentially Enter Cancer Cells. *Cancer Res.* **2009**, *69* (2), 537–546. https://doi.org/10.1158/0008-5472.CAN-08-2932.

(80)   Ye, J.; Pei, X.; Cui, H.; Yu, Z.; Lee, H.; Wang, J.; Wang, X.; Sun, L.; He, H.; Yang, V. C. Cellular Uptake Mechanism and Comparative in Vitro Cytotoxicity Studies of Monomeric LMWP-SiRNA Conjugate. *J. Ind. Eng. Chem.* **2018**, *63*, 103–111. https://doi.org/10.1016/j.jiec.2018.02.005.

(81)   Ramsey, J. D.; Flynn, N. H. Cell-Penetrating Peptides Transport Therapeutics into Cells. *Pharmacol. Ther.* **2015**, *154*, 78–86. https://doi.org/10.1016/J.PHARMTHERA.2015.07.003.

(82)   Erazo-Oliveras, A.; Muthukrishnan, N.; Baker, R.; Wang, T.-Y.; Pellois, J.-P. Improving the Endosomal Escape of Cell-Penetrating Peptides and Their Cargos: Strategies and Challenges. *Pharmaceuticals* **2012**, *5* (11), 1177–1209. https://doi.org/10.3390/ph5111177.

(83)   Poon, G. M. K.; Gariépy, J. *Cell-Surface Proteoglycans as Molecular Portals for Cationic Peptide and Polymer Entry into Cells*; 2007; Vol. 35, pp 788–793. https://doi.org/10.1042/BST0350788.

(84)   Bechara, C.; Sagan, S. Cell-Penetrating Peptides: 20 Years Later, Where Do We Stand? *FEBS Lett.* **2013**, *587* (12), 1693–1702. https://doi.org/10.1016/J.FEBSLET.2013.04.031.

(85)   Deshayes, S.; Plénat, T.; Aldrian-Herrada, G.; Divita, G.; Le Grimellec, C.; Heitz, F. Primary Amphipathic Cell-Penetrating Peptides: Structural Requirements and Interactions with Model Membranes. *Biochemistry* **2004**, *43* (24), 7698–7706. https://doi.org/10.1021/bi049298m.

(86)   Walrant, A.; Correia, I.; Jiao, C. Y.; Lequin, O.; Bent, E. H.; Goasdoué, N.; Lacombe, C.; Chassaing, G.; Sagan, S.; Alves, I. D. Different Membrane Behaviour and Cellular Uptake of Three Basic Arginine-Rich Peptides. *Biochim. Biophys. Acta - Biomembr.* **2011**, *1808* (1), 382–393. https://doi.org/10.1016/j.bbamem.2010.09.009.

(87)   Eiríksdóttir, E.; Konate, K.; Langel, Ü.; Divita, G.; Deshayes, S. Secondary Structure of Cell-Penetrating Peptides Controls Membrane Interaction and Insertion. *Biochim. Biophys. Acta - Biomembr.* **2010**, *1798* (6), 1119–1128. https://doi.org/10.1016/j.bbamem.2010.03.005.

(88)   Neundorf, I.; Rennert, R.; Hoyer, J.; Schramm, F.; Löbner, K.; Kitanovic, I.; Wölfl, S. Fusion of a Short HA2-Derived Peptide Sequence to Cell-Penetrating Peptides Improves Cytosolic Uptake, but Enhances Cytotoxic Activity. *Pharm. 2009, Vol. 2, Pages 49-65* **2009**, *2* (2), 49–65. https://doi.org/10.3390/PH2020049.

(89) Henriques, S. T.; Melo, M. N.; Castanho, M. A. R. B. Cell-Penetrating Peptides and Antimicrobial Peptides: How Different Are They? *Biochemical Journal*. Portland Press Ltd October 1, 2006, pp 1–7. https://doi.org/10.1042/BJ20061100.

(90) Gronewold, A.; Horn, M.; Ranđelović, I.; Tóvári, J.; Muñoz Vázquez, S.; Schomäcker, K.; Neundorf, I. Characterization of a Cell-Penetrating Peptide with Potential Anticancer Activity. *ChemMedChem* **2017**, *12* (1), 42–49. https://doi.org/10.1002/cmdc.201600498.

(91) Reichart, F.; Horn, M.; Neundorf, I. Cyclization of a Cell-Penetrating Peptide via Click-Chemistry Increases Proteolytic Resistance and Improves Drug Delivery. *J. Pept. Sci.* **2016**, *22* (6), 421–426. https://doi.org/10.1002/psc.2885.

(92) Klein, A.; Haseloer, A.; Lützenburg, T.; Strache, J. P.; Neudörfl, J.; Neundorf, I. Building up Pt(II)-thiosemicarbazone-lysine-sC18 Conjugates. *ChemBioChem* **2020**, cbic.202000564. https://doi.org/10.1002/cbic.202000564.

(93) Reinhardt, A.; Neundorf, I. Design and Application of Antimicrobial Peptide Conjugates. *Int. J. Mol. Sci.* **2016**, *17* (5), 701. https://doi.org/10.3390/ijms17050701.

(94) Drexelius, M.; Reinhardt, A.; Grabeck, J.; Cronenberg, T.; Nitsche, F.; Huesgen, P. F.; Maier, B.; Neundorf, I. Multistep Optimization of a Cell-Penetrating Peptide towards Its Antimicrobial Activity. *Biochem. J.* **2021**, *478* (1), 63–78. https://doi.org/10.1042/BCJ20200698.

(95) Grabeck, J.; Lützenburg, T.; Frommelt, P.; Neundorf, I. Comparing Variants of the Cell-Penetrating Peptide SC18 to Design Peptide-Drug Conjugates. *Mol. 2022, Vol. 27, Page 6656* **2022**, *27* (19), 6656. https://doi.org/10.3390/MOLECULES27196656.

(96) Negrete-Hurtado, A.; Overhoff, M.; Bera, S.; De Bruyckere, E.; Schätzmüller, K.; Kye, M. J.; Qin, C.; Lammers, M.; Kondylis, V.; Neundorf, I.; Kononenko, N. L. Autophagy Lipidation Machinery Regulates Axonal Microtubule Dynamics but Is Dispensable for Survival of Mammalian Neurons. *Nat. Commun.* **2020**, *11* (1), 1–19. https://doi.org/10.1038/s41467-020-15287-9.

(97) Gronewold, A.; Horn, M.; Neundorf, I. Design and Biological Characterization of Novel Cell-Penetrating Peptides Preferentially Targeting Cell Nuclei and Subnuclear Regions. *Beilstein J. Org. Chem.* **2018**, *14* (1).

(98) Kardani, K.; Milani, A.; H. Shabani, S.; Bolhassani, A. Cell Penetrating Peptides: The Potent Multi-Cargo Intracellular Carriers. *https://doi.org/10.1080/17425247.2019.1676720* **2019**, *16* (11), 1227–1258. https://doi.org/10.1080/17425247.2019.1676720.

(99) Kurrikoff, K.; Langel, Ü. Recent CPP-Based Applications in Medicine. *https://doi.org/10.1080/17425247.2019.1665021* **2019**, *16* (11), 1183–1191. https://doi.org/10.1080/17425247.2019.1665021.

(100) Borrelli, A.; Tornesello, A. L.; Tornesello, M. L.; Buonaguro, F. M. Cell Penetrating Peptides as Molecular Carriers for Anti-Cancer Agents. *Mol. A J. Synth. Chem. Nat. Prod. Chem.* **2018**, *23* (2). https://doi.org/10.3390/MOLECULES23020295.

(101) Movafegh, B.; Jalal, R.; Mohammadi, Z.; Aldaghi, S. A. Poly-L-Arginine: Enhancing Cytotoxicity and Cellular Uptake of Doxorubicin and Necrotic Cell Death. *Anticancer. Agents Med. Chem.* **2019**, *18* (10), 1448–1456. https://doi.org/10.2174/1871520618666180412114750.

(102) Szeto, H. H. Cell-Permeable, Mitochondrial-Targeted, Peptide Antioxidants. *AAPS J.* **2006**, *8* (2), E277–E283. https://doi.org/10.1007/bf02854898.

(103) Szeto, H. H. Mitochondria-Targeted Peptide Antioxidants: Novel Neuroprotective Agents. *AAPS Journal*. Springer August 18, 2006, pp 521–531. https://doi.org/10.1208/aapsj080362.

(104) Zhao, T.; Liu, X.; Singh, S.; Liu, X.; Zhang, Y.; Sawada, J.; Komatsu, M.; Belfield, K. D. Mitochondria Penetrating Peptide-Conjugated TAMRA for Live-Cell Long-Term Tracking. *Bioconjug. Chem.* **2019**, *30* (9), 2312–2316. https://doi.org/10.1021/acs.bioconjchem.9b00465.

(105) Horton, K. L.; Kelley, S. O. Engineered Apoptosis-Inducing Peptides with Enhanced Mitochondrial Localization and Potency. *J. Med. Chem.* **2009**, *52* (10), 3293–3299. https://doi.org/10.1021/jm900178n.

(106) Klimpel, A.; Neundorf, I. Bifunctional Peptide Hybrids Targeting the Matrix of Mitochondria. *J. Control. Release* **2018**, *291*, 147–156. https://doi.org/10.1016/j.jconrel.2018.10.029.

(107) Apostolopoulos, V.; Bojarska, J.; Chai, T. T.; Elnagdy, S.; Kaczmarek, K.; Matsoukas, J.; New, R.; Parang, K.; Lopez, O. P.; Parhiz, H.; Perera, C. O.; Pickholz, M.; Remko, M.; Saviano, M.; Skwarczynski, M.; Tang, Y.; Wolf, W. M.; Yoshiya, T.; Zabrocki, J.; Zielenkiewicz, P.; Alkhazindar, M.; Barriga, V.; Kelaidonis, K.; Sarasia, E. M.; Toth, I. A Global Review on Short Peptides: Frontiers and Perspectives. *Molecules* **2021**, *26* (2), 430. https://doi.org/10.3390/molecules26020430.

(108) Langer, R.; Lund, D.; Leong, K.; Folkman, J. Controlled Release of Macromolecules: Biological Studies. *J. Control. Release* **1985**, *2* (C), 331–341. https://doi.org/10.1016/0168-3659(85)90055-0.

(109) Fuchs, S. M.; Raines, R. T. Pathway for Polyarginine Entry into Mammalian Cells. *Biochemistry* **2004**, *43* (9), 2438–2444. https://doi.org/10.1021/bi035933x.

(110) Hayashi, Y.; Yamauchi, J.; Khalil, I. A.; Kajimoto, K.; Akita, H.; Harashima, H. Cell Penetrating Peptide-Mediated Systemic SiRNA Delivery to the Liver. *Int. J. Pharm.* **2011**, *419* (1–2), 308–313. https://doi.org/10.1016/j.ijpharm.2011.07.038.

(111) Koppelhus, U.; Awasthi, S. K.; Zachar, V.; Holst, H. U.; Ebbesen, P.; Nielsen, P. E. Cell-Dependent Differential Cellular Uptake of PNA, Peptides, and PNA-Peptide Conjugates. *Antisense Nucleic Acid Drug Dev.* **2002**, *12* (2), 51–63. https://doi.org/10.1089/108729002760070795.

(112) Guidotti, G.; Brambilla, L.; Rossi, D. Cell-Penetrating Peptides: From Basic Research to Clinics. *Trends Pharmacol. Sci.* **2017**, *38* (4), 406–424. https://doi.org/10.1016/J.TIPS.2017.01.003.

(113) Henninot, A.; Collins, J. C.; Nuss, J. M. The Current State of Peptide Drug Discovery: Back to the Future? *Journal of Medicinal Chemistry.* American Chemical Society February 22, 2018, pp 1382–1414. https://doi.org/10.1021/acs.jmedchem.7b00318.

(114) Rotem, R.; Heyfets, A.; Fingrut, O.; Blickstein, D.; Shaklai, M.; Flescher, E. Jasmonates: Novel Anticancer Agents Acting Directly and Selectively on Human Cancer Cell Mitochondria. *Cancer Res.* **2005**, *65* (5), 1984–1993. https://doi.org/10.1158/0008-5472.CAN-04-3091.

(115) Raviv, Z.; Cohen, S.; Reischer-Pelech, D. The Anti-Cancer Activities of Jasmonates. *Cancer Chemother. Pharmacol.* **2013**, *71* (2), 275–285. https://doi.org/10.1007/S00280-012-2039-Z/FIGURES/4.

(116) Yeruva, L.; Pierre, K. J.; Carper, S. W.; Elegbede, J. A.; Toy, B. J.; Wang, R. C. JASMONATES INDUCE APOPTOSIS AND CELL CYCLE ARREST IN NON-SMALL CELL LUNG CANCER LINES. *http://dx.doi.org/10.1080/01902140601059604* **2009**, *32* (10), 499–516. https://doi.org/10.1080/01902140601059604.

(117) Fingrut, O.; Flescher, E. Plant Stress Hormones Suppress the Proliferation and Induce Apoptosis in Human Cancer Cells. *Leuk. 2002 164* **2002**, *16* (4), 608–616. https://doi.org/10.1038/sj.leu.2402419.

(118) Klippel, S.; Jakubikova, J.; Delmore, J.; Ooi, M.; Mcmillin, D.; Kastritis, E.; Laubach, J.; Richardson, P. G.; Anderson, K. C.; Mitsiades, C. S. Methyljasmonate Displays In Vitro and In Vivo Activity against Multiple Myeloma Cells. *Br. J. Haematol.* **2012**, *159* (3), 340. https://doi.org/10.1111/J.1365-2141.2012.09253.X.

(119) Fingrut, O.; Reischer, D.; Rotem, R.; Goldin, N.; Altboum, I.; Zan-Bar, I.; Flescher, E. Jasmonates Induce Nonapoptotic Death in High-Resistance Mutant P53-Expressing B-Lymphoma Cells. *Br. J. Pharmacol.* **2005**, *146* (6), 800. https://doi.org/10.1038/SJ.BJP.0706394.

(120) Goldin, N.; Arzoine, L.; Heyfets, A.; Israelson, A.; Zaslavsky, Z.; Bravman, T.; Bronner, V.; Notcovich, A.; Shoshan-Barmatz, V.; Flescher, E. Methyl Jasmonate Binds to and Detaches Mitochondria-Bound Hexokinase. *Oncogene 2008 2734* **2008**, *27* (34), 4636–4643. https://doi.org/10.1038/onc.2008.108.

(121) Jarocka-Karpowicz, I.; Markowska, A. Jasmonate Compounds and Their Derivatives in the Regulation of the Neoplastic Processes. *Mol. 2021, Vol. 26, Page 2901* **2021**, *26* (10), 2901. https://doi.org/10.3390/MOLECULES26102901.

(122) Tong, Q. S.; Jiang, G. S.; Zheng, L. D.; Tang, S. T.; Cai, J. Bin; Liu, Y.; Zeng, F. Q.; Dong, J. H. Natural Jasmonates of Different Structures Suppress the Growth of Human Neuroblastoma Cell Line SH-SY5Y and Its Mechanisms. *Acta Pharmacol. Sin. 2008 297* **2008**, *29* (7), 861–869. https://doi.org/10.1111/j.1745-7254.2008.00814.x.

(123) Åmand, H. L.; Rydberg, H. A.; Fornander, L. H.; Lincoln, P.; Nordén, B.; Esbjörner, E. K. Cell Surface Binding and Uptake of Arginine- and Lysine-Rich Penetratin Peptides in Absence and Presence of Proteoglycans. *Biochim. Biophys. Acta - Biomembr.* **2012**, *1818* (11), 2669–2678. https://doi.org/10.1016/J.BBAMEM.2012.06.006.

(124) von Heijne, G. Mitochondrial Targeting Sequences May Form Amphiphilic Helices. *EMBO J.* **1986**, *5* (6), 1335. https://doi.org/10.1002/J.1460-2075.1986.TB04364.X.

(125) Rajan, R.; Balaram, P. A Model for the Interaction of Trifluoroethanol with Peptides and Proteins. *Int. J. Pept. Protein Res.* **1996**, *48* (4), 328–336. https://doi.org/10.1111/J.1399-3011.1996.TB00849.X.

(126) MacPhee, C. E.; Perugini, M. A.; H. Sawyer, W.; Howlett, G. J. Trifluoroethanol Induces the Self-Association of Specific Amphipathic Peptides. *FEBS Lett.* **1997**, *416* (3), 265–268. https://doi.org/10.1016/S0014-5793(97)01224-6.

(127) Manning, M. C.; Woody, R. W. Theoretical CD Studies of Polypeptide Helices: Examination of Important Electronic and Geometric Factors. *Biopolymers* **1991**, *31* (5), 569–586. https://doi.org/10.1002/BIP.360310511.

(128) Henrietta Lacks: Science Must Right a Historical Wrong. *Nature*. Nature Research September 3, 2020, p 7. https://doi.org/10.1038/d41586-020-02494-z.

(129) McKinnon, K. M. Flow Cytometry: An Overview. *Curr. Protoc. Immunol.* **2018**, *2018*, 5.1.1-5.1.11. https://doi.org/10.1002/cpim.40.

(130) Jobin, M. L.; Alves, I. D. On the Importance of Electrostatic Interactions between Cell Penetrating Peptides and Membranes: A Pathway toward Tumor Cell Selectivity? *Biochimie* **2014**, *107* (Part A), 154–159. https://doi.org/10.1016/J.BIOCHI.2014.07.022.

(131) Holohan, C.; Van Schaeybroeck, S.; Longley, D. B.; Johnston, P. G. Cancer Drug Resistance: An Evolving Paradigm. *Nature Reviews Cancer*. Nature Publishing Group October 24, 2013, pp 714–726. https://doi.org/10.1038/nrc3599.

(132) Chen, Z.-P. P.; Li, M.; Zhang, L.-J. J.; He, J.-Y. Y.; Wu, L.; Xiao, Y.-Y. Y.; Duan, J.-A. A.; Cai, T.; Li, W.-D. D. Mitochondria-Targeted Drug Delivery System for Cancer Treatment. *J. Drug Target.* **2016**, *24* (6), 492–502. https://doi.org/10.3109/1061186X.2015.1108325.

(133) Roise, D.; Schatz, G. Mitochondrial Presequences. *J. Biol. Chem.* **1988**, *263* (10), 4509–4511. https://doi.org/10.1016/S0021-9258(18)68809-X.

(134) Jarocka-Karpowicz, I.; Markowska, A. Therapeutic Potential of Jasmonic Acid and Its Derivatives. *Int. J. Mol. Sci. 2021, Vol. 22, Page 8437* **2021**, *22* (16), 8437. https://doi.org/10.3390/IJMS22168437.

(135) Gräslund, A.; Madani, F.; Lindberg, S.; Langel, Ü.; Futaki, S. Mechanisms of Cellular Uptake of Cell-Penetrating Peptides. *J. Biophys.* **2011**, *2011*. https://doi.org/10.1155/2011/414729.

9. Attachment

9.1. Supplementary data
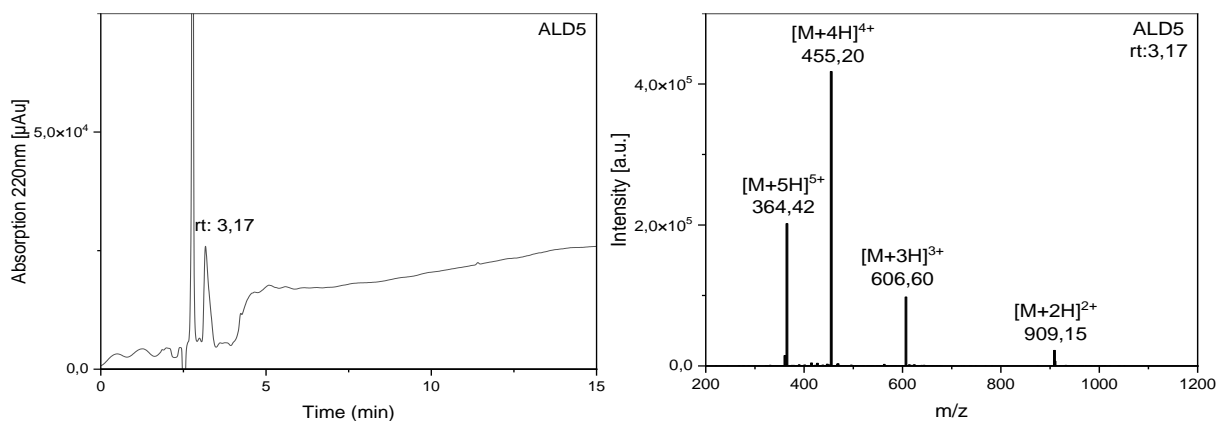
Figure S 1. UV-chromatogram and ESI-MS spectrum of ALD5 after purification. Sample was recorded using a gradient from 10-60 % ACN in water within 15 min.
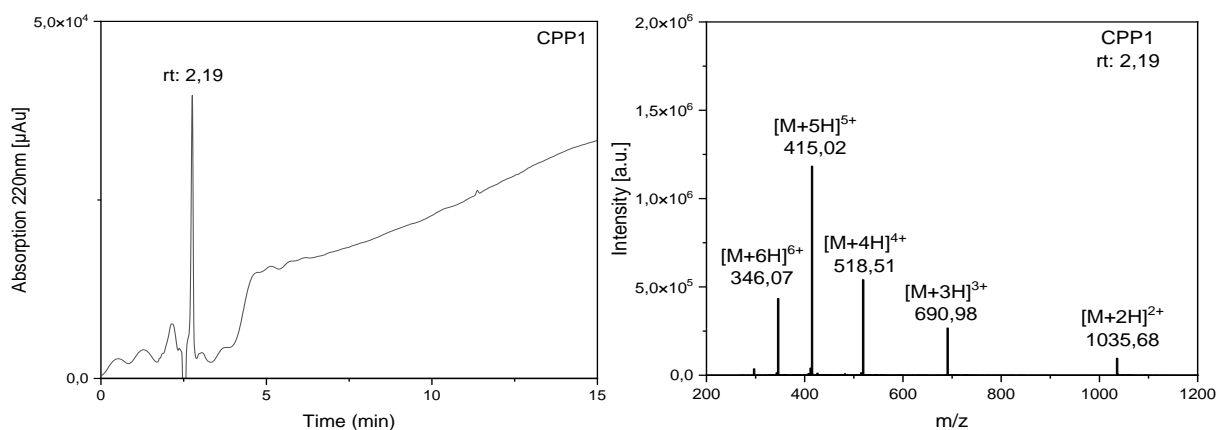
Figure S 2. UV-chromatogram and ESI-MS spectrum of CPP1 after purification. Sample was recorded using a gradient from 10-60 % ACN in water within 15 min.
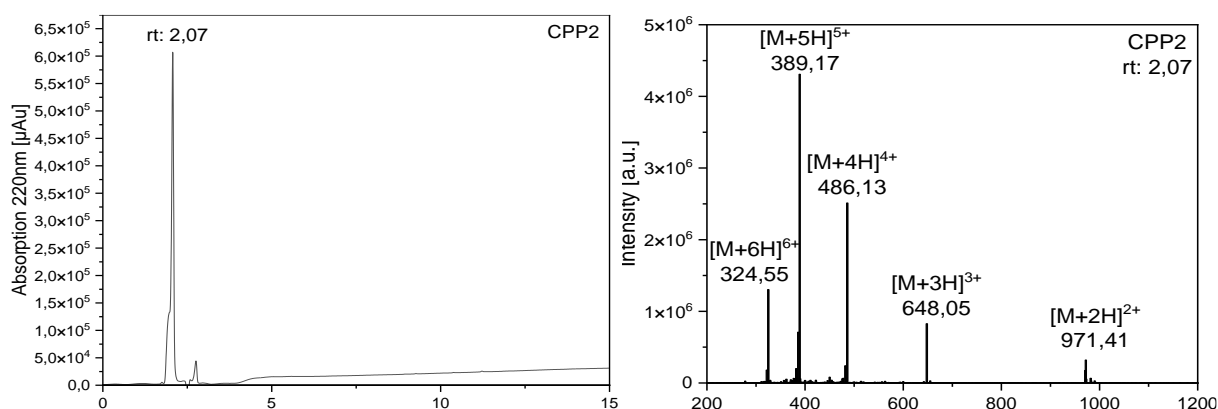
Figure S 3. UV-chromatogram and ESI-MS spectrum of CPP2 after purification. Sample was recorded using a gradient from 10-60 % ACN in water within 15 min.
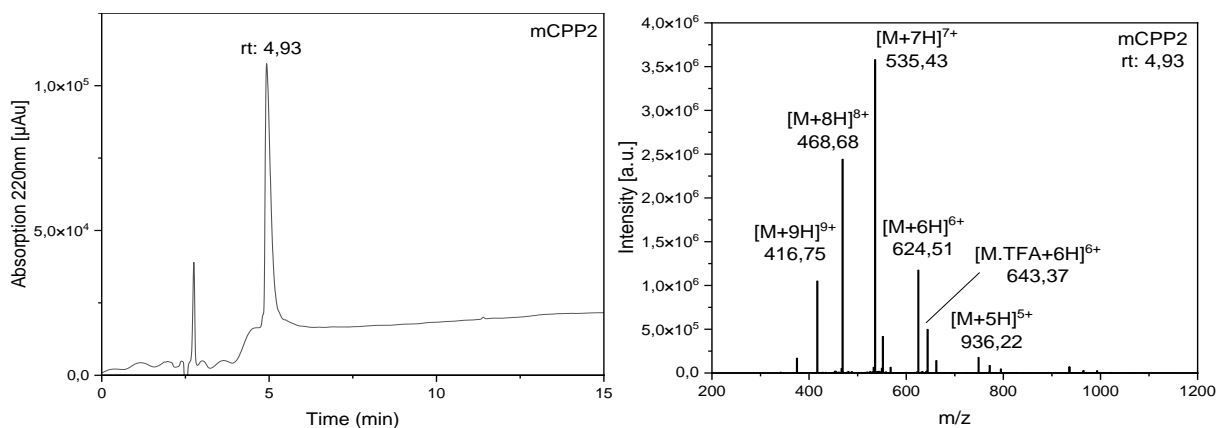
Figure S 5. UV-chromatogram and ESI-MS spectrum of mCPP2 after purification. Sample was recorded using a gradient from 10-60 % ACN in water within 15 min.
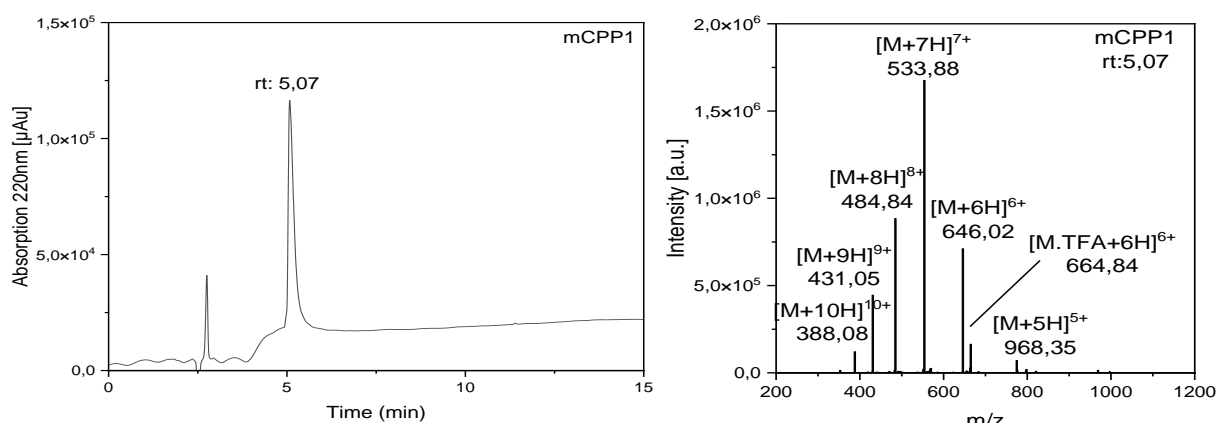
Figure S 4. UV-chromatogram and ESI-MS spectrum of mCPP1 after purification. Sample was recorded using a gradient from 10-60 % ACN in water within 15 min.
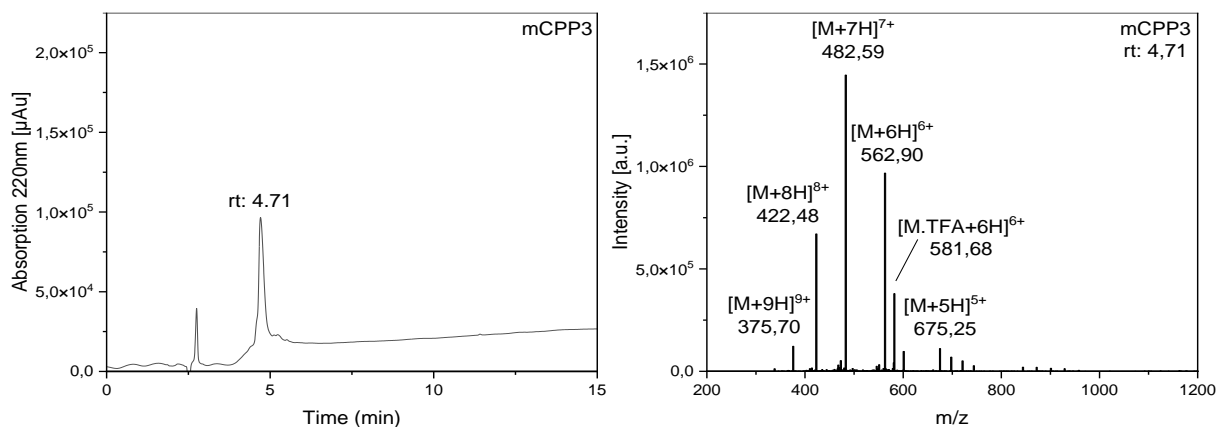
Figure S 6. UV-chromatogram and ESI-MS spectrum of mCPP3 after purification. Sample was recorded using a gradient from 10-60 % ACN in water within 15 min.
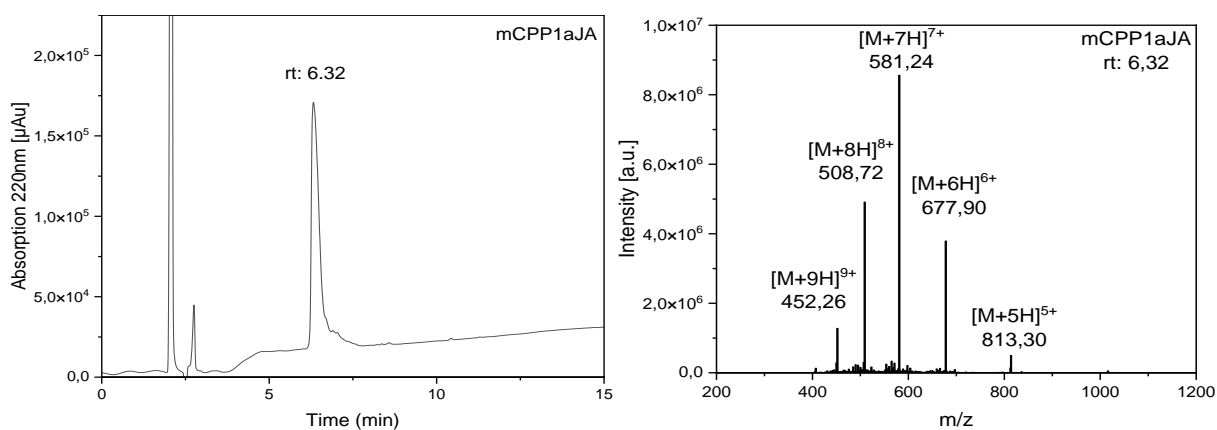
Figure S 7. UV-chromatogram and ESI-MS spectrum of mCPP1aJA after purification. Sample was recorded using a gradient from 10-60 % ACN in water within 15 min.
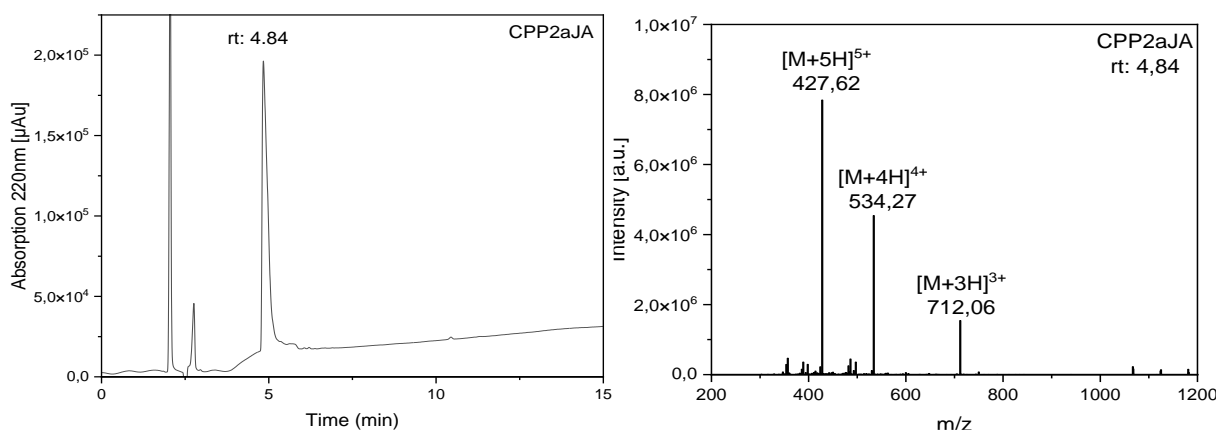
Figure S 9. UV-chromatogram and ESI-MS spectrum of CPP2aJA after purification. Sample was recorded using a gradient from 10-60 % ACN in water within 15 min.
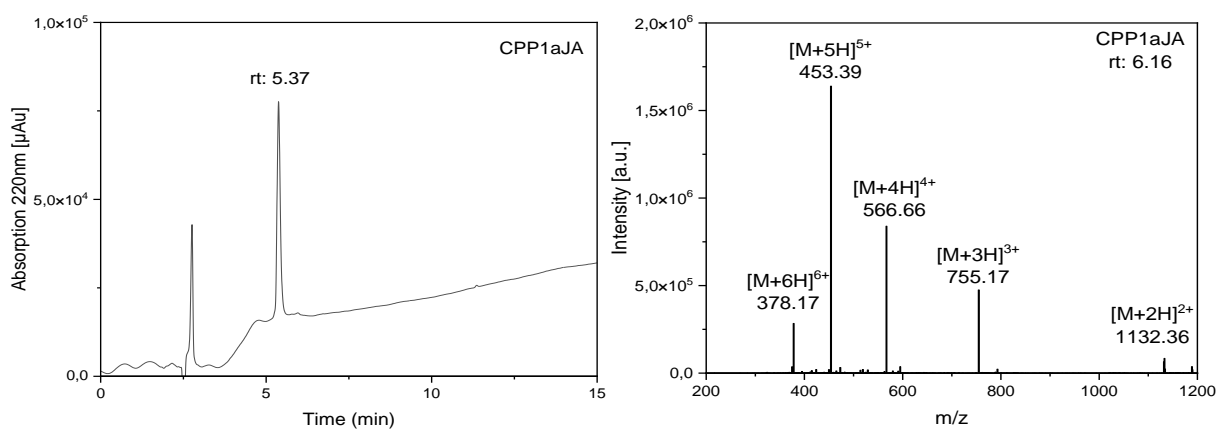
Figure S 8. UV-chromatogram and ESI-MS spectrum of CPP1aJA after purification. Sample was recorded using a gradient from 10-60 % ACN in water within 15 min.
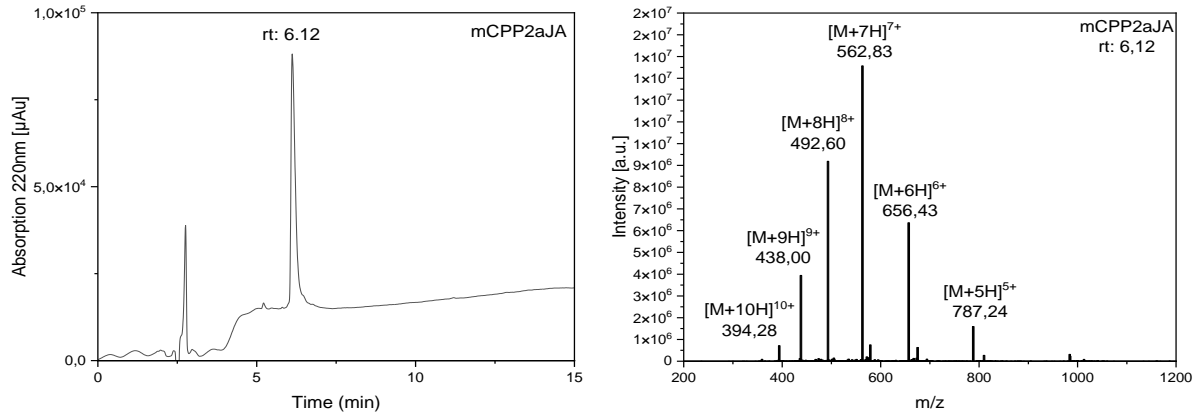
Figure S 10. UV-chromatogram and ESI-MS spectrum of mCPP2aJA after purification. Sample was recorded using a gradient from 10-60 % ACN in water within 15 min.
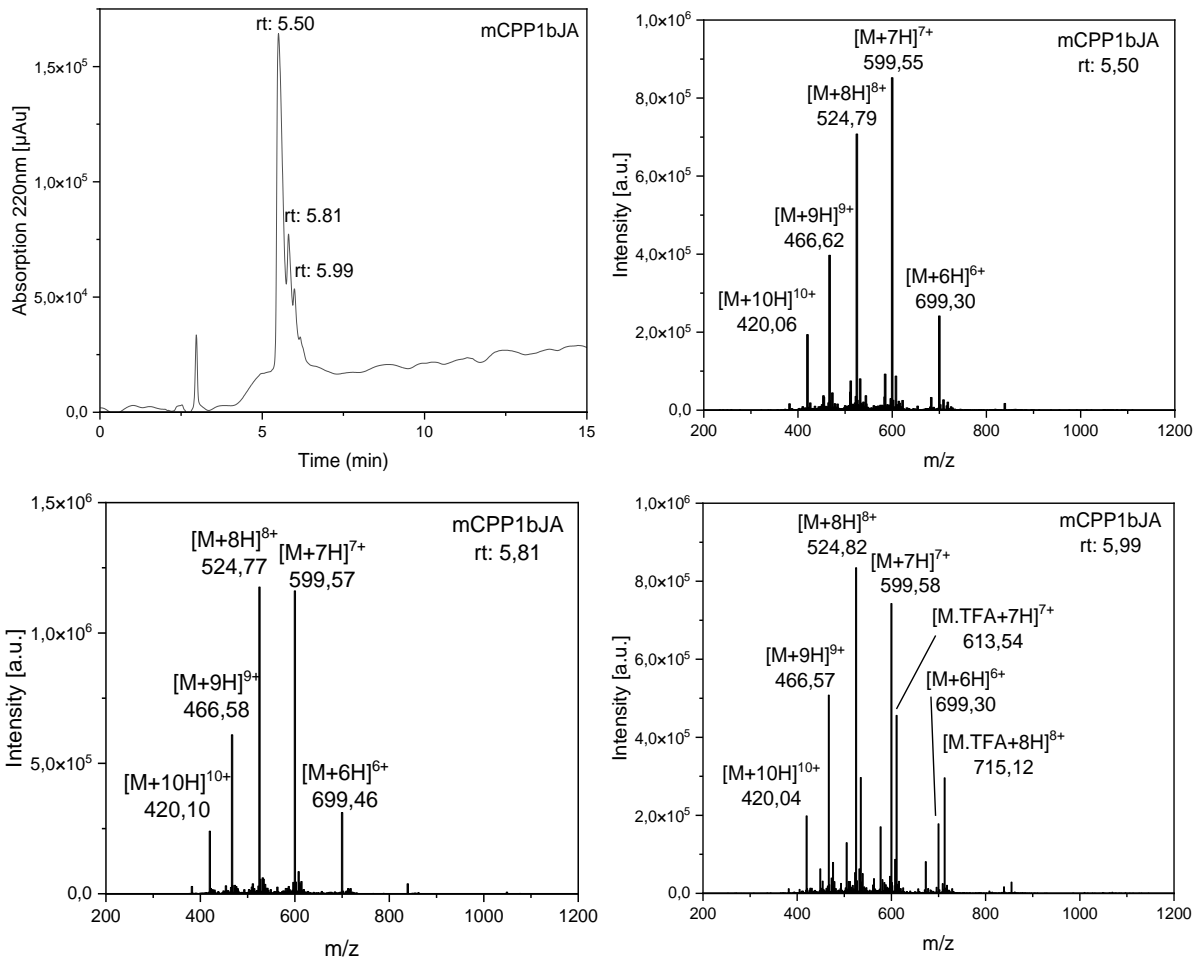
Figure S 11. UV-chromatogram and ESI-MS spectrum of mCPP1bJA after purification. Sample was recorded using a gradient from 10-60 % ACN in water within 15 min.
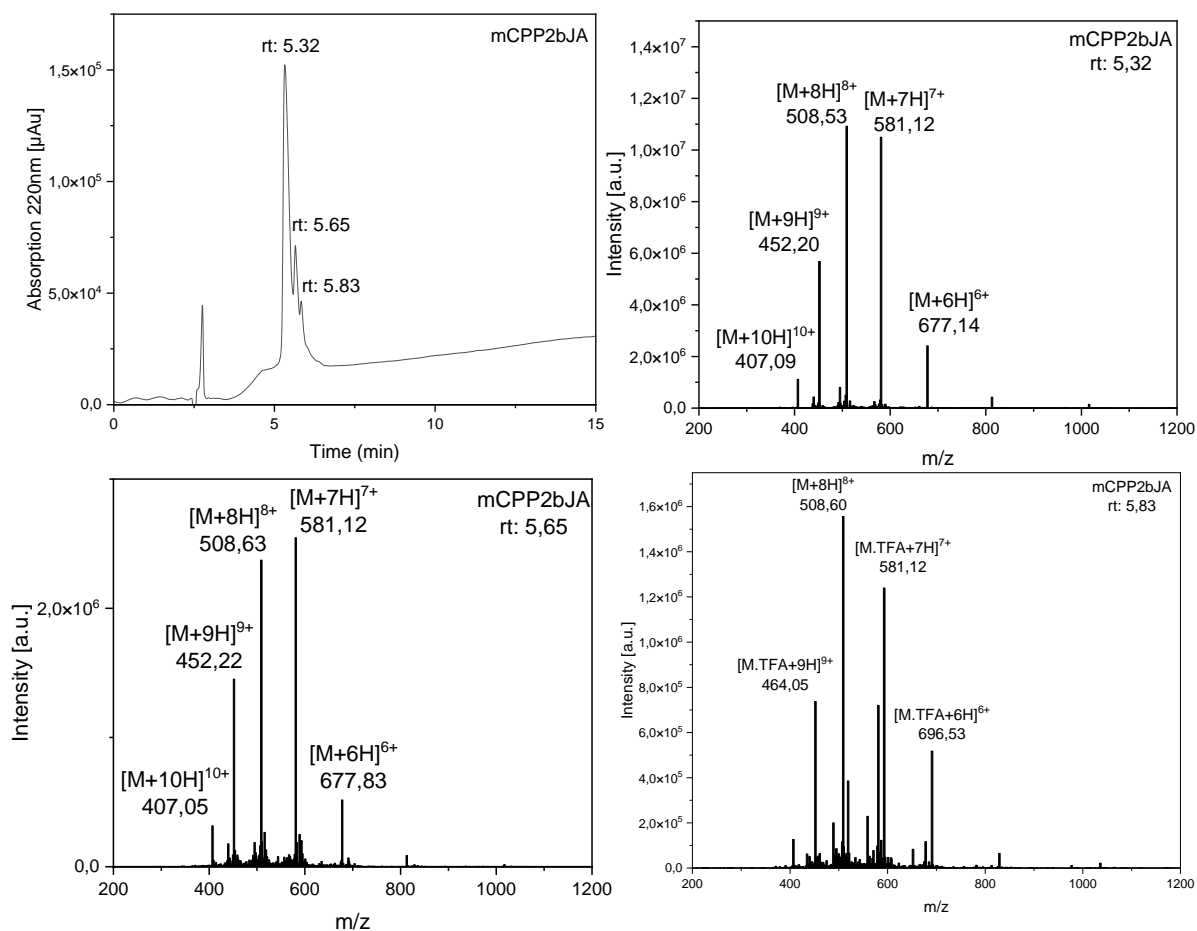
Figure S 12. UV-chromatogram and ESI-MS spectrum of mCPP2bJA after purification. Sample was recorded using a gradient from 10-60 % ACN in water within 15 min.
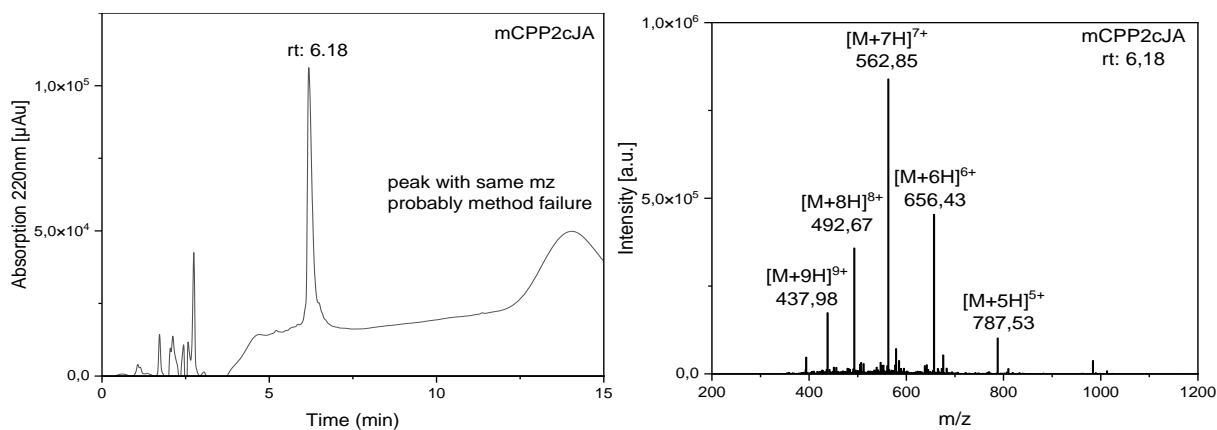
Figure S 13. UV-chromatogram and ESI-MS spectrum of mCPP2cJA after purification. Sample was recorded using a gradient from 10-60 % ACN in water within 15 min.
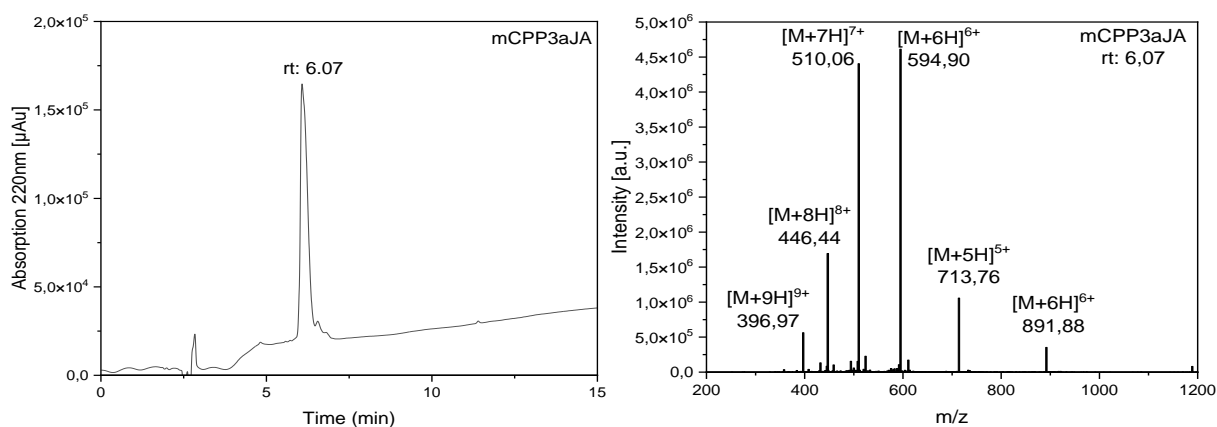
Figure S 15. UV-chromatogram and ESI-MS spectrum of mCPP3aJA after purification. Sample was recorded using a gradient from 10-60 % ACN in water within 15 min.
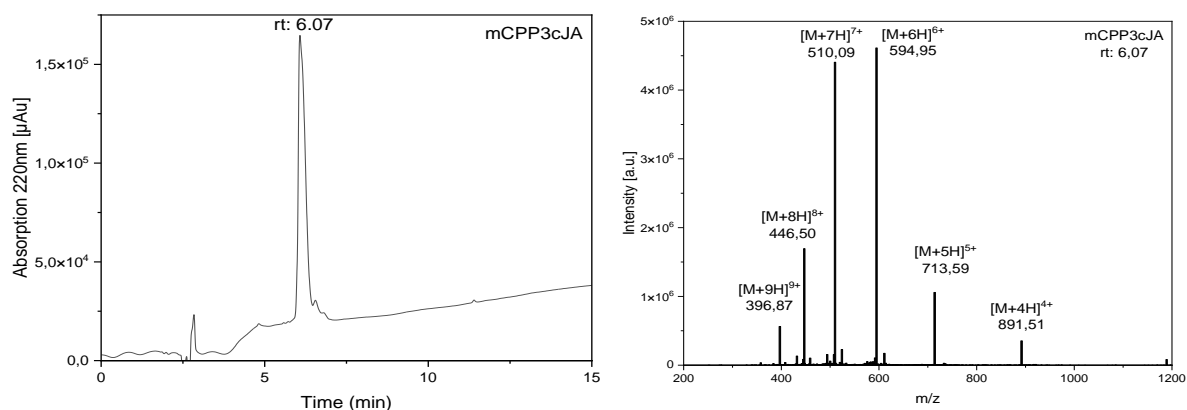
Figure S 16. UV-chromatogram and ESI-MS spectrum of mCPP3cJA after purification. Sample was recorded using a gradient from 10-60 % ACN in water within 15 min.
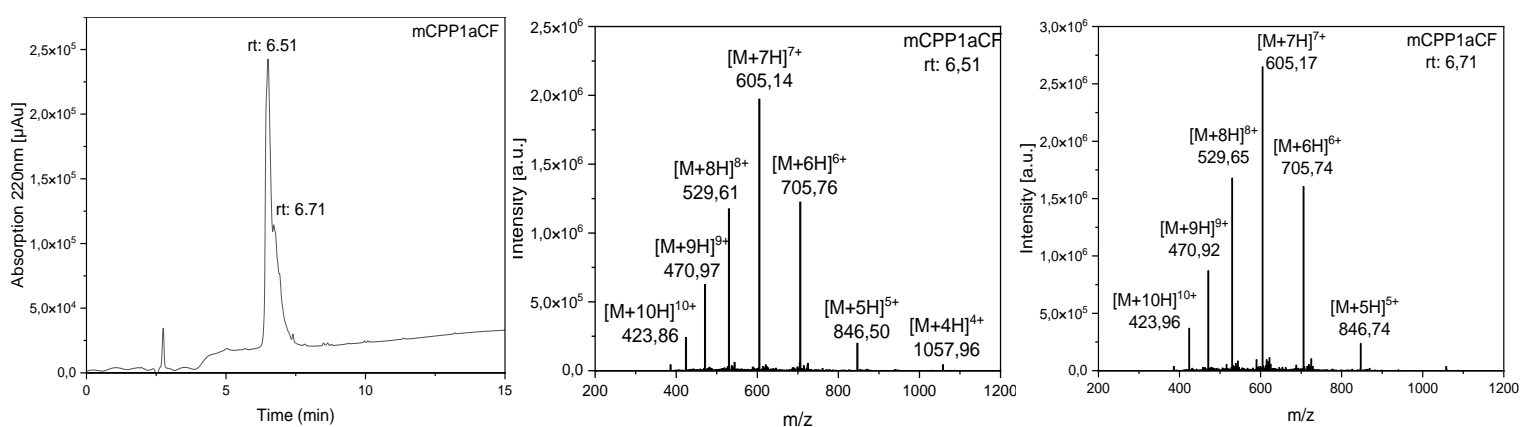
Figure S 14. UV-chromatogram and ESI-MS spectrum of mCPP1aCF after purification. Sample was recorded using a gradient from 10-60 % ACN in water within 15 min.
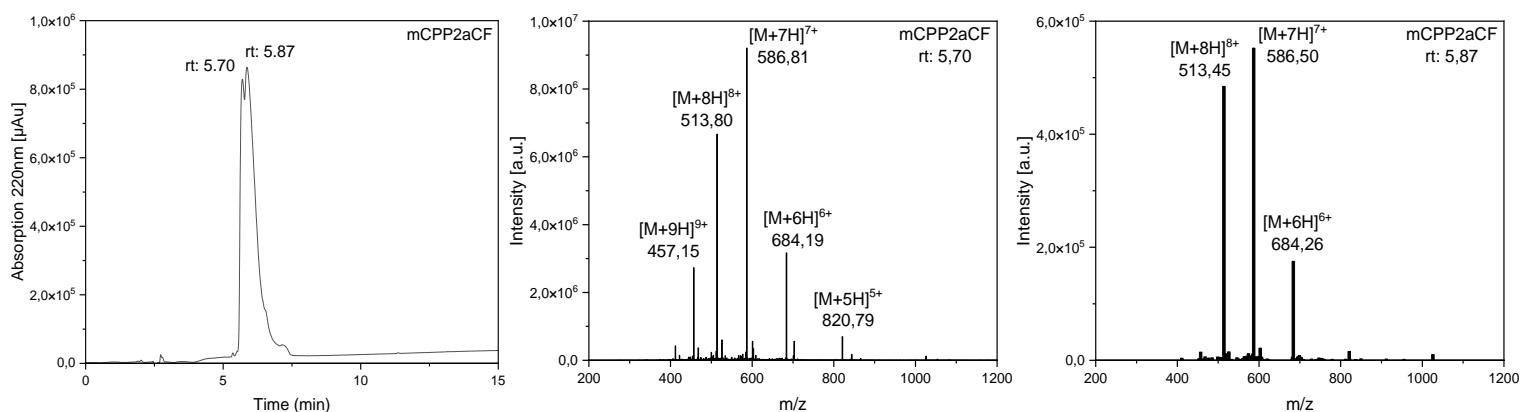
Figure S 18. UV-chromatogram and ESI-MS spectrum of mCPP2aCF after purification. Sample was recorded using a gradient from 10-60 % ACN in water within 15 min.
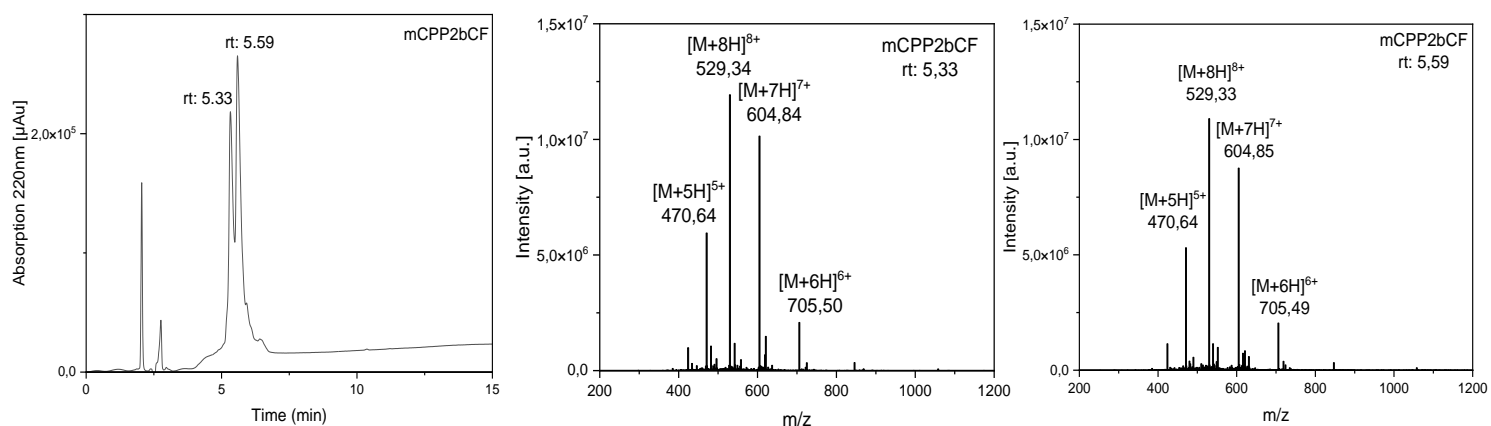
Figure S 19. UV-chromatogram and ESI-MS spectrum of mCPP2bCF after purification. Sample was recorded using a gradient from 10-60 % ACN in water within 15 min.
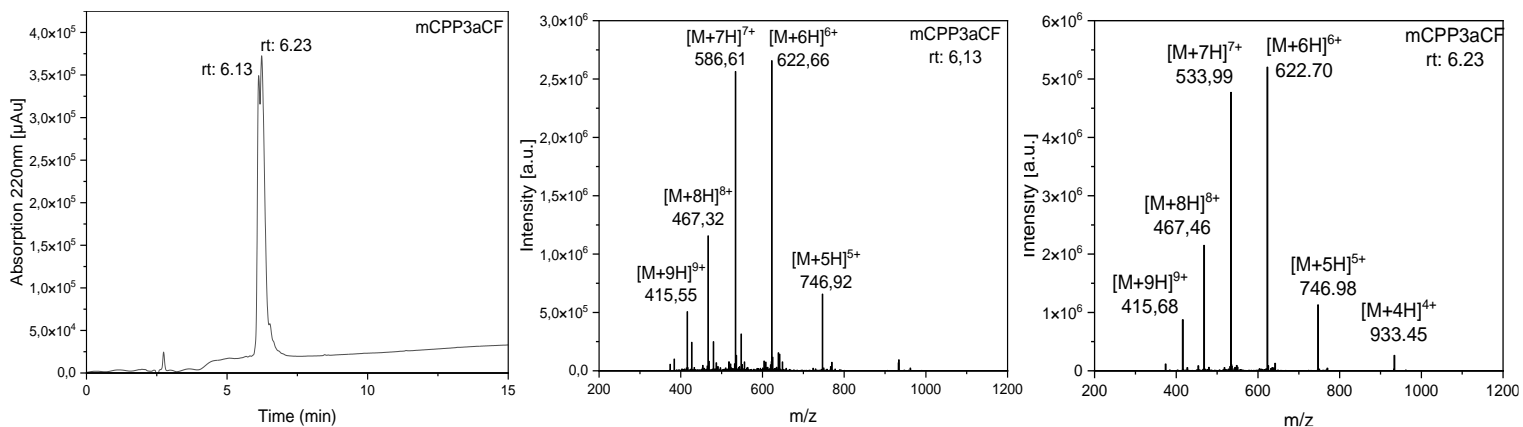
Figure S 17. UV-chromatogram and ESI-MS spectrum of mCPP3aCF after purification. Sample was recorded using a gradient from 10-60 % ACN in water within 15 min.
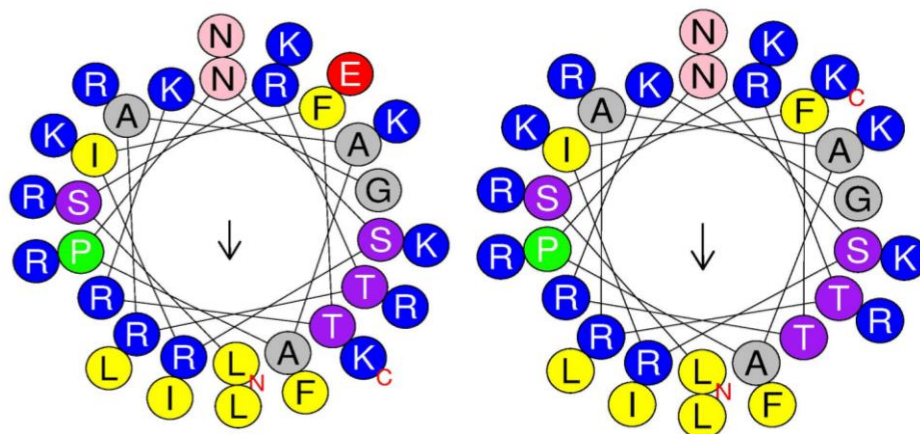
Figure S 20. Helix projection with size proportional to residues. mCPP1b (left), mCPP2b (right). Colors refers to residues properties: blue for hydrophilic/positively charged aa, yellow for hydrophobic/non-polar aa, grey, pink and purple for uncharged aa, green for special aa, red for hydrophilic/negatively charged aa. Additionally terminal aa are marked with a red letter; N for N-termini and C for C-termini.
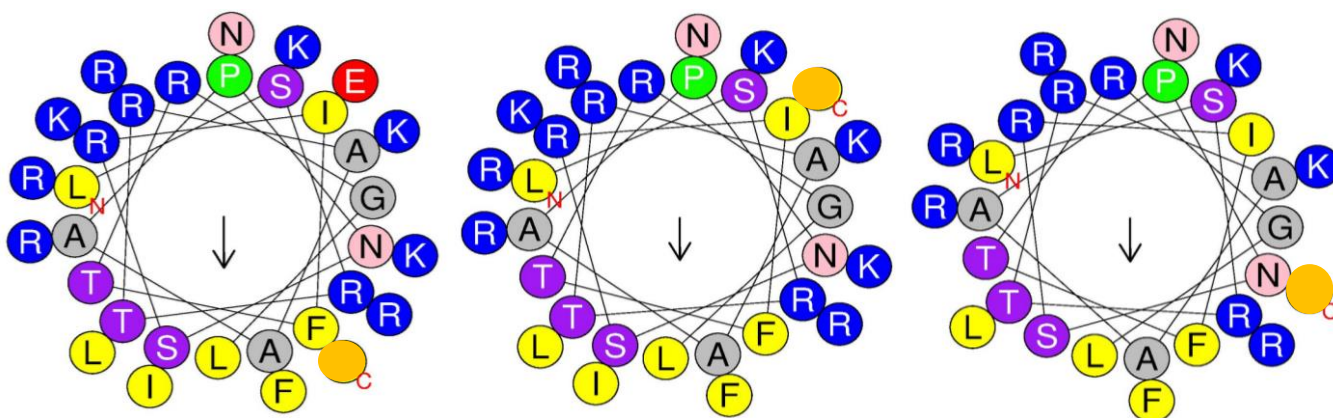
Figure S 21. Helix projection with size proportional to residues. mCPP1a (left), mCPP2a (middle), mCPP3a (right). Colors refers to residues properties: blue for hydrophilic/positively charged aa, yellow for hydrophobic/non-polar aa, grey, pink and purple for uncharged aa, green for special aa, red for hydrophilic/negatively charged aa and payload cou-pling position in orange. Additionally terminal aa are marked with a red letter; N for N-termini and C for C-termini.
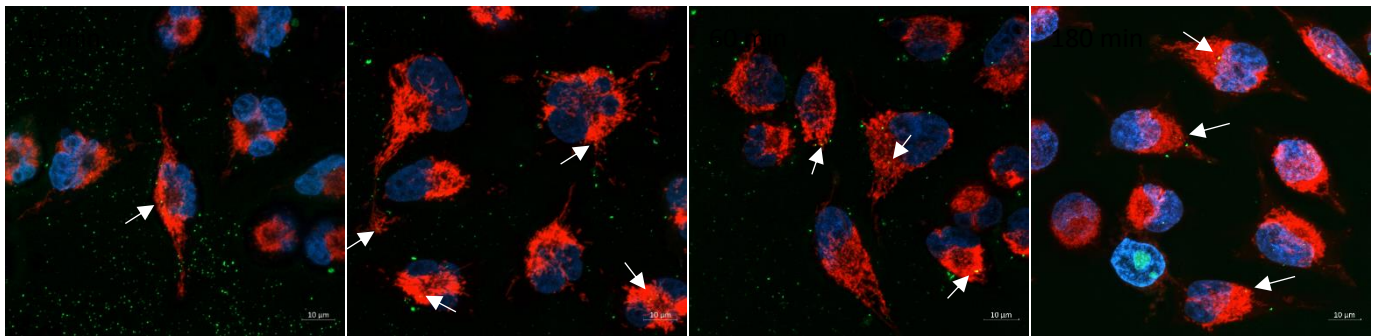
Figure S 22. Confocal images of mCPP2aCF unfixed. Samples were incubated with CMXRos mitotracker (red) for 30 min then with mCPP2aCF (green) for 15, 30, 60 or 180 min (left to right) at 5µM and finally with Hoechst (blue) nucleus dye for 10 min. Co-localization spots are indicated with an arrow.
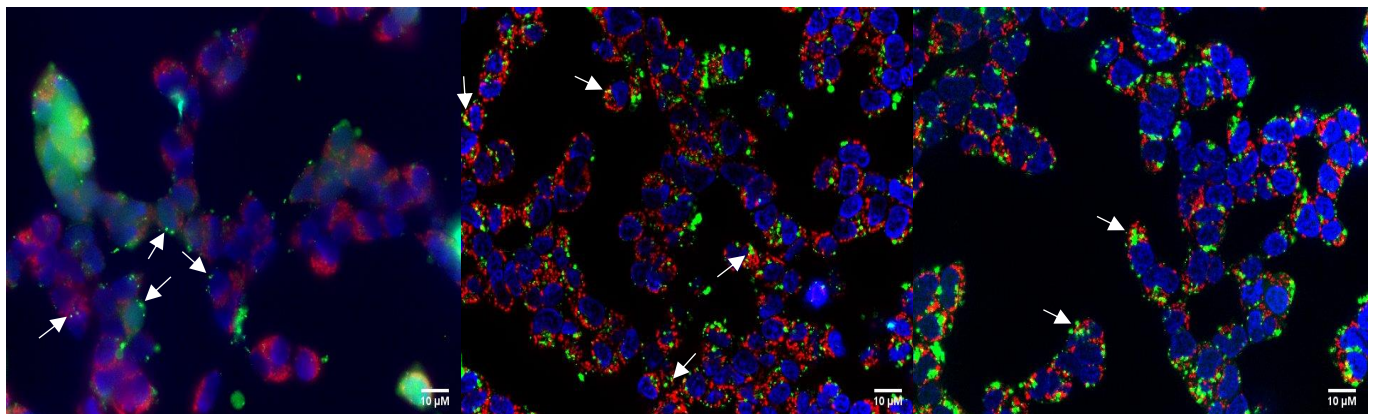
Figure S 23. Microscopy images in HEK-293 cells. Samples were incubated with CMXRos mitotracker (red) for 30 min then with mCPP-CF (green) for 30 min at 5µM and finally with Hoechst (blue) nucleus dye for 10 min. mCPP2aCF (left) mCPP2bCF (middle) mCPP3aCF (right). Co-localization spots are indicated with an arrow.

9.2. List of abbreviations

aa: amino acid

ACN: acetonitrile

ADP: adenosine diphosphate

ALD5: aldehyde dehydrogenase 5

AMP: adenosine monophosphate

APAF1: apoptotic peptidase activating factor 1

ATP: adenosine triphosphate

Bcl-2: B cell lymphoma 2

CF: 5(6) -carboxyfluorescein

CPP: cell-penetrating peptide

CoA: coenzyme a

Dde: 2-acetyldimenone

DIC: N, N'-diisopropyl carbodiimide

DIPEA: N, N-diisopropylethylamine

DLC: delocalized lipophilic cations

Dde: N-(1-(4,4-dimethyl-2,6-dioxocyclohexylidene)ethyl)

DNA: deoxyribonucleic acid

DQA: Dequalinium

ESI-MS: electrospray ionization mass spectrometry

ETC: electron transport chain

Et$_2$O: diethylether

EtOH: ethanol

EPR: enhanced permeability and retention

$FADH_2$: flavin adenine dinucleotide

FBS: fetal bovine serum

h: hours

HATU: 1-[bis(di-methylamino)methyl]-1H-1,2,3-triazole[4,5-b]pyridinium-3-oxidehexa-fluoro-phosphate

HEK-293: human embryonic kidney 293 cell line

Hela: human cervical carcinoma cell line

H_2O_2: hydrogen peroxide

HPLC: high performance liquid chromatography

IMM: inner mitochondrial membrane

IMS: inter membrane space

JA: jasmonic acid

mCPP: mitochondria targeted cell-penetrating peptide

MIM: mitochondrial import machinery

min: minutes

Molt-4: human acute lymphoblastic leukemia cell line

MOMP: mitochondrial outer membrane permeabilization

MPP: mitochondrial processing peptidase

mtDNA: mitochondrial deoxyribonucleic acid

mtPP: mitochondrial penetrating peptide

Mw: molecular weight

m/z: mass to charge ratio

NADH: nicotinamide adenine dinucleotide

NC: nanocarrier

O2-·: superoxide anion

OMM: outer mitochondrial membrane

OXPHOS: oxidative phosphorylation

OXA: oxidative assembly complex

PAM: presequence translocase associated motor

PARP-1: poly(ADP-ribose) polymerase-1

PBS: phosphate buffer saline

PI: propidium iodide

PPi: inorganic pyrophosphate

PS: phosphatidylserine

RIP: receptor interacting protein

ROS: reactive oxygen species

rt: room temperature

SAM: sorting and assembly machinery

SPPS: solid phase peptide synthesis

SS: Szeto-Schiller

TFE: 2,2,2-trifluoroethanol

TCA: tricarboxylic acid cycle

TIM: translocase of the inner membrane

TIS: triisopropylsilane

TOM: translocase of the outer membrane

TPP: Triphenylphosphonium

VDAC: voltage dependent anion channel

9.4. List of tables

9.5. Supplementary figures

I would like to extend those words to Pr. Dr. Norbert Sewald and Dr. Marcel Frese, for organizing and creating this European funding program, it was a great opportunity to work on a meaningful project and to discover the work of others.

Maintenant je souhaite remercier ma famille et mes amis pour leur soutien tout au long de ces 3 années. A mes parents, pour nos appels sabaticaux qui ont réduit la distance qui nous séparait. Le soutien, l'écoute et les conseils tout du long qui font du bien au moral. A mon grand frère dont j'essaye de suivre la trace avec ce doctorat, merci d'avoir été une source d'inspiration et de conseils. A notre petit chat Luffy, qui se fait vieux, merci d'avoir été un bon chat tout du long et pour son bref accompagnement en Allemagne. A mon frère Ludovic, que la vie n'a pas toujours facilité, merci d'être un si bon ami, un soutien inconditionnel, un exemple de détermination et une fontaine à bons moments. Je crois que ces 3 années ont fortement consolidé notre lien. A ma chère Marie, pour son soutien psychologique, son écoute et son empathie. Je suis heureux que l'on ait pris l'initiative de se retrouver et j'espère que ce lien perdurera. A tous mes gurlucks, bien que l'on n'ait pas pu se voir au quotidien à chaque retrouvaille c'était tout comme. Merci d'avoir supporté mon choix de vacances qui fut fort en déception mais surtout merci d'être des amis sur qui je peux compter en tout temps. A mon amie Hélène, pour avoir partagé mes galères le long du chemin.

9.7. Declaration

Hiermit versichere ich an Eides statt, dass ich die vorliegende Dissertation selbstständig und ohne die Benutzung anderer als der angegebenen Hilfsmittel und Literatur angefertigt habe. Alle Stellen, die wörtlich oder sinngemäß aus veröffentlichten und nicht veröffentlichten Werken dem Wortlaut oder dem Sinn nach entnommen wurden, sind als solche kenntlich gemacht. Ich versichere an Eides statt, dass diese Dissertation noch keiner anderen Fakultät oder Universität zur Prüfung vorgelegen hat; dass sie - abgesehen von unten angegebenen Teilpublikationen und eingebundenen Artikeln und Manuskripten - noch nicht veröffentlicht worden ist sowie, dass ich eine Veröffentlichung der Dissertation vor Abschluss der Promotion
nicht ohne Genehmigung des Promotionsausschusses vornehmen werde. Die Bestimmungen dieser Ordnung sind mir bekannt. Darüber hinaus erkläre ich hiermit, dass ich die Ordnung zur Sicherung guter wissenschaftlicher Praxis und zum Umgang mit wissenschaftlichem Fehlverhalten der Universität zu Köln gelesen und sie bei der Durchführung der Dissertation zugrundeliegenden Arbeiten und der schriftlich verfassten Dissertation beachtet habe und verpflichte mich hiermit, die dort genannten Vorgaben bei allen wissenschaftlichen Tätigkeiten zu beachten und umzusetzen. Ich versichere, dass die eingereichte elektronische Fassung der eingereichten Druckfassung vollständig entspricht.

Teilpublikationen:

> **Gayraud, F***.; Klußmann, M*.; Neundorf, I. Recent Advances and Trends in Chemical CPP–Drug Conjugation Techniques. Molecules 2021, 26 (6), 1591. https://doi.org/10.3390/molecules26061591.

> * These authors contributed equally to this work.

Posterpräsentationen:

> **Gayraud, F***.; Neundorf, I. Mitochondria targeted drug deliver – a new approach in cancer treatment, *EPS 2022 in the Young Investigators Mini Symposium*

9.8. Curriculum vitae

Personal data

Name	Félix Gayraud
Birth date	09.03.1996
Birth place	Paris, France

Education

Since 04.2020	PhD study in biochemistry University of Cologne Development of peptide-drug conjugates targeting mitochondria within the ITN Magic Bullet::Reloaded under the supervision of Pr. Dr. Ines Neundorf
2017-2019	Master of science in molecular chemistry Sorbonne Université
2014-2017	Bachelor of science in Chemistry Sorbonne Université

Félix Gayraud

In Köln, 19.06.2023